2012

The feasibility of using megavoltage CT for the treatment planning of HDR cervical brachytherapy with shielded tandem and ovoid applicators

Jeffrey Roger Kemp
Louisiana State University and Agricultural and Mechanical College

THE FEASIBILITY OF USING MEGAVOLTAGE CT FOR THE TREATMENT PLANNING OF HDR CERVICAL BRACHYTHERAPY WITH SHIELDED TANDEM AND OVOID APPLICATORS

A THESIS

Submitted to the Graduate Faculty of the
Louisiana State University and
Agricultural and Mechanical College
in partial fulfillment of the
requirements for the degree of
Master of Science

In

The Department of Physics and Astronomy

by
Jeffrey Roger Kemp
B.S., Brigham Young University, 2009
August 2012

Acknowledgments

I thank Dr. Michael Price for his many hours of discussion, treatment planning and thesis editing. Without his mentorship, this project would not have been possible. I also thank him for his encouragement and support as he helped me to further develop as an independent researcher and physicist. The skills I have learned from Dr. Price will be invaluable to my success as a medical physicist.

I also thank my committee members, Dr. John Gibbons, Dr. Kent Gifford, Dr. Rongying Jin, Dr. Kip Matthews, and Dr. Charlie Wood. Their input and expertise has clarified and improved the quality of my research, helping to produce a study robust enough to contribute to the field of medical physics. I especially thank Dr. Kip Matthews. He has generously shared his resources and time which was been a great help.

I thank my wonderful wife for the loving encouragement and sacrifice to help me get through graduate school. I also thank my daughters Emily and Katie. They have helped me to relax and laugh when needed. My family has been a great strength and support to me for which I am eternally grateful.

I thank the other physicists and physicians participating in my research, namely Dr. Joe Dugas, Kara Ferachi, Dr. Jonas Fontenot, Bryan Mason, Dan Neck, Dr. Brent Parker, Laura Rechner, Dr. Nathan Sheets and Dr. Noam Van der Wald. They invested a considerable amount of time in performing organ segmentation and catheter reconstruction on numerous image sets.

Other people I thank are Dr. Sheldon Johnson, Connel Chu, Ricky Hesston, my professors, and colleagues. These individuals have answered many of my questions or provided support in numerous ways that have helped me to accomplish this research.

Table of Contents

List of Tables

List of Figures

Abstract

Purpose/Objectives: A drawback of tandem and ovoid (T&O) ICBT is exposure of the posterior bladder and anterior rectal walls to relatively high isodoses. To mitigate this effect, intra-ovoid shielding may be used to reduce dose to these OARs. However, metal artifacts present in images acquired via kVCT make anatomy segmentation and catheter localization difficult for the purpose of 3D treatment planning. We present a method that combines MVCT-based imaging and applicator modeling to increase the quality of 3D treatment plans for shielded T&O ICBT.

Materials/Methods: Using Oncentra's TPS, 9 participants from multiple institutions performed organ segmentation and catheter reconstruction for KVCT and MVCT data sets acquired of a water phantom containing bladder and rectum surrogates and various HDR T&O applicators: Nucletron's CT/MR compatible (CTMR), Nucletron's shielded Fletcher Williamson (FW) and (3) Varian's shielded Fletcher-Suit-Delclos style (FSD). The dimensions of OAR structures were determined using in-air kVCT and physical measurements. By comparing the 3D volumes and centroid-to-perimeter (C2P) measurements of individual OAR contours, segmentation accuracy was assessed in regions exhibiting artifact under kVCT (1cm superior and inferior to shielding). Comparing the TPS-defined coordinate of the most distal dwell position to that of the true position (determined using radiographs of a fiducial affixed to the applicators), assessed catheter reconstruction accuracy. For Nucletron devices, this metric was also quantified using an applicator-model for localization.

Results: The percentage of points for C2P measurements that differ (greater than 2mm) from the true contour extents decreased under MVCT for the shielded T&Os (78.4 vs. 71.3%), while the converse is observed for the CTMR. Similarly, the volume of the OAR surrogates follows the same trend. This is attributed to the lack of metal artifacts as well as the decrease in the contrast of low Z materials observed when utilizing MVCT. Catheter reconstruction accuracy improved by 26% under MVCT for

shielded T&Os, was invariant for the CTMR and within 2.29mm of the true position using applicator modeling.

Conclusions: The quality of MVCT 3D ICBT treatment plans of shielded T&O is comparable to MVCT CTMR treatment plans. Further improvements were observed when using an applicator model for catheter reconstruction.

Chapter 1 Introduction

1.1 Brachytherapy for the Treatment of Cervical Cancer

It is estimated that in 2012 in the United States 12,200 women will be diagnosed with cervical cancer of which 4,210 will result in death (National Cancer Institute, 2011). For early or non-bulky disease (typically FIGO stages IB-IVA), the current standard of care is a combination of external beam radiotherapy (EBRT) and intracavitary brachytherapy (ICBT). EBRT is administered first to sterilize regional and local pelvic disease as well as decrease the volume of the primary tumor. ICBT is then used to boost dose delivered to the diseased area with minimal dose to surrounding normal tissue (Viswanathan, et al., 2007). High-dose rate (HDR) brachytherapy (*i.e.* >12 Gy/hr) is a common form of ICBT for the treatment of cervical cancer and has a typical fractionation scheme of 5.5-7 Gy per fraction for 4-5 fractions (Viswanathan, et al., 2011). Through the combination of these two radiotherapy delivery methods, local control of cervical cancer for a large patient population has been achieved (Saibishkumar, et al., 2005).

Brachytherapy is ideally suited for the treatment of cervical cancer for several reasons. Radiation is emitted from brachytherapy sources isotropically, falling off inversely with the square of the distance. This makes it possible to deliver therapeutic doses to diseased tissue while minimizing dose to surrounding normal tissues. Additionally, while localization of the vagina and uterus is of concern when utilizing EBRT, placing the source *in vivo* aids in accurate dose delivery to the desired tissues (Viswanathan, et al., 2007). A distinct disadvantage of ICBT is the inevitable dose delivered to the bladder and rectum. As such, the delivery of therapeutic levels of radiation via ICBT is often limited by these two organs. Common complications due to overdosing of the bladder and rectum include proctitis, fistulas, cystitis and bladder and rectal ulceration (Kapp, et al., 1997).

1.2 Administration of Intracavitary Brachytherapy via Tandem and Ovoid Applicators

A variety of applicators have been developed to administer ICBT. One of the most common applicators utilized in the administration of ICBT is the tandem and ovoid (T&O) applicator (see Figure 1-1).

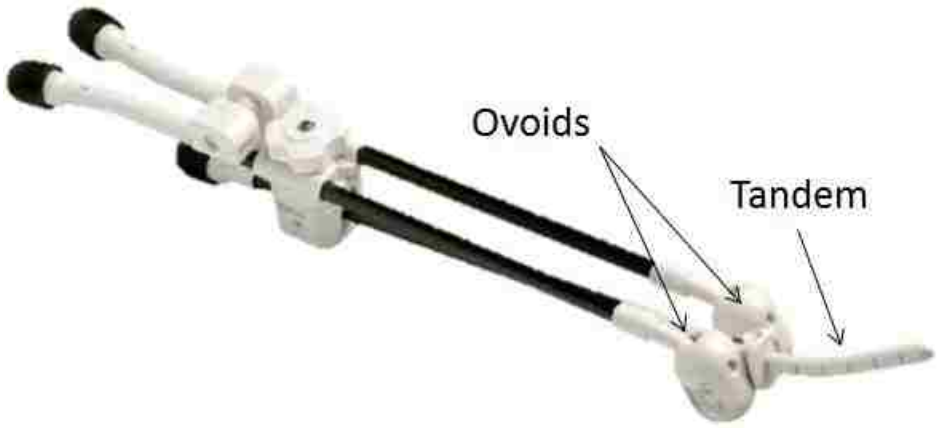

Figure 1-1: Nucletron's CT/MR compatible applicator. This is the current, clinical tandem and ovoid applicator used at Mary Bird Perkins Cancer Center in Baton Rouge, LA where this study was performed.

The tandem is a hollow stainless steel or plastic rod that extends through the cervix into the uterus. To accommodate variations in patient anatomy, tandems are available in multiple angles of anteversion. In addition, the applicator has two catheter tubes that are positioned laterally to the tandem. These channels are capped with ovoids, plastic oval ellipsoids that are seated in the vaginal fornices. The purpose of the ovoids is to broaden the dose distribution into the paracervical regions, while the tandem delivers dose to the cervical, endometrial and uterine tissues (Bentel, 1996).

1.3 Shielded Ovoids for the Tandem and Ovoid Applicator

Ovoids containing shields at their posterior and anterior ends may be used to mitigate dose to the bladder and rectum, minimizing the aforementioned late sequelae (see Figure 1.2). Intra-ovoid shields are commonly constructed of tungsten, titanium or stainless steel. The implementation of intra-ovoid shielding has been demonstrated to substantially reduce dose to the bladder and rectum when compared to equivalent treatments delivered utilizing unshielded ovoids (Yorke, et al., 1987)

(Williamson, 1990) (Verellen, et al., 1994) (Williamson, et al., 2002). Of the shielded applicators developed, tungsten shielded ovoids have proven most effective, reducing dose to the bladder and rectum by up to 48% compared to equivalent treatments delivered using unshielded ovoids (Williamson, 1990).

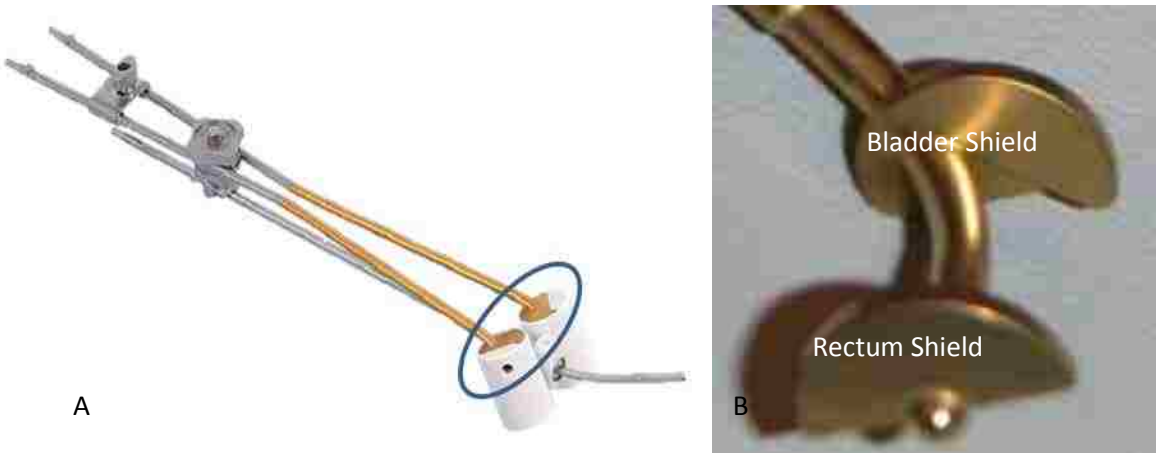

Figure 1-2: Nucletron's shielded Fletcher-Williamson applicator. (A) External image showing the anterior bladder shields. (B) Ovoid tube with ovoid cap removed showing the bladder (anterior) and rectum (posterior) shields.

1.3.1 Shielded Ovoid-Induced Image Artifact

The main disadvantage associated with shielded ovoids is the introduction of image obscuring metal artifacts in treatment planning CT data sets. High Z shields scatter significant portions of the imaging beam. The inability of CT filtered backprojection algorithms to compensate for these heterogeneities is manifest in severe, anatomy-obscuring metal artifact, which in turn limits the ability of physicians and physicists to accurately locate source dwell positions and contour the organs at risk (OAR) within the treatment planning system (TPS). A comparison of CT scans obtained of a Varian unshielded CT/MR compatible applicator and a Nucletron shielded Fletcher (tungsten shields) applicator can be seen in Figure 1-3 (A) and (B), respectively. Extensive metal artifact is observed in the case of the tungsten shielded applicator, severely limiting accurate OAR segmentation and applicator localization. For this reason, many clinics choose to use CT/MR-compatible applicators for ICBT.

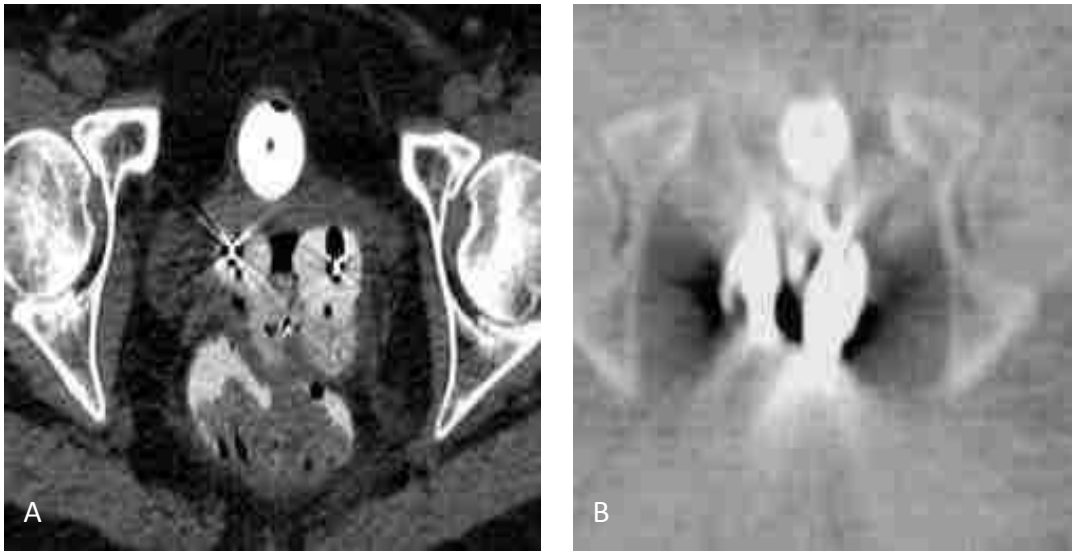

Figure 1-3: A transverse pelvic CT scan of typical patient anatomy with (A) an unshielded, CT/MR Fletcher applicators and (B) a tungsten shielded Fletcher applicator. For the CT/MR compatible applicator, minimal metal artifact can be seen from the source position markers within the ovoids when compared with the metal artifact present in the CT slice of the shielded Fletcher applicator. (Roeske, et al., 2003)

1.3.2 Image Artifact Reduction Methods

Attempts to reduce the presence of high Z metal artifact in CT image sets have met with limited success. Multiple methods of CT artifact reduction are considered in this section.

Roeske *et al.* explored the use of CT projection-interpolation algorithms to mitigate metal artifacts due to the Fletcher-Suit applicator (2003). Linear or higher order CT projection-interpolation algorithms have previously proven effective in reducing metal artifact due to high Z objects with minimal structural integrity (surgical clips, dental fillings, etc.) yielding near artifact-free CT data sets (Glover & Pelc, 1981) (Hsieh, 1998) (Kalendar, et al., 1987). These same methods were applied for phantom and patient CT data sets obtained of the stainless steel, unshielded Fletcher-Suit applicator. While this technique offered the benefits of ease of use and short computational time, results met with limited success (see Figure 1-4). Clinical implementation of this technique remains limited to smaller, high Z objects as it has not yet yielded sufficient metal artifact reduction to warrant clinical implementation.

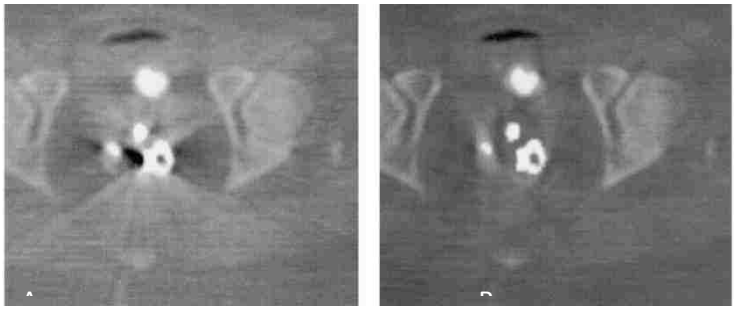

Figure 1-4: CT scan showing the top of the ovoids, tandem and contrast in the Foley catheter (A) before and (B) after CT projection-interpolation algorithm artifact reduction (Roeske, et al., 2003).

Another approach to reduce CT artifact is iterative statistical CT image-reconstruction which more accurately model CT detector response and the physical process of signal acquisition (Williamson, et al., 2002). This method is capable of yielding nearly artifact-free CT imaging of soft tissues near high Z metal objects (see Figure 1-5). This method is limited however in that it relies on an accurate *a priori* model of the metal object, including its pose (position and orientation), shape and a well-defined attenuation map. The inability to correctly determine 3D applicator pose has limited the iterative statistical CT image-reconstruction approach (Williamson, et al., 2002) (Yazdia, et al., 2005). Attempts have been made to improve these methods using generalized iterative forward projection matching (gIFPM) reliant on three 2D x-ray projections. It was reported that pose localization errors were less than 1.5 mm and 2^{o} for orientation angles (Pokhrel, et al., 2011). This method of mitigating metal artifact is not yet clinically availably nor have its capabilities been proven for CT acquisition of shielded ovoids.

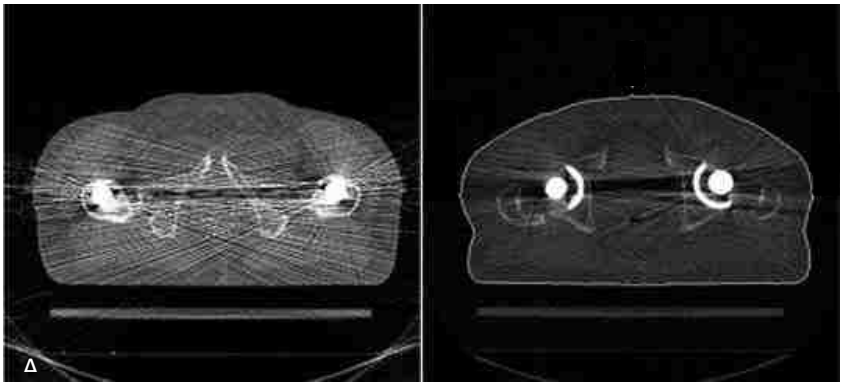

Figure 1-5: A transverse pelvic CT slice through a patient's hip prostheses (A) before and (B) after metal artifact reduction (Yazdia, et al., 2005).

Several attempts have been made to develop clinically viable, CT-compatible shielded ICBT T&O applicators. The first of these, the "Weeks" applicator, utilized tungsten-shielded source carriers that are loaded post-CT acquisition (Weeks & Montana, 1997). This applicator was based off the shielded Fletcher-Suit-Delclos applicator with mini-colpostats (both systems are shown in Figure 1-6 and Figure 1-7). The affixed Fletcher shields were replaced with manually loaded tungsten shields that are inserted in conjunction with ^{137}Cs source loading (see Figure 1-7(left)) (Weeks & Montana, 1997). The main disadvantage of the Weeks applicator, preventing clinical implementation, is the inability for remote afterloading resulting in increased exposure to clinical staff for low dose rate (LDR) procedures and no possible treatment for HDR or pulsed-dose-rate (PDR) applications.

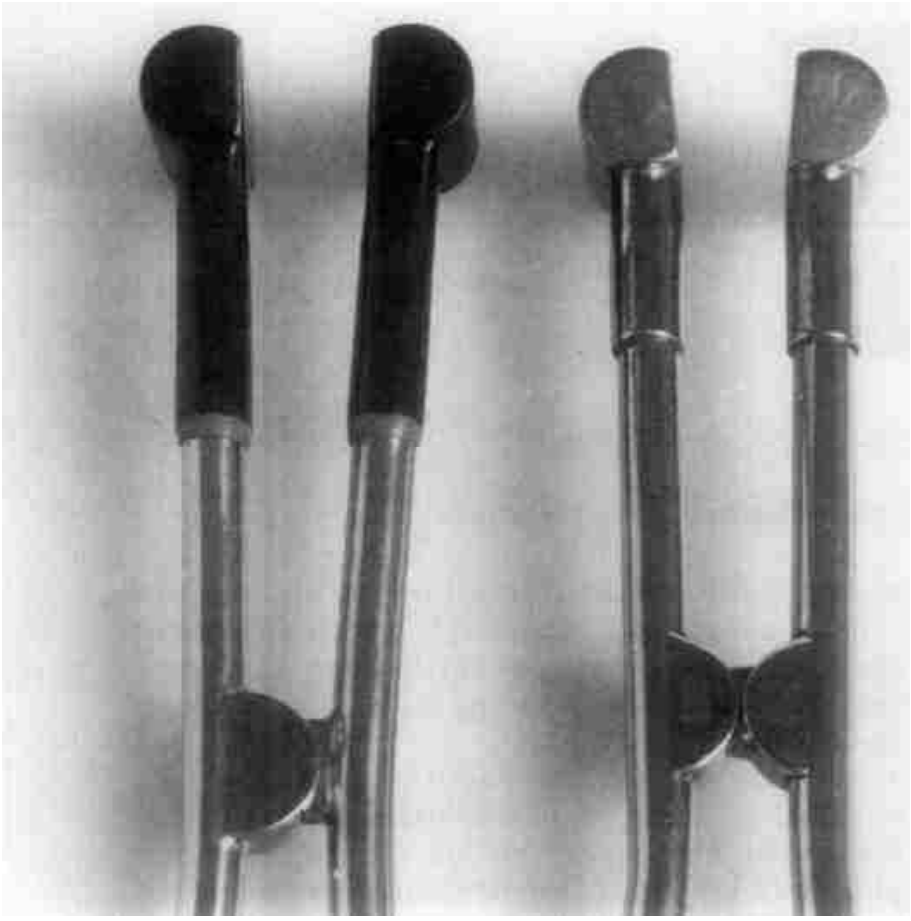

Figure 1-6: Side-by-side comparison of the second generation Weeks ovoids (left) and the Fletcher-Suit-Delclos ovoids (right) showing their similarity. The second generation Weeks ovoids were composed of Aluminum. The change from plastic ovoid tubing to aluminum improved the rigidity of the applicator (Weeks & Montana, 1997).

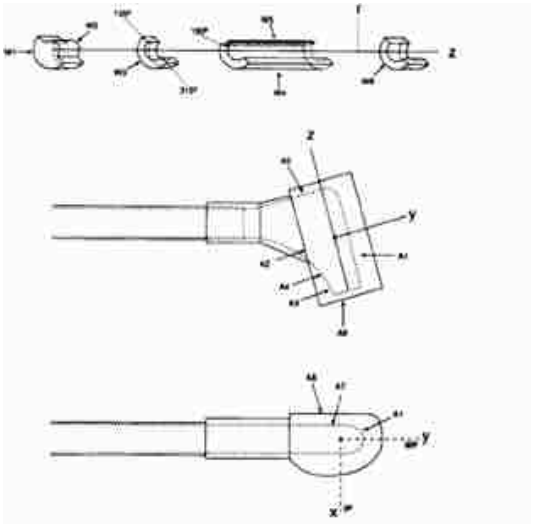

Figure 1-7: Schematic of the Weeks ovoids with the catheter tube (top), a lateral view of the post-CT added shielded source carrier (middle) and an anterior view of the post-CT added shielded source carrier (bottom). (Weeks & Montana, 1997)

A prototype CT/MR compatible Fletcher Williamson applicator with moveable interovoid shields (the Anatomically Adaptive Applicator or A^3) has also been developed in an attempt to reduce metal artifact in CT data sets (see Figure 1-8). It has been shown that this applicator yields artifact-free images of patient anatomy with metal artifact limited to a region contained within the ovoid (see Figure 1-9) (Price, et al., 2009). A step-and-shoot method of CT acquisition is used to acquire artifact-free CT images. MR compatibility is achieved through the use of carefully selected MR-compliant materials. Although several centers are initiating clinical trials utilizing the A^3 applicator, it is not available for clinical use at this time.

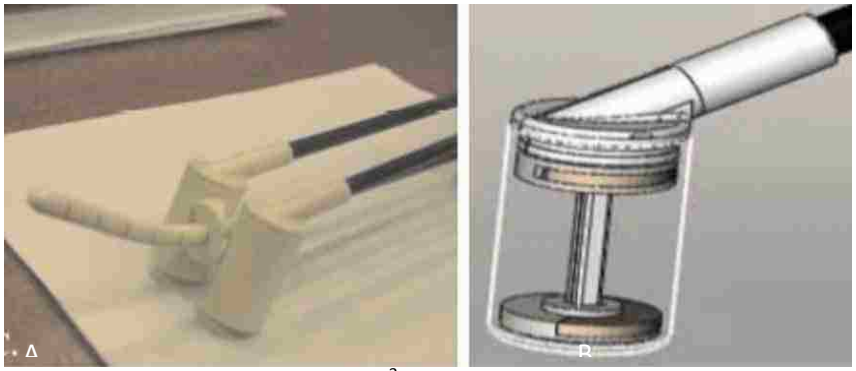

Figure 1-8: Price's CT/MR compatible shielded A^3 applicator. The external appearance of the applicator (A) and interovoid shields (B). (Price, 2008)

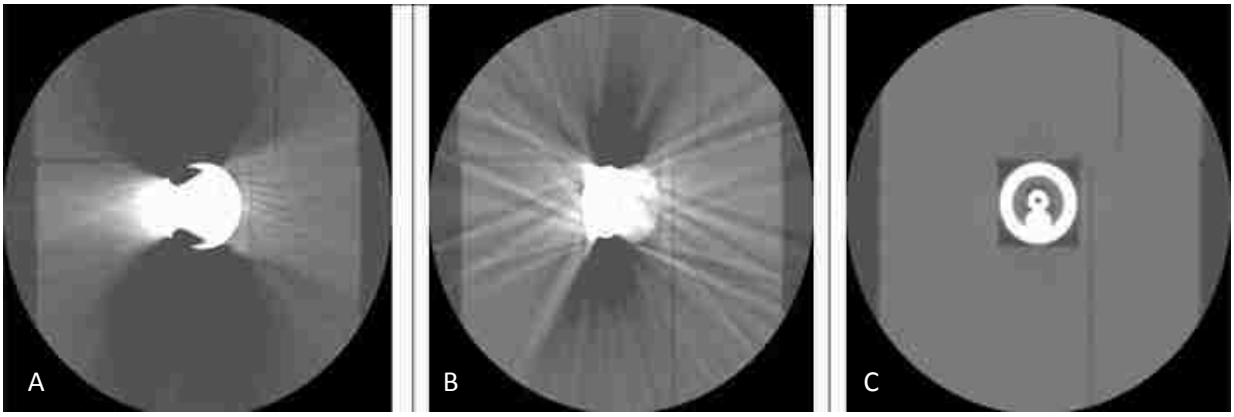

Figure 1-9: Comparison of reconstructed axial CT slices through the bladders shields of the shielded Fletcher-Suit-Delclos applicator (A), the shielded Fletcher Williamson applicator (B) and Price's A^3 applicator (C)

1.4 Megavoltage Computed Tomography for Planning Shielded Ovoid ICBT Treatments

Alternatively, the use of megavoltage CT (MVCT) may pose a viable solution for artifact-free imaging of shielded tandem and ovoid applicators. An MVCT imaging beam is more penetrating than a Kilovoltage CT (kVCT) beam; as energy increases, linear attenuation decreases with relatively more radiation arriving at the CT detector panels. For example, at 60 keV (typical kVCT scan mean energy), the linear attenuation coefficient (μ) of tungsten is 71 cm^{-1} whereas at 3.5 MV (average energy of 0.75 MeV), μ is equal to 1.71 cm^{-1}, a decrease by a factor of $\approx$40. An increase in energy also results in an increase in penetration through CT detectors yielding a decrease in image contrast and resolution. However, it has been demonstrated that helical tomotherapy yields CT data sets acceptable for patient alignment and delineation of many soft tissue structures (Meeks, et al., 2005). Also, multiple studies have demonstrated that MVCT data sets continue to display sufficient contrast to facilitate critical structure segmentation even when high Z objects, such as hip prosthesis, spinal stabilization rods and dental appliances are present (see Figure 1-10) (Hansen, et al., 2006), (Aubin, 2006), (Yank, et al., 2010), (Korol, et al., 2010). One study has explored the feasibility to utilizing MVCT for the treatment planning

of a shielded Fletcher-Suit-Delclos applicator, concluding that MVCT images for clinical LDR gynecological brachytherapy are acceptable for 3D, MVCT-based dose planning (Wagner, et al., 2009).

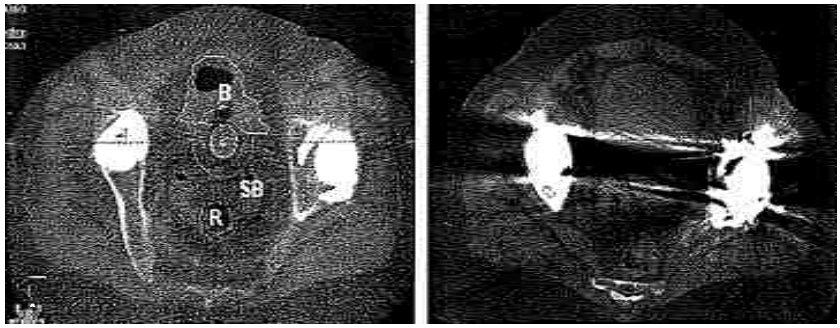

Figure 1-10: CT scans of a cervical ICBT T&O patient with hip prostheses with (A) a MVCT scanner and (B) a kVCT scanner. It is noted that in image (A), MV energy, the scan quality was sufficient for physician organ segmentation of the rectum (R), small bowl/sigmoid colon (SB) and the bladder (B). (Korol, et al., 2010)

MVCT imaging of patients containing metallic objects often results in negligible metal artifacts when compared to equivalent scans acquired via kVCT. It is not yet known if MVCT scans of a patient containing shielded HDR tandem and ovoid applicators are of sufficient quality to allow 3D treatment planning of a gynecologic ICBT treatment, to localize source dwell positions and to segment OARs (bladder, rectum and sigmoid colon). The purpose of this work is to investigate the use of MVCT imaging to acquire artifact-free or nearly-artifact-free imaging data sets of a shielded applicator in a patient-surrogate phantom for ICBT organ segmentation and catheter reconstruction.

1.5 Hypothesis and Specific Aims

Metrics[1] quantifying the accuracy of (a) organ segmentation and (b) intracavitary brachytherapy catheter reconstruction will agree within ±2 mm/±15 cc and ±2 mm, respectively, of known values for

[1]Organ segmentation two- and three-dimensional metrics: centroid-to-perimeter (CTP) measures (2D) as well as volume comparisons (3D). The three-dimensional dwell position metric is a comparison of the distal-most origin of catheter reconstruction relative to applicator reference markers. The two-dimensional organ segmentation metric was chosen to be 2mm as this was within 1mm of the systematic error. The three-dimensional organ segmentation metric was chosen to be 15cc, a volume representing 5%-12% of surrogate organ structure volumes. For three-

image sets acquired via mega-voltage computed tomography (MVCT) for shielded tandem and ovoid (T&O) brachytherapy applicators imaged in a water phantom containing surrogate organ structures.

1.5.1 Aim 1. Water Phantom Development and Image Acquisition

First, a water phantom containing structures acting as surrogates for patient rectums and bladders will be constructed. Second, kVCT and MVCT image sets will be acquired for three (3) HDR T&O-type ICBT applicators: a Nucletron unshielded, CT/MR compatible Fletcher applicator, a Nucletron shielded Fletcher-Williamson applicator and a Varian shielded Fletcher-Suit-Delclos-style applicator.

1.5.2 Aim 2. Organ Segmentation and Catheter Reconstruction

Medical physicists and physicians from multiple institutions will segment the bladder and rectum on both kVCT and MVCT data sets for all applicator types and perform catheter reconstruction for kVCT and MVCT image sets. In the case of the Nucletron applicators, an additional catheter reconstruction will be performed with the assistance of the Oncentra Brachy applicator modeling TPS plugin.

1.5.3 Aim 3. Determination of Organ Segmentation and Catheter Reconstruction Accuracy

The quality of the resulting treatment plans will be evaluated based on the accuracy of the participant organ segmentation and catheter reconstruction. Organ segmentation accuracy will be determined via two-dimensional centroid-to-perimeter (CTP) measurements and three-dimensional volume comparison. CTP values will be compared with bladder and rectum structure scans in air to obtain values which will be designated as CTP-diff. Overall structure volumes will be compared with volumes measured via water displacement to obtain values designated as VOL-diff. Catheter reconstruction accuracy will be determined for each applicator tube by comparing the location of the distal-most, participant-defined dwell positions relative to applicator reference markers, with control values measured via radiograph; this measure will be referred to as MD-diff.

---

dimensional dwell position metric, 2mm was chosen because this is outside the specifications of the mechanical accuracy of the afterloader (+/-1mm).

Chapter 2 Methods and Materials

2.1 Aim 1: Water Phantom Development and Image Acquisition

To achieve the aims of this study, a water phantom was constructed to provide participants with image sets containing surrogate bladder and rectum structures as well as clinically viable applicator positioning relative to these structures. The water phantom consisted of a water tank, structure immobilization devices, bladder and rectum surrogates, and various T&O applicators.

2.1.1 Tandem and Ovoid Applicators

The imaging properties of three different HDR T&O applicators were investigated in this study: the Nucletron CT/MR compatible Fletcher applicator (CTMR), the Nucletron shielded Fletcher-Williamson applicator (FW) and the Varian shielded Fletcher-Suit-Delclos-style applicator (FSDs) (see Figure 2-1).

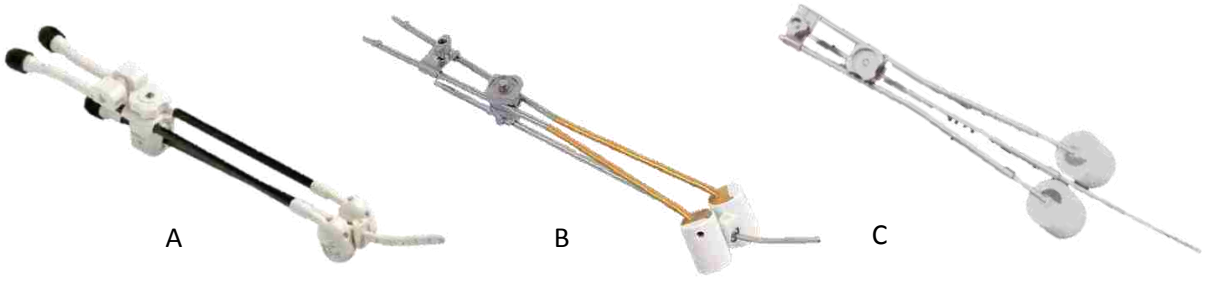

Figure 2-1: HDR T&O applicators used in this study. (A) Nucletron's CT/MR compatible applicator. (B) Nucletron's Fletcher-Williamson applicator. (C) Varian's Fletcher-Suit-Delclos-style applicator.

The CTMR applicator is the current, clinical applicator used at Mary Bird Perkins Cancer Center (MBPCC) in Baton Rouge, LA where this study was conducted. It is composed of special composite, low Z plastics which mitigate artifact in CT and MR images, facilitating 3D ICBT treatment planning and dose analysis.

The FW applicator catheters are constructed of stainless steel and the ovoids consist of polysulfone caps surrounding Densimet-17 (tungsten alloy, Z=74, ρ = 17g/cm^3) bladder and rectal shields

(Horton, et al., 2005). The bladder and rectum shields are 2.0 and 2.1 mm thick, respectively, and are welded to the applicator tubes in an orientation that optimizes shielding to the posterior bladder and anterior rectal walls for ideal insertions (see Figure 2-2). For ideal insertions, these shields yield a dose reduction in the bladder and rectum greater than 40% for ideal anatomy positioning relative to the ovoid shields.

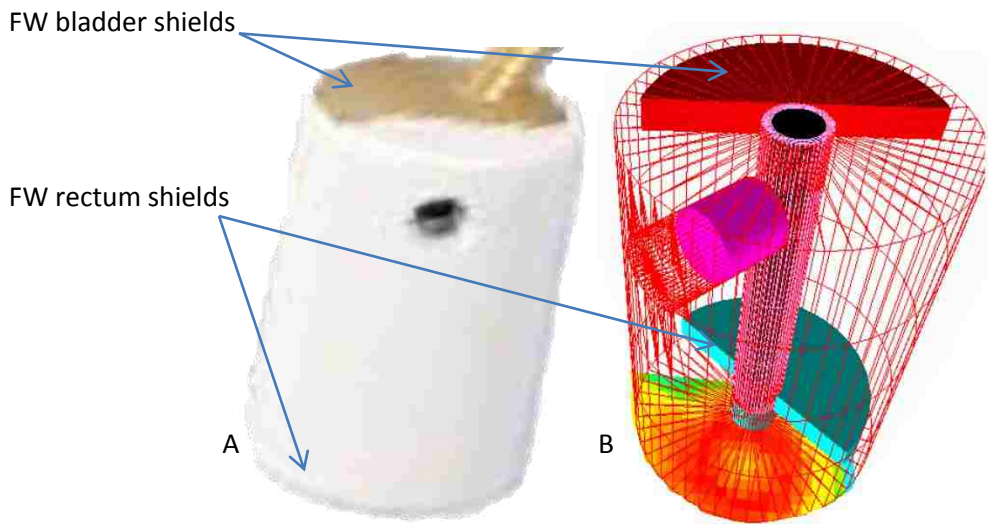

Figure 2-2: (A) The exterior of the FW ovoid (rectal shield not visible) and (B) a schematic of the interior of the FW ovoid, mainly the bladder and rectum shields. (Price, 2008)

The Varian Fletcher-Suit-Delclos-style applicator catheters and inter-colpostatic shields are constructed of stainless steel ($\rho \approx 8$ g/cm^3, $Z \approx 27$ (exact composition proprietary)) and the ovoid caps are acetal (Naydenov & Ryzhikov, 2005). The manufacturer reports that the stainless steel shields are capable of reducing dose in the bladder and rectum by up to 20% (Varian Medical Systems, 2009). While this is less than half the dose reduction achieved with FW ovoid shields, the intent is to provide an applicator capable of shielding the bladder and rectum while yielding CT data sets with sufficient visibility to facilitate organ segmentation and catheter reconstruction.

For all applicators investigated, a tandem tube angle of 30 degrees and an ovoid diameter of 25 mm were chosen because all applicator sets include components of these specifications and these sizes

are commonly utilized clinically. Clinical source position markers were used for investigations of the CTMR applicators (see Figure 2-3). Source position markers are made of a thin metal strand with larger metallic markers placed periodically along the strand. These markers are used clinically in patient CT scans to represent actual source paths during treatment and to aid physicists and physicians in accurately choosing dwell positions within the TPS. Source position markers were not used for the Nucletron Fletcher-Williamson or the Varian Fletcher-Suit Delclos-style applicators because image artifacts inhibit visualization of source position markers. Clinical treatment planning for shielded applicators typically involves localizing the catheter tube tip end, measuring a fixed distance (which is institution dependent) inferior to the tip end and placing the source in the middle of the catheter tube.

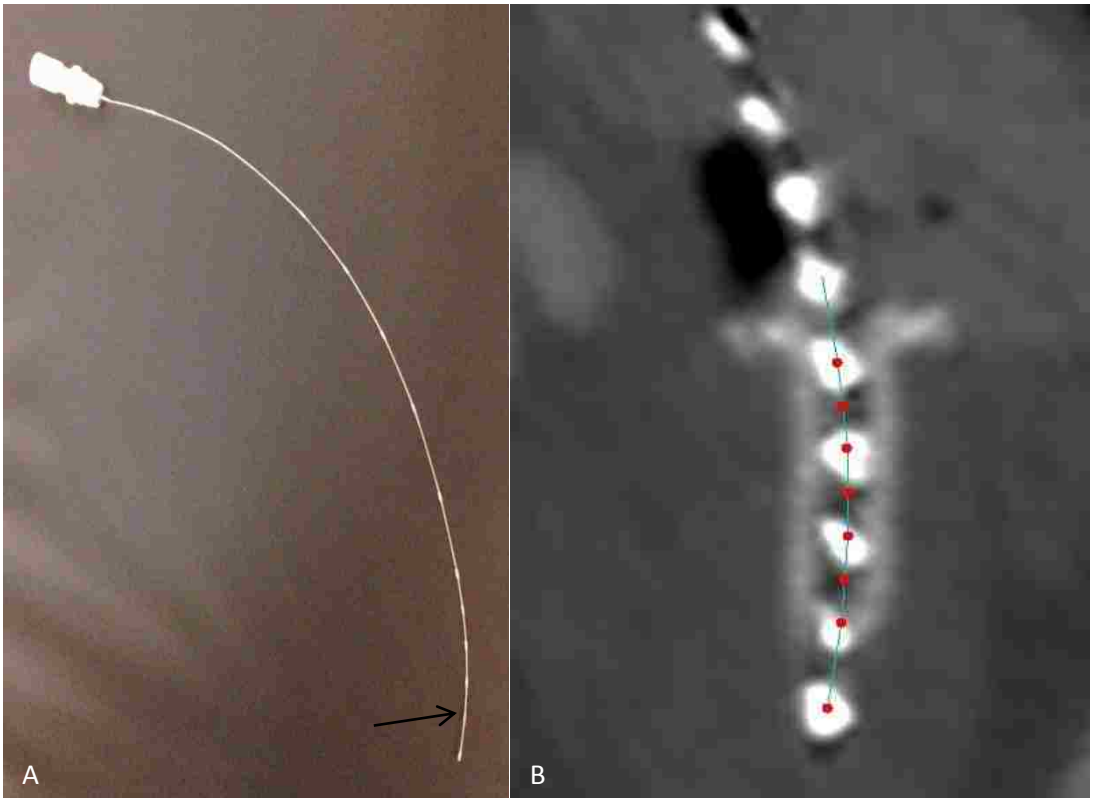

Figure 2-3: CTMR applicator source position markers. (A) Metallic markers along wire strand (a single marker pointed out by black arrow) representing various source positions within the catheter. (B) Sagittal CT slice showing the source position markers (white marks) and planned TPS dwell positions (red dots along green reconstructed catheter).

For each applicator catheter tube (the tandem and both ovoids), applicator reference markers were attached to facilitate Aim 3 of the study (see Figure 2.4). These markers were ≈1.2 mm in length

and 1 mm in diameter and made of stainless steel. To determine the correct applicator reference marker size, various sizes were imaged on kVCT and MVCT scanners until the markers were visually present for both kV and MV image sets with default window (=500) and level (=1) settings while minimizing metal artifact. For the ovoid catheters, applicator reference markers were placed directly behind the ovoids. In the case of the shielded ovoids, a 5 mm wooden spacer was placed between the ovoid tube and the marker so as to limit artifact interference from the stainless steel tubes. For the tandem tubes, the markers were placed 3 cm inferior from the tip. Again, a wooden spacer (1 mm thick) was utilized for tandem tubes from the shielded applicators.

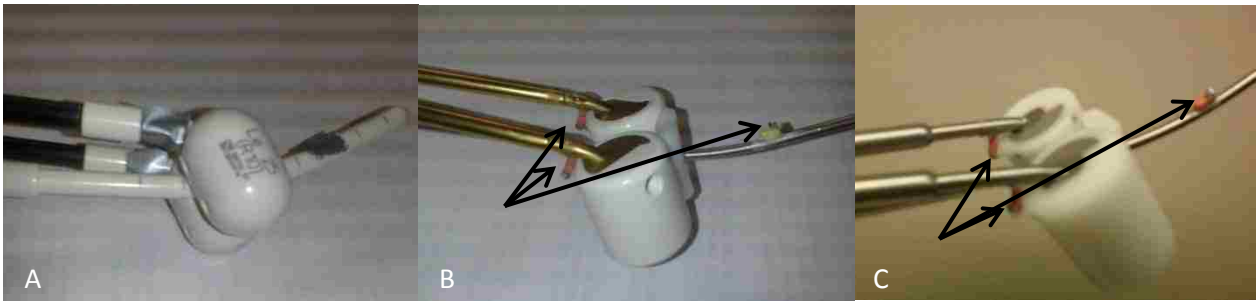

Figure 2-4: Attachment of fiducial markers to the tandem and ovoids for (A) the CT/MR compatible applicator (markers attached with duct tape), (B) the Fletcher-Williamson applicator and (C) the Fletcher-Suit-Delclos-style applicator. The spacers can be seen on both the FW and FSDs applicators moving the markers outside of the regions containing image obscuring artifact. Arrows designate ovoid catheter markers with wooden spacers.

2.1.2 Water Phantom Constituents: Bladder and Rectum Surrogate Structures

Surrogate anatomic structures were developed with realistic size (diameter and volume), shape and positioning relative to the T&O applicator. Multiple patient CT scans were gleaned from the MBPCC database and analyzed to develop the general geometry typical of OARs (bladder, rectum and sigmoid colon) encountered clinically.

2.1.2.1 Development of Bladder and Rectum Surrogate Structures

First-generation surrogate patient rectums and bladders were composed of iodinated contrast/saline filled latex material deformed into irregular shapes using duct tape (see Figure 2.5). These structures could be filled to known volumes facilitating the comparison between actual and TPS-

generated volumes. To secure the structures within the phantom water tank, the rectum structures were attached via duct tape and the bladder was mounted on a rod suspended superior to the assembled applicator and surrogate rectum. The lack of rigidity of these structures proved problematic as motion of water within the tank during scanning induced surrogate structure motion, hindering the acquisition of reproducible image sets. Further details regarding the development of the first generation phantom are included in Appendix A.

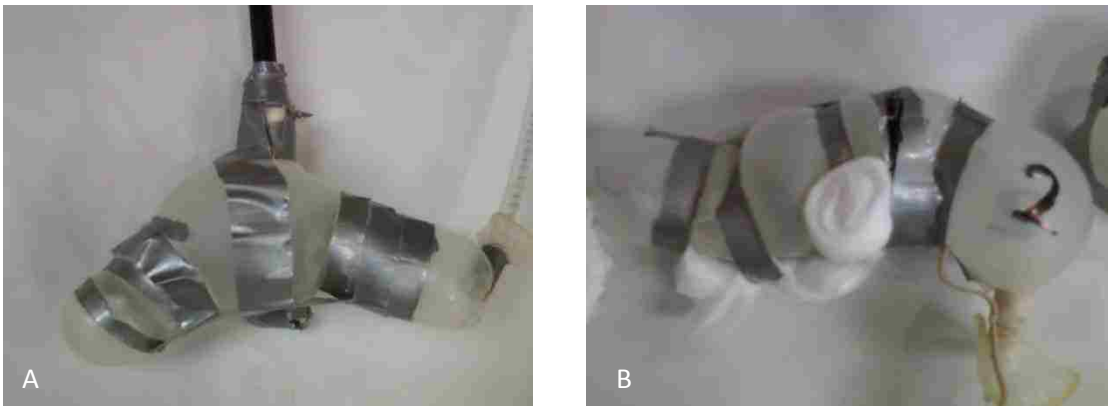

Figure 2-5: Initial attempts at constructing surrogate patient bladder (A) and rectum (B)

2.1.2.2 Aquaplast Bladder and Rectum Surrogates

A rigid substitute with a physical density similar to bladder and rectal tissue was needed to overcome the problem of surrogate structure motion. Aquaplast was chosen for two main reasons: rigidity at room temperature and a physical density (ρ=1.08 g/cm^3) (RPD, 2011) similar to bladder and rectal tissues (1.04 g/cm^3) (Awschalom, 1983). Typically, aquaplast is used as surface bolus in the clinic for areas of irregular surfaces due to its (a) malleability and (b) rigidity at room temperature. Bladder and rectum surrogate structures were made by molding heated aquaplast around the first generation structures described in Section 2.1.2.1 (see Figure 2-6 and Figure 2-7).

The process of molding the aquaplast resulted in variations of wall thickness, typical of variations seen in patient anatomy. The minimum wall thickness was about 0.5 mm. A re-sealable cap was fitted to each structure to allow for partial filling with water and air to mimic expected organ content. Four rectums and two bladders were constructed. A pseudo urethra was added to the bladder

in order to secure the bladder structure to the water tank via a mounted rod and thereby prevent motion of the bladder structure during CT scans. For each structure, laser/ovoid alignment markings were placed on the structure to ensure a reproducible setup for 3D image acquisition (see Figure 2-8).

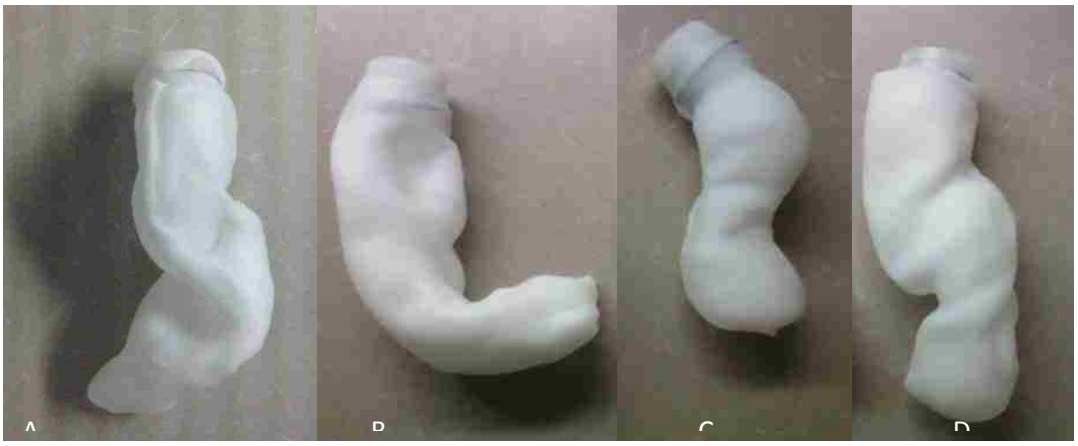

Figure 2-6: Second-generation aquaplast rectum surrogate structures. (A) Test surrogate rectum, (B) surrogate rectum-1, (C) surrogate rectum-2 and (D) surrogate rectum-3.

Figure 2-7: Second-generation aquaplast bladder surrogate structures. (A) Test surrogate bladder and (B) surrogate bladder used for all image sets containing a T&O applicator.

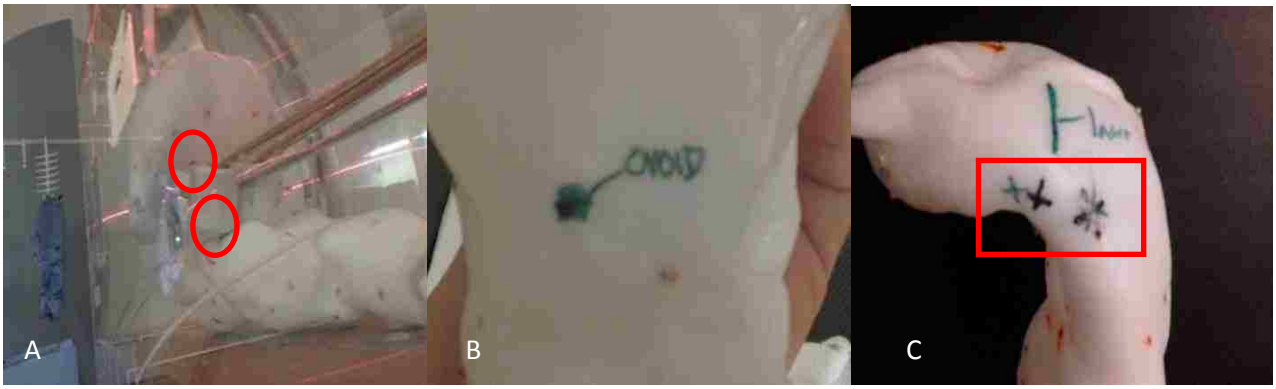

Figure 2-8: Laser/ovoid alignment markings added to the bladder and rectum surrogate structure. (A) The applicator in the water phantom aligned to the bladder and rectum surrogate structures (bladder and rectum ovoid alignment markings outlined in red), (B) Bladder ovoid marking and (C) Rectum ovoid markings (outlined in red) with green marks for shielded applicators and black for the CTMR applicator.

One bladder and one rectum were used solely as “pre-test” structures to validate the ability of participants to use the Oncentra TPS organ segmentation tools. The three remaining rectum surrogate structures and bladder, combined with the three different applicators, yielded nine different image sets for organ segmentation and catheter reconstruction for each imaging modality.

The physical volume of each structure was measured via water displacement to facilitate volume comparisons between measured and segmented volumes. Volumes were measured via displacing a structure in a large, water-filled beaker and, upon removing the structure, re-filling the beaker to the same water level using a graduated cylinder with +/-0.4 ml accuracy (see Figure 2-9). The measured values are included in Table 2-1. The volumes of the test rectum and bladder structures are 189 ±0.8 ml and 300 ±1 ml respectively. The measured volumes of rectum-1, rectum-2, rectum-3, and the main phantom bladder are 160 ±0.8 ml, 125 ±0.7 ml, 184 ±0.8 ml and 265 ±1 ml, respectively.

Figure 2-9: Organ surrogate volume measurements via water displacement. (A) Submersion of surrogate rectum structure, water level is recorded from a ruler. (B) Water is added using the graduate cylinder to the same level displaced by the surrogate rectum structure.

Table 2-1: Bladder and rectum surrogate structure control volumes determined via water displacement.

Bladder and Rectum Surrogate Structure Measured Volumes					
Test Structures		**Main Structures**			
Bladder	**Rectum**	**Bladder**	**Rectum-1**	**Rectum-2**	**Rectum-3**
300 ±1 ml	189 ±0.8 ml	265 ±1 ml	160 ±0.8 ml	125 ±0.7 ml	184 ±0.8 ml

2.1.2.3 Bladder and Rectum Surrogate Structure Fiducial Markers

To facilitate the 2D organ segmentation stated in aim 3, fiducial markers were added to all surrogate bladder and rectum structures except for the test set. Fiducial markers facilitate the

determination of an axial cross section of each surrogate organ capable of being localized for kV and MV image sets. Three sets of three fiducial markers were embedded in each rectal structure wall: (1) superior to the ovoid region, (2) directly posterior to the ovoids (same axial CT slice) and (3) inferior to the ovoids. Similarly, for the bladder, there were also three sets of three fiducial markers embedded into each bladder structure wall: (1) to the left lateral of the ovoids, (2) directly anterior to the ovoids and (3) to the right lateral of the ovoids.

Fiducial markers capable of being visually present on both kV and MV image sets without introducing metal artifact into kVCT data sets were needed. Clinical fiducial markers used with kVCT were nearly indiscernible on MV image sets. A variety of high Z objects with various sizes were tested (different paper clips and pushpins mainly) and it was determined that suitable fiducial markers could be obtained by cutting a typical pushpin (diameter =1 mm) into ≈1.25 mm lengths. To improve their visibility on MVCT scans, a second marker was placed superior to previously attached markers. The end product yielded sufficient visibility on both kVCT and MVCT data sets (see Figure 2-10).

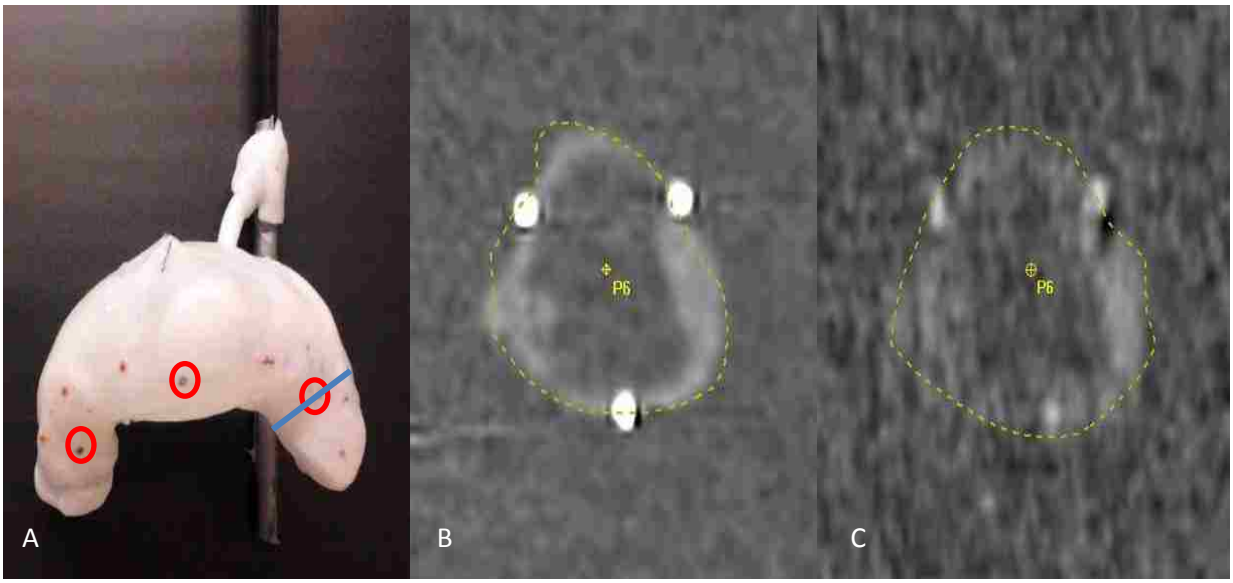

Figure 2-10: Examples of the surrogate structure fiducial markers. (A) Fiducial markers attached to the outer surface of the bladder surrogate structure (encircled in red). The blue line represents the plane from which images (B) and (C) were acquired. KVCT (B) and MVCT (C) scans in the ECS view of the bladder for the sets of markers depicted by the blue line in (A).

It was assured that one set of fiducial markers for each structure lay within the artifact region. The artifact region is defined as the region of slices containing metal artifact due to ovoid shielding (see Figure 2-11). The fiducial markers were placed on each rectum such that one set of markers would be located in the artifact region.

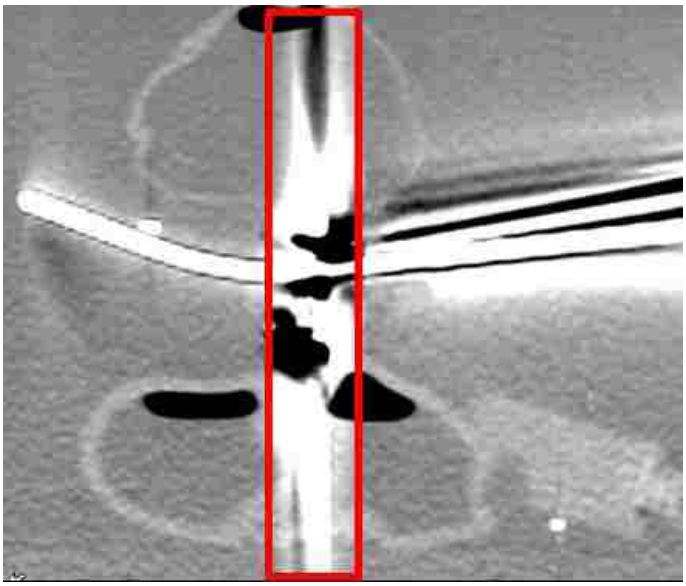

Figure 2-11: Sagittal kVCT slice of the FW applicator demonstrating the "artifact region" of each applicator.

2.1.3 Phantom Alignment

Reproducible phantom alignment was critical for accurate comparisons of kVCT and MVCT image sets for each bladder/rectum arrangement. The process for phantom alignment was:

1. First, the water tank was aligned with the CT coordinate system. To accomplish this, the water tank was squared with the CT patient table using a rigid table attachment utilized for patient immobilization. Two slabs of SolidWater® (Gammex RMI, Middleton, WI) were then placed within the phantom water tank and immobilized in the right superior corner using plastic spacers (see Figure 2-12). Using markings on the SolidWater®, the phantom was aligned laterally with the overhead CT lasers (see Figure 2-12). Water was then filled to markings on the tank that placed the water level ≈2cm above the anterior portion of the phantom bladder.

Figure 2-12: Overhead view of the Solidwater®/CT laser alignment. A black, plastic spacer (in red box) was used to immobilize the SolidWater® within the water tank.

2. Next, the rectum was immobilized atop the solid water using rubber bands and aligned laterally with the overhead CT lasers (see Figure 2-13). Alignment in the superior/ inferior direction was accomplished in the following step.

Figure 2-13: Surrogate rectum structure alignment. The structure was attached to the Solidwater® using rubber bands and then aligned laterally with the overhead CT lasers.

3. One of the three T&O applicators investigated was then attached to the clinical applicator mount and aligned with the rectum via the ovoid alignment marks in the posterior ovoid caps touching the rectum (see Figure 2-15). The tandem tube was aligned with the overhead CT lasers (see Figure 2-14). This alignment procedure also facilitated the superior/inferior rectum alignment within the water tank, being based off of the T&O applicator positioning within the water tank.

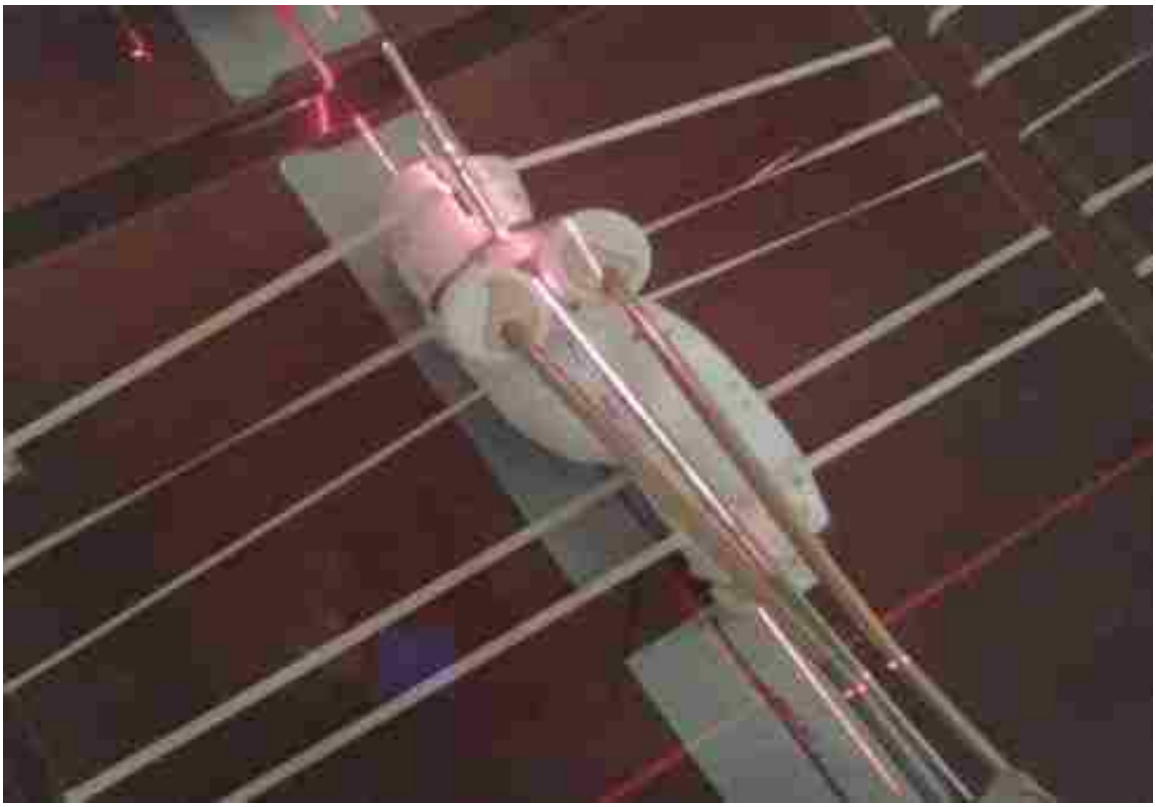

Figure 2-14: Overhead view of T&O applicator alignment with surrogate rectum structure. The T&O applicator was aligned with the overhead CT laser.

4. The bladder was then immobilized in the water tank via a rod and mount, and aligned via ovoid alignment markings that resulted in the anterior portion of the ovoid caps touching the bladder (see Figure 2-8and Figure 2-15). The anterior side of the bladder was simultaneously aligned with the overhead CT lasers (see Figure 2-16).

Figure 2-15: Ovoid contact with the bladder and rectum ovoid alignment markings.

Figure 2-16: Surrogate bladder structure alignment with the overhead CT lasers. Note: a difference in the internal and external overhead CT lasers is seen in this figure. To avoid problems with alignment mismatch between the internal and external CT lasers, all parts of the phantom were aligned to the internal CT lasers.

A lateral view of the completed phantom can be seen in Figure 2-17. It is worth noting that the relative spatial locations of the bladder, rectum and applicator are not typically this close in patients. However, this setup resembles a “worst case scenario” encountered clinically when poor or lack of vaginal packing provides insufficient bladder and rectal wall displacement. It also aids in achieving a reproducible setup via ovoid/structure alignment markings. The setup also should result in the largest adverse effects to the results of organ segmentation and catheter reconstruction due to metal artifacts.

Figure 2-17: Water phantom assembled for scanning on the TomoTherapy Hi-Art II MVCT scanner. This image also shows the bladder attachment arm and the applicator mount.

2.1.4 Image Acquisition: kVCT versus MVCT

kVCT image sets were acquired using a GE Lightspeed RT 16 CT scanner (General Electric Medical Systems, Fairfield, CT). The MBPCC gynecological ICBT HDR treatment imaging protocol was followed. The MVCT image sets acquired using the TomoTherapy Hi-Art II MVCT scanner (TomoTherapy, Madison, WI) with parameters set as close to the kVCT parameters as allowed by the Hi-Art system other than energy. The imaging parameters used in this study are tabulated in Table 2-2.

Table 2-2: Imaging parameters for both the kV and MV imaging modalities used in this study.

Kilovoltage CT (GE Lightspeed 16RT)		**Megavoltage CT (TomoTherapy Hi-Art)**	
kVp	120	E(MV)	3.5
Slice Thickness (mm)	1.25	Slice Thickness (mm)	2 (minimum)
SFOV (cm)	50	SFOV (cm)	40
Pixel Size (mm^2)	0.976 x 0.976	Pixel Size (mm^2)	0.76 x 0.76
Voxel Size (mm^3)	1.19	Voxel Size (mm^3)	1.16
Image Size	512 x 512	Image Size	512 x 512

2.2 Aim 2. Participant Organ Segmentation and Catheter Reconstruction

2.2.1 Physicist and Physician Participation

Seven physicists and two physicians from multiple institutions participated in this study. Institutions included MBPCC (Baton Rouge, LA), the University of Texas MD Anderson Cancer Center (Houston, TX), the University of Texas Medical Branch at Galveston (Galveston, TX), and the University of North Carolina School of Medicine (Chapel Hill, NC). Each participant was proficient with the Oncentra Brachy TPS for planning cervical ICBT T&O treatments. A variety of questions were asked of the participants to ascertain their skill with organ segmentation and catheter reconstruction. As shown in Table 2-3, there were no specific qualifications for participating in the study other than (a) working currently as a clinical medical physicist/physician and (b) familiarity with the Oncentra Brachy TPS. Experience as a medical physicist/physician ranged from 1-17 years (this does not indicate an equivalent number of years of experience with ICBT). It was not clinical practice for all participants to segment the bladder and rectum structures; some clinics rely on dose calculations using the ICRU 38-defined bladder and rectum points. Regarding experience with planning of patient cases with shielded T&O applicators, "infrequent" refers to any time period longer than three months between shielded T&O insertion plans.

Each participant was provided with seven image sets, including one pre-test image set, which was the same for all participants. The primary purpose of the pre-test image set was to confirm the familiarity of the participant to perform organ segmentation using Oncentra Brachy's TPS. All resulting reconstructed volumes were within ±17.5cc of known volumes. The remaining six image sets were comprised of kV and MV image sets for each applicator with various combinations of rectum structures with the bladder structure. Image set assignments were made randomly to prevent participant bias towards a given modality or method of segmentation/catheter reconstruction. The image set assignments are shown in Table 2-4.

Table 2-3: Participant experience prior to participation in the study.

Participant Experience									
	Physicist 1	Physicist 2	Physicist 3	Physicist 4	Physicist 5	Physicist 6	Physicist 7	Physician 1	Physician 2
Years in Clinic?	17	4	12	9	3	8	8.5	2	2
Board Certified? (Y/N)	yes	yes	yes	yes	no, 1&2	yes	yes	no	no
# of ICBT Insertions Planned (6 months)	4	10	24	5	1	1	2	5	10
Clinical Practice to Segment Bladder/Rectum?	no	yes	yes	yes	yes	yes	yes	yes	yes
Experience Planning Shielded T&O Insertions?	yes	no	yes	no	no	yes	yes	yes	yes
If so, with what frequency?	infrequent	N/A	infrequent	N/A	N/A	infrequent	infrequent	infrequent	infrequent

Table 2-4: Participant image set assignment. Every third participant has the same image sets however each participant's image sets were individually randomized to help eliminate bias towards certain applicators or imaging modalities.

Physicist 1	Physicist 2	Physicist 3	Physicist 4	Physicist 5	Physicist 6	Physicist 7	Physician 1	Physician 2
Test	Test	Test	Test	Test	Test	Test	Test	Test
CTMR kV 2	FSDs kV 1	FSDs kV 2	FSDs MV 1	CTMR MV 3	FW kV 1	FSDs MV 1	CTMR kV 1	CTMR MV 1
CTMR MV 3	CTMR kV 2	FW kV 1	CTMR MV 2	FW kV 3	FW MV 2	FW kV 2	FSDs kV 3	FW MV 2
FW MV 1	FSDs MV 2	FW MV 2	CTMR kV 1	FSDs MV 2	FSDs MV 3	FW MV 3	FW kV 2	FW kV 1
FSDs MV 2	FW MV 1	FSDs MV 3	FSDs kV 3	CTMR kV 2	FSDs kV 2	FSDs kV 3	FSDs MV 1	CTMR kV 3
FSDs kV 1	CTMR MV 3	CTMR MV 1	FW kV 2	FSDs kV 1	CTMR kV 3	CTMR kV 1	FW MV 3	FSDs MV 3
FW kV 3	FW kV 3	CTMR kV 3	FW MV 3	FW MV 1	CTMR MV 1	CTMR MV 2	CTMR MV 2	FSDs kV 2

2.2.2 Participant Instructions

Participants were provided with detailed instructions serving four main purposes: 1) provide each participant with a general overview of the study and their role therein, 2) give basic TPS setup guidelines (Lanczos Window smoothing, region of interest (ROI) voxel size, etc.), 3) provide clarification regarding organ segmentation and catheter reconstruction for phantom structures (how to contour the bladder with the attachment arm present in multiple slices) and 4) give detailed DICOM export instructions. A copy of the instruction is included in Appendix B.

2.2.3 Organ Segmentation

Participants were asked to perform organ segmentation for both the bladder and rectum surrogate structures in each of the seven image sets assigned. Instructions were provided regarding caveats due to phantom construction such as the surrogate structure mounting hardware as well as the extents to which the surrogate structures should be segmented. Participants were instructed to use their best judgment to contour as if fiducial markers were not present.

2.2.4 Catheter Reconstruction

Following clinical protocol, the participant performed catheter reconstruction on the six image sets containing a T&O applicator. For the CTMR compatible applicator, participants choose source dwell positions utilizing source position markers for guidance, as these markers are used clinically to simulate the location of the source dwell positions during treatment.

For the shielded applicators, participants were instructed to define the distal-most source dwell position 7 mm inferior to the applicator tube tip. This method is used due to the inability to visualize source position markers on CT data sets acquired of shielded T&O applicators. As mentioned previously (see Section 1.3.1), the stainless steel catheter tubes and tungsten/stainless steel ovoid shields introduce image obscuring artifact into CT data sets, preventing the physicists or physicians from visualizing source position markers.

2.2.5 Catheter Reconstruction with Nucletron's Applicator Modeling

Catheter reconstruction was performed by the investigator utilizing Nucletron's Applicator Modeling plugin (AMp) for both of the Nucletron applicators: the CTMR and the FW. The AMp utilizes a 3D digital reconstruction of an applicator, with correct dimensions and shape, to aid in catheter reconstruction for cases where applicator localization cannot otherwise be determined (see Figure 2-18).

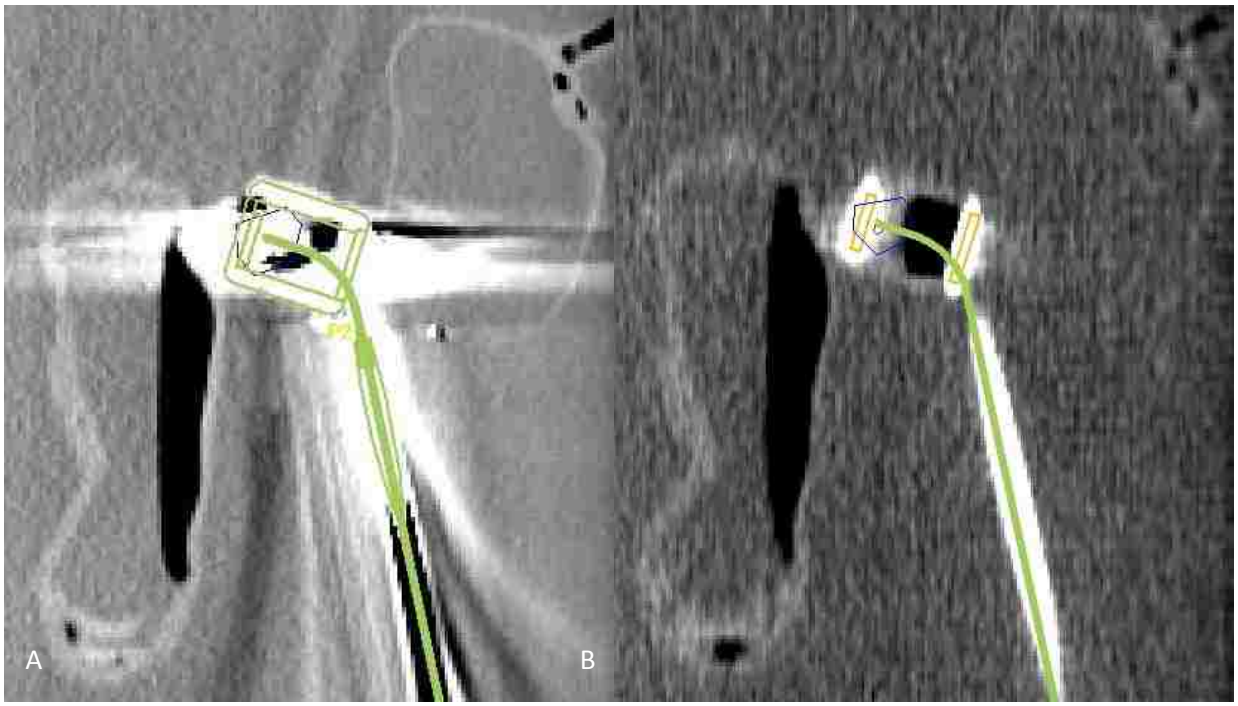

Figure 2-18: Visual example of AMp catheter reconstruction in the presence of CT metal artifact in (A) kVCT and (B) MVCT data sets.

The AMp digital model position and orientation can be adjusted via rigid translation and rotation as well as non-rigid deformation (see Figure 2-19). However, in this study only rigid transformations were utilized. Twelve treatment plans were generated using the AMp—six for the CTMR applicator and six for the FW applicator which included a plan for each bladder/rectum combination.

The accuracy of the AMp was determined by comparing the distance between the applicator reference marker and the AMp-defined distal-most dwell position with the same measure obtained via radiograph—the control measures (discussed in further detail in Section 2.3.2).

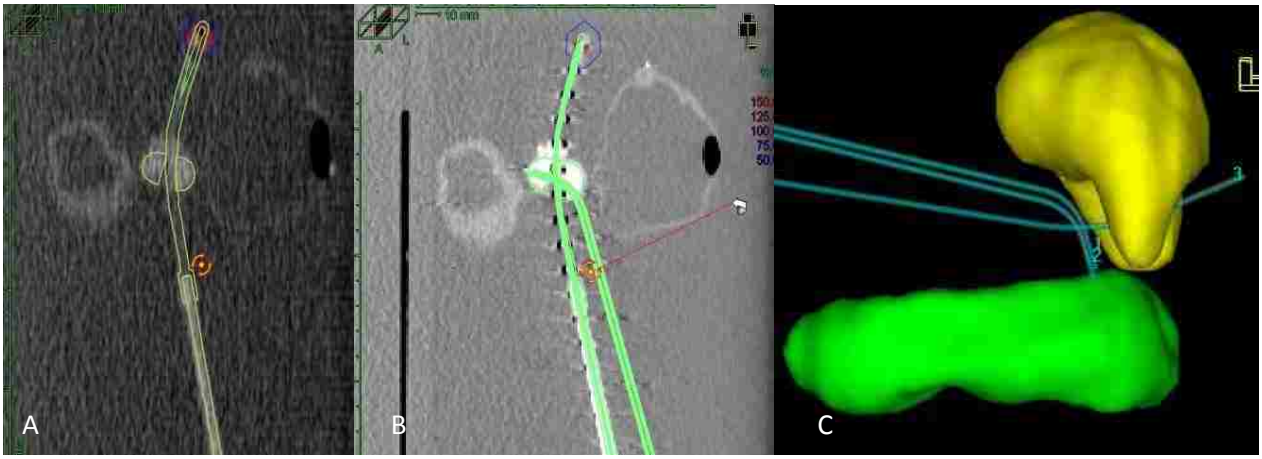

Figure 2-19: Application of the Applicator Modeling plugin (AMp). (A) Catheter manipulation of the tandem tube as it is being manipulated while the ovoid tubes remain in place. (B) Manipulation of the entire applicator. All tubes are being rotated around a central pivot point (red circle is pivot point). (C) A completed model in place within the water phantom (yellow is the bladder structure and green is the rectum structure).

2.3 Aim 3. Organ Segmentation and Catheter Reconstruction Analysis

2.3.1 Organ Segmentation Comparison: Two- and Three-dimensional Methods

Two-dimensional CTP measurements and three-dimensional volume comparisons were used to quantify the accuracy of organ segmentation. The methods discussed in the following sections were derived from methodologies presented in the literature and have been shown to be reliable for assessing and quantifying the quality of organ segmentation (Jameson, et al., 2010).

2.3.1.1 Two-dimensional CTP Analysis

The following procedure was followed for two-dimensional analysis of the organ segmentation accuracy:

1. The centroid was found for each set of fiducial markers on each rectum and bladder structure (three sets of three markers per structure). For rectum structures, this produced one centroid point superior to the artifact region, one within the artifact region and one inferior to the artifact region. For the bladder structure, due to the plane within which measurements were made (coronal, sagittal or extra coordinate system (ECS)), all slices used for measurement had at least one measure for which artifact could be an influencing factor.

The process for finding the centroid is as follows:

a. Using the ECS within Oncentra, a reconstructed CT slice was dervied in which all three fiducial markers of a given set were visible (see Section 2.1.2.3). This was accomplished by centering the ECS coordinate system on a fiducial marker (see Figure 2-20 A) and then manipulating the other two planes until the axes were visually centered through each of the other two markers in all three planes. (see Figure 2-20 B).

b. With all three markers present in the derived slice, Oncentra Brachy's "distance" tool was used to construct lines between each fiducial marker creating a triangle. The geometric center or centroid was then found by marking the intersection of the triangles medians, which are the lines joining each vertex (fiducial marker) with the midpoint of the opposite side (see Figure 2-20 C).

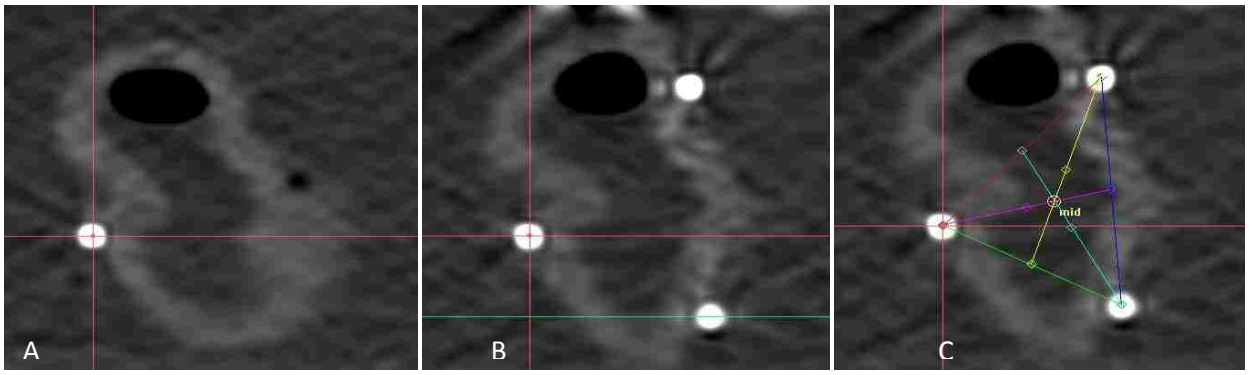

Figure 2-20: Method for determining the centroid of each set of fiducial markers. (A) Find a CT slice with one of the markers and center the ECS coordinate system in that point. (B) Manipulate the ECS coordinate system until the centers of all points are visible in the same slice. (C) Draw the medians of the triangle. The point where the three medians intersect is the centroid.

c. Using the "point" tool, a point was placed at the intersection of the medians, which is, by definition, the centroid of the three fiducial markers.

d. The process was repeated for each set of three fiducial markers (three sets of three markers on each bladder and rectum structure) in each image set.

2. To perform distance measurements, the "Distance and Angle" tool was used. The Distance and Angle tool reports the lengths of two lines with a common endpoint and calculates the

angle between those two lines (see Figure 2-21). To use the "Distance and Angle" tool, a line is extended to a point (in this case the centroid), the point is selected by clicking the mouse and then another line may be extended from that point. The "Distance and Angle" tool then displays the length of each line, the angle between the two lines and the total length of both lines. Clinical testing of the beta version of the Distance and Angle tool by Dr. Michael Price at MD Anderson Cancer Center showed the tool to have an accuracy of ±0.5 mm (Price, 2007).

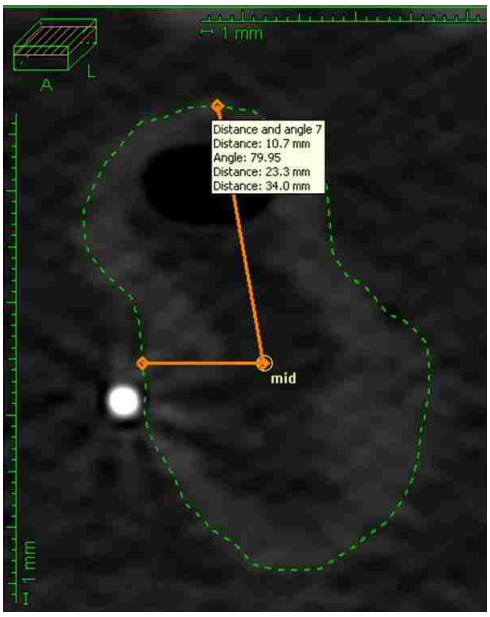

Figure 2-21: Example of use of Oncentra's "Distance and Angle" tool on an axial CT slice of a surrogate rectum structure.

a. First, a slice was found containing the centroid (see Figure 2-22). For all rectum structures, all but one centroid was found in the axial slice. The other slice was found in the ECS coordinate system. For the bladder structure, the right lateral point was found in the coronal plane, the midpoint was found in the sagittal plane, and the left lateral point was found in the ECS view. The ECS view was only utilized when the three standard views failed to provide consistent images. (see Figure 2-23). When utilizing

the ECS, prior to each measurement, the coordinate system was squared with the water tank to minimize errors in using a non-rigid coordinate system.

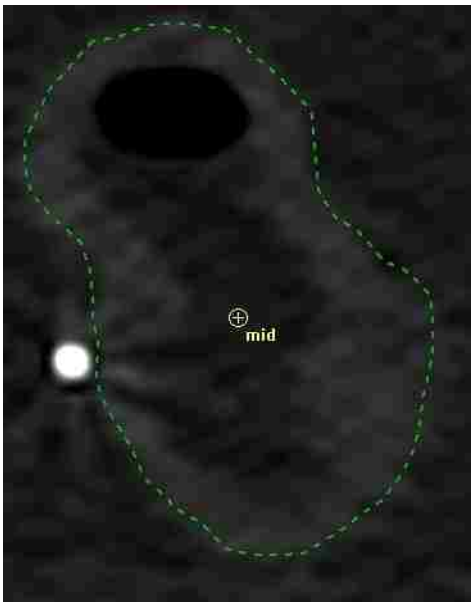

Figure 2-22: Axial CT slice of a surrogate rectum containing the centroid. This is an example of the slices used for two-dimensional CTP distances discussed in this section.

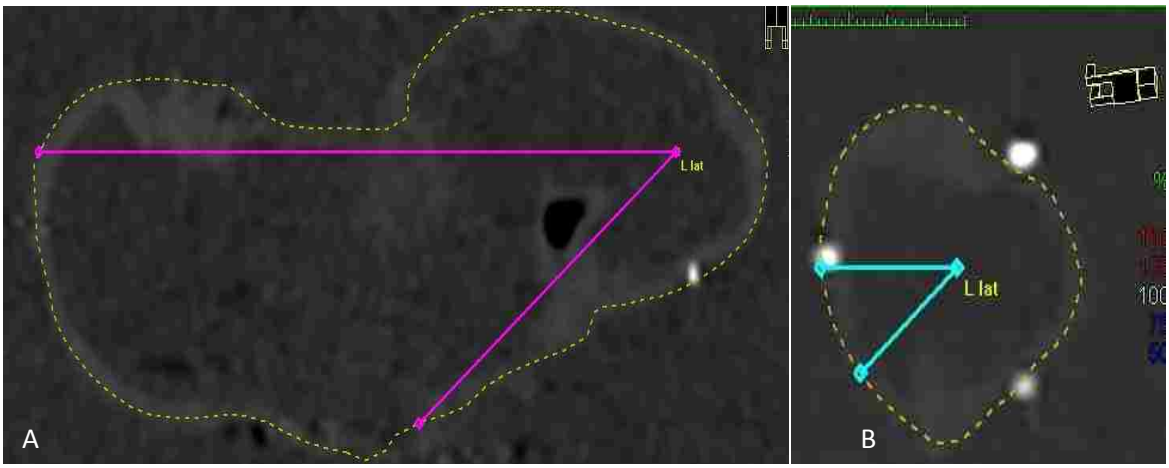

Figure 2-23: Comparison of CTP distance measurements for the surrogate bladder structure in (A) the coronal view and (B) the ECS view. Zoom settings were the same for each image.

b. In a slice containing the centroid, a horizontal line was drawn from the left extending to the centroid and then another line was extended from the centroid back out to the participant-defined segmentation perimeter. Distances were recorded for angles of 0, 40, 80, 120, 160, 200, 240, 280 and 320 degrees as shown

in Figure 2-24 A and B. Measurements were recorded and compared to control values obtained via from scans of the surrogates in air. The differences were called CTP-diff. Phantom scans in air, rather than in water, were used to determine control values because of the sharp air/aquaplast border (see Figure 2-24)

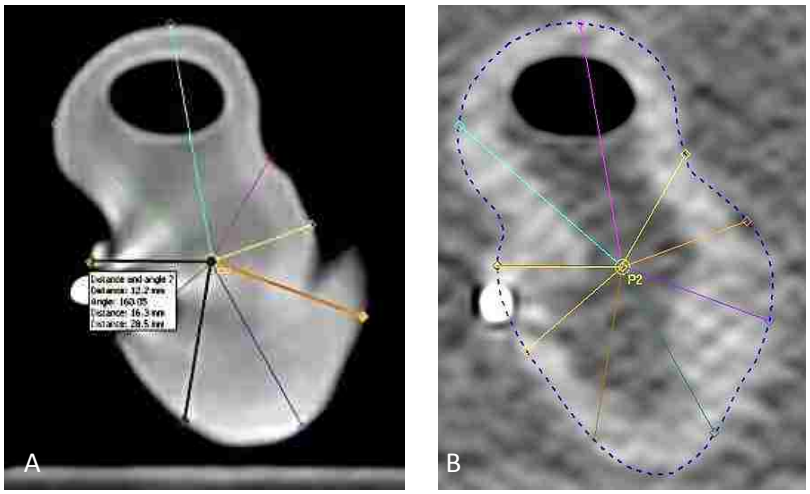

Figure 2-24: Images showing the method for making 2D organ segmentation measurements for (A) the phantom scans in air and (B) the participant-defined organ segmentation. The small box seen in (A) shows how the "distance and angle" tool reports angle. The window and level values for both images are 500 and 1, respectively.

For two-dimensional CTP analysis, the systematic error was dependent upon the ROI pixel size of 2.0 x 2.0 mm^2 defined within the TPS. Because the pixel size was larger than the kV and MV pixels, the uncertainty for such measurements is independent of imaging modality. For any point chosen within Oncentra, whether OAR contours or prescription points, the TPS treats those points as if they were placed in the center of the corresponding ROI. This yields a maximum deviance from the true value of ½ the diagonal of the pixel or in the case of a 2.0 x 2.0 mm^2 pixel size, ±1.4 mm. This difference must be accounted for both at the centroid and at the perimeter. Incorporating the uncertainty of the "Distance and Angle" tool (±0.5 mm) results in an overall systematic uncertainty of±2.0 mm. Because both the control values and measured values were determined within the TPS, the systematic uncertainty is the same for both.

2.3.1.2 Three-dimensional Reconstructed Volume Analysis

The accuracy of participant organ segmentation was also quantified by the difference between the control and TPS-reconstructed volumes (VOL-diff) (see Figure 2-25). The control volumes were determined by displacement (see 2.1.2.1). Within the treatment planning system, each participant segmented the bladder and rectum for each image set following the participant instructions (see Section 2.2.2) as well as clinical practice. Upon completing the organ segmentation, the TPS displays the volume (in cc) of the reconstructed volume which was used for comparison against the control volumes.

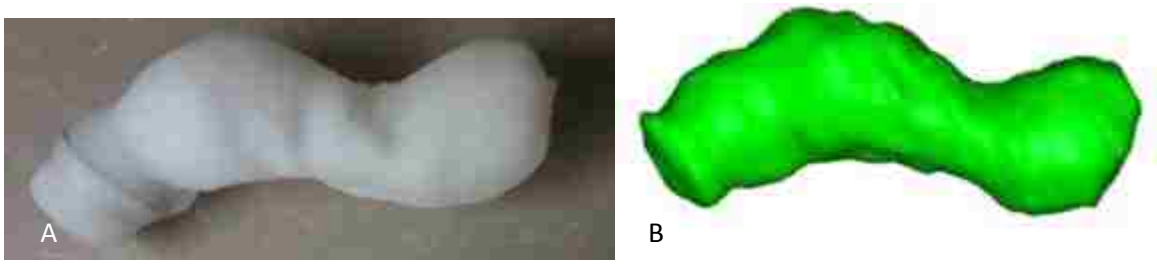

Figure 2-25: (A) Rectum surrogate structure control volume and (B) participant-TPS generated rectum surrogate structure based on participant segmentation

The supposed manufacturer-reported systematic uncertainty of the treatment planning system is ±1 voxel for segmented OARs. This appeared questionable due to the variations in structure volumes (125 ml-265 ml) and the dependence of structure volume on the voxels it contains (if ½ or more of a voxel is within a contour line, the voxel is counted towards the entire structure volume). A method was devised to determine the expected variation between control volumes (determined via water displacement) and TPS reconstructed volumes. Utilizing the Oncentra "Magic Wand" tool which generates OAR contours based on pixel value rather than user approximation, the bladder and rectum structures were segmented on the kVCT phantom scans in air (with a high-contrast aquaplast/air border). The uncertainty in measurements was then determined by comparing the volumes of the phantom scans in air with the actual structure volumes, yielding a difference which we used as the

systematic uncertainty. Each structure volume was measured three times for both control volumes and air volumes. The results of these measurements can be seen in Table 2-5.

Table 2-5: Comparison of control volumes determined via phantom scans in air as well as via water displacement. These results were used to determine the systematic uncertainty of the treatment planning system.

VOL-diff Comparisons: Systematic Error Analysis –Phantom Scan in Air vs. Control Volumes						
		Volume (cc)			**Difference**	
Bladder	**air**	245.8	±	0.2	**Absolute**	17.7
	control	263.5	±	2.7	**Percent**	7%
Rectum 1	**air**	139.3	±	0.5	**Absolute**	21.0
	control	160.3	±	0.5	**Percent**	14%
Rectum 2	**air**	109.2	±	0.2	**Absolute**	16.1
	control	125.3	±	0.5	**Percent**	14%
Rectum 3	**air**	154.7	±	0.4	**Absolute**	29.6
	control	184.3	±	0.5	**Percent**	17%

Within Table 2-5, a marked difference between the bladder and rectum structures percent difference is observed. The rectum structures had a mean percent difference of 15% whereas the bladder percent difference was only 7%. It is proposed by the investigator that this is due to the difference in the overall segmented perimeters for axial slices of the bladder and rectum structures. Whereas the rectum structures had a smaller diameter (≈2-5cm) and extended over a larger range of slices (100-121 slices), the bladder had a larger volume for a smaller range of slices (volume of 263 cc for only 60 slices). To illustrate the effect this could have an example is given. For any given slice, you can have two structures with the same area—one similar to a square (bladder) and one similar to a rectangle (rectum). The square-like shape will have a smaller perimeter than the rectangular-shaped object, meaning it has fewer pixels around its border, resulting in less overall systematic error represented in the rectangular-shaped object (bladder). It seems this would explain the reason for a 7% difference between the air and control volumes for the bladder structure when the rectum structures

averaged a 15% difference. Due to these differences, it is proposed that the systematic uncertainty for each individual structure should be reported and a mean value not be taken.

2.3.2 Three Dimensional Catheter Reconstruction Analysis

Each participant in this study performed catheter reconstruction for the six image sets containing T&O applicators. For the CTMR applicator, dwell positions were based off source dwell position markers, which represent actual source dwell locations. For the shielded FW and FSDs applicators, the participants were instructed to define the distal-most source dwell position 7 mm inferior to the applicator tube tip. This method is used due to the applicator tubes being constructed of stainless steel which inhibits source position marker visualization, most notably in regions of strong artifacts caused by the ovoid shields.

To determine the accuracy of catheter reconstruction, a distance measurement from the distal-most dwell position to the applicator reference marker—marker-to-dwell difference or MD-diff, was used for comparison. Control values were obtained by radiographing each applicator ovoid and tandem tube separately and measuring the distance between the center of the distal-most, procedurally-defined dwell position and the closest point of the applicator reference marker (see Figure 2-26). Distances were measured 10 times with IP65 SPi digital calipers with reported ±0.02 mm accuracy. Measured values are reported in Table 2-6.

Table 2-6: Distances from the distal dwell position to applicator fiducial markers for the respective applicators.

Distal Dwell-to-Applicator Reference Marker Distance	CTMR	FW	FSDs
Tandem (mm)	23.03±0.20	23.57±0.23	23.70±0.17
Right Ovoid (mm)	23.47±0.18	21.66±0.25	25.11±0.23
Left Ovoid (mm)	20.71±0.19	21.88±0.17	24.44±0.18

To perform distance measurements within the TPS, *x, y* and *z* coordinates for the distal dwell positions and applicator reference markers were utilized. To localize the applicator reference marker, a TPS point was placed in the general region of the marker. Then, utilizing axial, coronal and sagittal views, the point was moved to the part of the reference marker closest to the dwell position in each view (see Figure 2-26).

The systematic uncertainty for the control measures was based off the uncertainty of the IP65 SPi calipers used (±0.02 mm) (see Figure 2-26(A)). To determine the uncertainty in TPS measured values, voxel size must be accounted for. As mentioned in Section 2.3.1.1, Oncentra's TPS measurements are based off the center of pixels and voxels. For a comparison of 3D points, the furthest a point could differ and still be associated with a given voxel is half the diagonal from the center of the voxel, which is 0.9 mm for kV and 1.1 mm for MV. This error must be accounted for in both the dwell position and the applicator reference marker point yielding a final systematic uncertainty of ±1.3 mm and ±1.6 mm for kV and MV imaging, respectively.

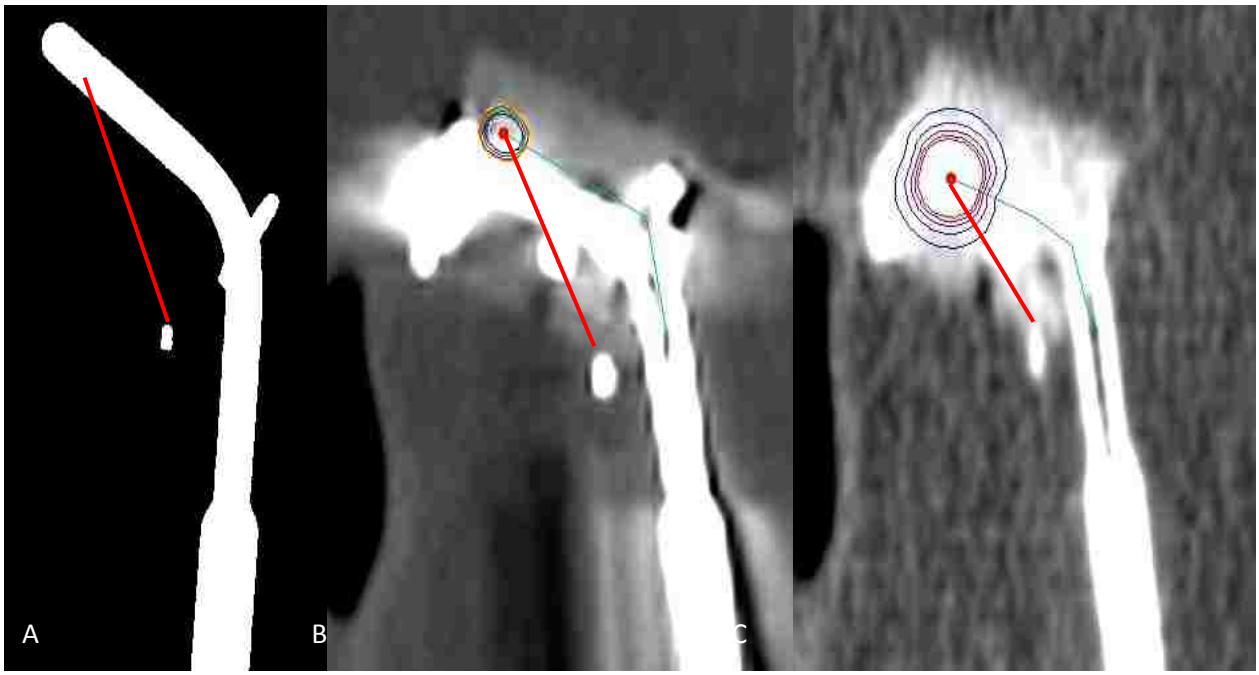

Figure 2-26: Method of determining the accuracy of the participant-defined source dwell position. (A) Scan of the radiograph from which control distances were measured. (B) kVCT and (C) MVCT of the left ovoid for the FSDs applicator.

2.4 Statistical Tests

A number of statistical tests were conducted to determine if the variables CTP-diff, VOL-diff, and MD-diff obtained from MV imaging differed significantly from the same variables obtained from kV imaging. A two-proportion t-test was used to determine if the percent of observations meeting the hypothesis criteria within MVCT data sets differed significantly from the percent of observations meeting the hypothesis criteria within kVCT data sets. A paired t-test was used to determine if mean values differed significantly between MV and kV imaging for two- and three-dimensional organ segmentation comparisons. An unpaired t-test was used to determine if participant-defined catheter reconstruction differed significantly between CTMR kVCT data sets and shielded applicator MVCT data sets. A paired, t-test was used to validate the Nucletron AMp (compared with results obtained following current, clinical procedure).

Though no Gaussian curve fitting was performed for this data it was determined that results sufficiently represented a normal distribution and that the number of degrees of freedom would be sufficient to determine statistical significance. Results with a p-value less than 0.05 were determined to be statistically significant. Microsoft Excel was used for all statistical analysis. Inherent capabilities for comparing means were utilized for the student t-tests.

Two-proportion t-test results were calculated as follows:

1. The pooled sample proportion was calculated,

$$\mathrm{p} = \frac{p_1 n_1 + p_2 n_2}{n_1 + n_2}$$

where p is the pooled sample proportion, p_1 is the proportion of points meeting the specified criteria from data set 1, p_2 is the proportion of points meeting the specified criteria from data set 2, n_1 is the sample size for data set 1 and n_2 is the sample size for data set 2.

2. Next, the standard error (SE) was calculated using the pooled sample proportion and sample sizes:

$$SE = \sqrt{p * (1 - p) * \left[\frac{1}{n_1} + \frac{1}{n_2}\right]}$$

3. Utilizing the standard error and proportion results for data sets 1 and 2, a t-value was obtained which was used as input for a t-distribution table to obtain a probability or p-value:

$$t = (p_1 - p_2)/SE$$

Chapter 3 Results and Discussion

3.1 Aim 1: Water Phantom Development

Figure 3-1: Completed water phantom setup for scanning on GE's Lightspeed RT kVCT scanner.

KV and MV image sets were acquired of all three T&O applicators in the water phantom shown in Figure 3-1. The CTMR kV and MV image sets exhibited no gross, anatomy-obscuring artifacts. Conversely, for the shielded FW and FSDs applicators, extensive metal artifacts were observed for all axial slices containing ovoid shields when imaged with kVCT. Qualitatively comparing shielded ovoid CT data sets, kV images acquired of the FW ovoids demonstrated much more severe artifacts compared to its FSDs ovoids. This was expected due to the composition of the ovoid shielding—FW Densimet-17 shields ($\rho = 17 g/cm^3$) (Horton, et al., 2005) compared with the FSDs applicator stainless steel shields ($\rho \approx 8 g/cm^3$) (Elert, et al., 2004).

The average image acquisition time for the kVCT scanner was ≈15-20 seconds whereas TomoTherapy's MV scanner averaged ≈10 minutes per phantom scan. The kVCT scanner was capable of much shorter scan times due to its 16 slice detector array (giving a pitch of 11.25 mm/rotation vs. 2 mm/rotation for MV) as well as faster gantry rotation (60 rpm for kV vs. 10 rpm for MV). Select slices for

each imaging modality for each applicator for a given bladder/rectum arrangement are shown in Figure 3-4. The same slice was chosen for each transverse and sagittal slice showing the reproducibility of the phantom setup. The window and level values were 500 and 1, respectively.

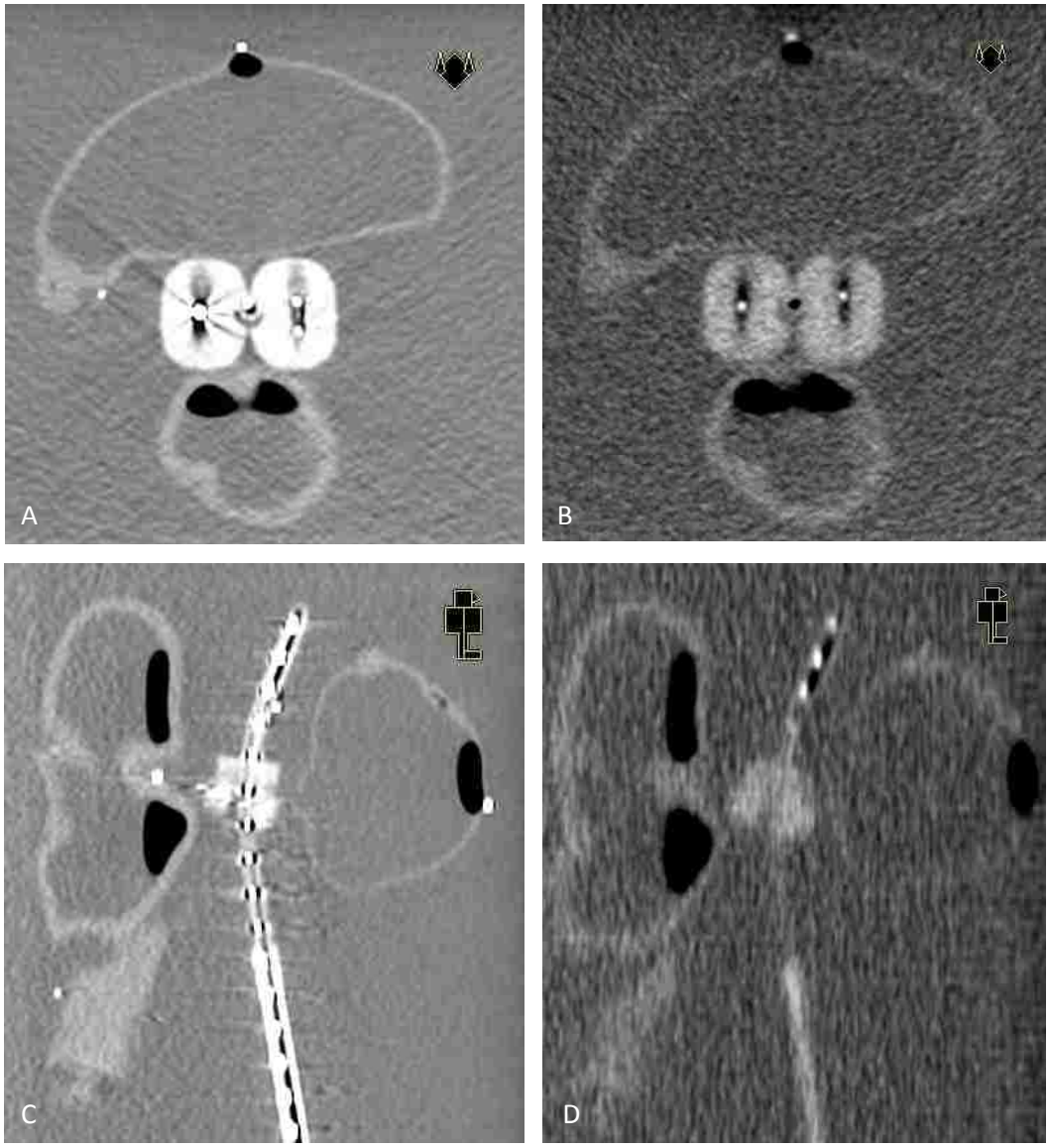

Figure 3-2: Corresponding axial and sagittal CT slices of kV and MV acquisitions for Nucletron's unshielded CT/MR compatible Fletcher applicator. Images (A) and (C) are the transverse and sagittal slices, respectively, acquired via kV imaging. Images (B) and (D) are the transverse and sagittal slices, respectively, acquired via MV imaging. Also, using fiducial markers, the same slice was chosen for both kV and MV images for both transverse and sagittal slices. Window and level values were 500 and 1, respectively.

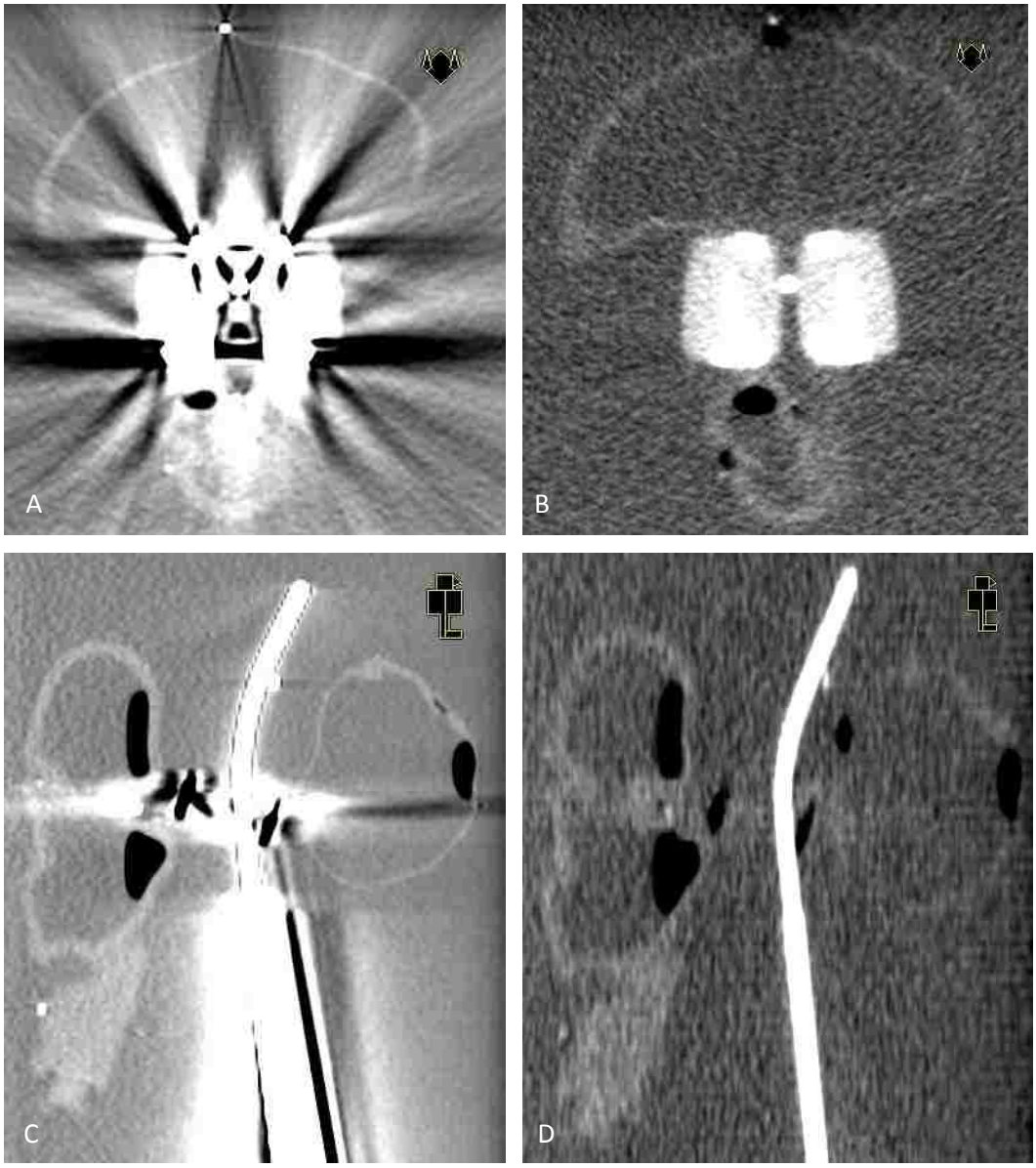

Figure 3-3: Corresponding axial and sagittal CT slices of kV and MV acquisitions for Varian stainless steel shielded Fletcher-Suit-Delclos-style applicator. Images (A) and (C) are the transverse and sagittal slices, respectively, acquired via kV imaging. Images (B) and (D) are the transverse and sagittal slices, respectively, acquired via MV imaging. Also, using fiducial markers, the same slice was chosen for both kV and MV images for both transverse and sagittal slices. Window and level values were 500 and 1, respectively.

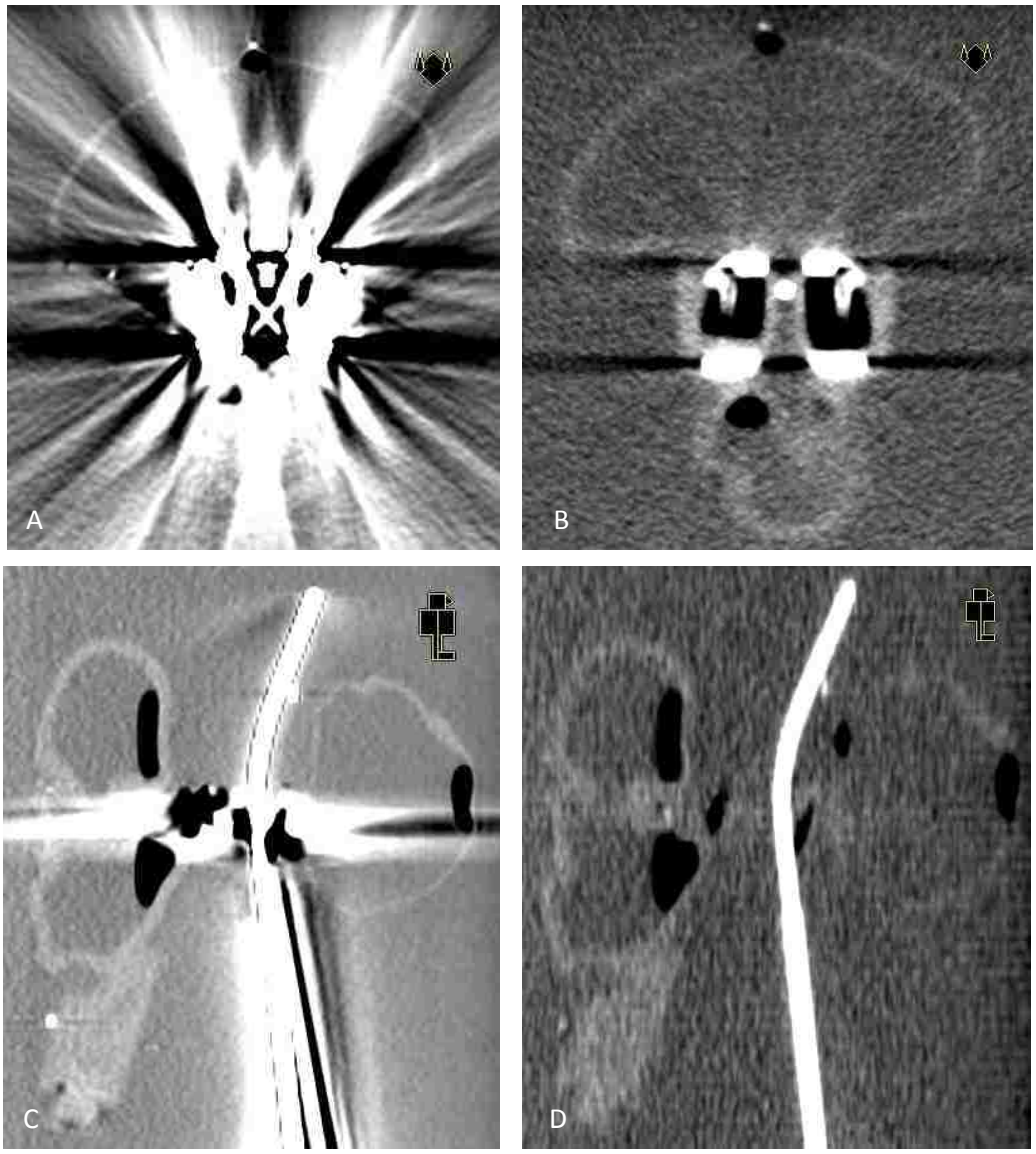

Figure 3-4: Corresponding axial and sagittal CT slices of kV and MV acquisitions for Nucletron tungsten shielded Fletcher-Williamson applicator. Images (A) and (C) are the transverse and sagittal slices, respectively, acquired via kV imaging. Images (B) and (D) are the transverse and sagittal slices, respectively, acquired via MV imaging. Also, using fiducial markers, the same slice was chosen for both kV and MV images for both transverse and sagittal slices. Window and level values were 500 and 1, respectively.

3.2 Aim 2: Participant Organ Segmentation and Catheter Reconstruction

3.2.1 Physicist and Physician Organ Segmentation and Catheter Reconstruction

The reported time required for physicists and physicians to complete organ segmentation and catheter reconstruction ranged from four to five hours. Participant-determined window and level values varied greatly for both kV and MV imaging modalities (see Table 3-1). The maximum and minimum

window and level values suggest that window and level settings are not determined by imaging modality but by user preference. In the pre-test image set, bladder and rectum structures, the reconstructed pre-test volumes were within ±17.5 cc of the control volumes for all participants verifying participant familiarity with Oncentra Brachy's TPS (see Section 2.2.1). The accuracy of organ segmentation and catheter reconstruction is reported in Section 3.3.

Table 3-1: Minimum and maximum window and level values reported for participant's organ segmentation and catheter reconstruction.

Reported Window and Level Values				
	kVCT		**MVCT**	
	Minimum	**Maximum**	**Minimum**	**Maximum**
Window	172	2879	250	2000
Level	-6	1982	-51	489

3.2.2 Investigator Catheter Reconstruction via Oncentra Applicator Modeling Plugin

Catheter reconstruction was performed for all image sets utilizing the Nucletron Oncentra Applicator Modeling plugin. The primary AMp tools utilized for catheter reconstruction were "Anchor Points" and "Catheter Manipulation." The average time to perform catheter reconstruction was 4-5 minutes. Results are presented in Section 3.3.3.1.

3.3 Organ Segmentation and Catheter Reconstruction Results

All participant results for organ segmentation and catheter reconstruction measurements are included in Appendix C. The following subsections present the analysis and discussion of organ segmentation and catheter reconstruction results. In the tables and figures, applicators are listed in order of increasing atomic number—CTMR (no shielding, Z≈6), FSDs (stainless steel shields, Z≈27), and FW (tungsten shields, Z≈74).

3.3.1 Organ Segmentation: CTP Comparisons

Two-dimensional organ segmentation accuracy was based on measurements from the centroid of a given CT slice to the participant-segmented perimeter (CTP) using the Oncentra "Distance and

Angle" tool. As the positioning of the surrogate bladder and rectum structures differed from one another as well as variations in physical characteristics (shape, wall thickness, etc.), results for bladder and rectum structures were analyzed separately.

3.3.1.1 Results and Analysis for Bladder Segmentation

For 2D organ segmentation analyses of the surrogate bladder, fewer CTP measurements met the ±2 mm criteria on MVCT data sets than on kVCT data sets. As reported in Table 3-2, kVCT data sets of the CTMR, FSDs and FW applicators resulted in 79%, 80% and 77% of points meeting the ±2 mm criteria, respectively; whereas on MVCT data sets, these percentages decreased to 65%, 65% and 67%, respectively. A two-proportion t-test determined that the percentage of CTPs meeting the 2 mm criteria in FSDs MVCT data sets was significantly less than the percentage of CTPs meeting the 2 mm criteria in CTMR kV data sets (65% vs. 79%, p=0.0004). The percentage of CTPs meeting the 2 mm criteria in FW MVCT data sets was significantly less than the percentage of CTPs meeting the 2 mm criteria in CTMR kV data sets (66% vs. 79%, p=0.001).

Table 3-2: Surrogate bladder CTP-diff results by applicator and imaging modality.

CTP-diff Results: Surrogate Bladder Structure									
		Number of CTPs that differ by:				Percent of CTPs that differ by:			
		[0-2mm]	[>2-5mm]	[>5-10mm]	[>10mm]	[0-2mm]	[>2-5mm]	[>5-10mm]	[>10mm]
CTMR	**kV**	188	53	2	0	77.4%	21.8%	0.8%	0.0%
	MV	158	78	7	0	65.0%	32.1%	2.9%	0.0%
FSDs	**kV**	196	45	2	0	80.7%	18.5%	0.8%	0.0%
	MV	158	72	13	0	65.0%	29.6%	5.3%	0.0%
FW	**kV**	184	50	6	2	75.7%	20.6%	2.5%	0.8%
	MV	161	72	9	1	66.3%	29.6%	3.7%	0.4%

Table 3-3 summarizes the statistical characteristics of the CTP-diff results for the surrogate bladder structure for all six data sets. The mean CTP-diff for all samples sets was within the 2 mm criterion. As determined by a paired t-test, the mean CTP-diff for the FSDs MVCT was significantly greater than the mean CTP-diff for the CTMR kVCT (1.0 mm vs. 0.7 mm, p=0.005). The mean CTP-diff for

the FW MVCT was not significantly different than the mean CTP-diff for the CTMR kVCT (0.7 mm vs. 0.7 mm, p=0.8). This suggests that surrogate bladder organ segmentation performed on MVCT data sets containing shielded FSDs and FW applicators is equivalent or slightly less accurate than organ segmentation perform on kVCT data sets of the unshielded CTMR applicator. This will be discussed further in subsection 3.3.1.4

Table 3-3: Summary of surrogate bladder CTP-diff results by applicator and imaging modality.

CTP-diff Results: Surrogate Bladder Structure *distances in mm						
		n	**Mean**	**σ**	**95% CI**	**Range**
CTMR	**kV**	243	0.7	1.7	0.5-0.9	12.7
	MV	243	1.1	1.9	0.9-1.4	12.2
FSDs	**kV**	243	0.6	1.5	0.4-0.8	10.4
	MV	243	1.0	2.2	0.7-1.3	13.7
FW	**kV**	243	0.6	2.4	0.3-0.8	25.6
	MV	243	0.8	2.3	0.4-1.0	15.6

3.3.1.2 Results and Analysis for Rectum Segmentation

For 2D organ segmentation analyses of the surrogate rectum, fewer CTP measurements met the ±2mm criteria on MVCT data sets than on kVCT data sets. As reported in Table 3-4, kVCT data sets of the CTMR, FSDs and FW applicators resulted in 85%, 81% and 79% of points meeting the ±2 mm criteria, respectively; on MVCT data sets, these numbers decreased to 75%, 78% and 73%, respectively. A two-proportion t-test determined that the percentage of CTPs meeting the 2 mm criteria in FSDs MVCT data sets was significantly less than the percentage of CTPs meeting the 2 mm criteria in CTMR kV data sets (85% vs. 78%, p=0.02). The percentage of CTPs meeting the 2 mm criteria in FW MVCT data sets was significantly less than the percentage of CTPs meeting the 2 mm criteria in CTMR kV data sets (85% vs. 73%, p=0.0006).

Table 3-4: Surrogate rectum CTP-diff results by applicator and imaging modality.

CTP-diff Results: Surrogate Rectum Structures									
		Number of points that differ by:				Percent of points that differ by:			
		[0-2mm]	[>2-5mm]	[>5-10mm]	[>10-15mm]	[0-2mm]	[>2-5mm]	[>5-10mm]	[>10-15mm]
CTMR	kV	210	31	2	0	86.4%	12.8%	0.8%	0.0%
	MV	183	49	8	3	75.3%	20.2%	3.3%	1.2%
FSDs	kV	193	41	8	1	79.4%	16.9%	3.3%	0.4%
	MV	193	44	6	0	79.4%	18.1%	2.5%	0.0%
FW	kV	188	35	19	1	77.4%	14.4%	7.8%	0.4%
	MV	181	60	2	0	74.5%	24.7%	0.8%	0.0%

Table 3-5 summarizes the statistical characteristics of the CTP-diff results for the surrogate rectum structure for all six data sets. The mean CTP-diff for all samples sets was within the 2 mm criteria. As determined by the paired t-test the mean CTP-diff for the FSDs MVCT was significantly greater than the mean CTP-diff for the CTMR kVCT (1.2 mm vs. 0.7 mm, p=1.7E-09). The mean CTP-diff for the FW MVCT was significantly greater than the mean CTP-diff for the CTMR kVCT (1.0 mm vs. 0.7 mm, p=0.02). This suggests that surrogate rectum organ segmentation performed on MVCT data sets acquired of the shielded FSDs and FW applicators is less accurate than organ segmentation perform on kVCT data sets of the unshielded CTMR applicator. This will be discussed further in subsection 3.3.1.4

Table 3-5: Summary of surrogate rectum CTP-diff results by applicator and imaging modality.

CTP-diff Results: Surrogate Rectum Structure						
		n	Mean	σ	95% CI	Range
CTMR	kV	243	0.6	1.4	0.5-0.8	10.3
	MV	243	1.3	2.1	1.0-1.6	15.4
FSDs	kV	243	0.5	2.0	0.3-0.8	16.9
	MV	243	1.2	1.6	1.0-1.5	11.7
FW	kV	243	0.5	2.5	0.3-0.9	18.8
	MV	243	1.0	1.5	0.8-1.2	9.9

3.3.1.3 Results and Analyses for Bladder and Rectum Artifact Regions

The results of the 2D organ segmentation analyses lean towards the conclusion that MVCT yields poorer quality and less-accurately segmented image sets than kVCT (see Section 1.4). These

results, however, were based off of CTP's in all regions of segmenting, two-thirds of which was non-artifact region. To more directly assess the influence of MVCT's leser metal artifacts on segmentation performance, results were analyzed exclusively for the artifact region of the T&O applicators (Section 2.1.2.3-artifact region definition). Results are separated by structure due to variations in surrogate structure construction and placement relative to T&O applicators.

For 2D organ segmentation analyses of the surrogate bladder artifact regions, fewer CTP measurements met the ±2 mm criteria on MVCT data sets than on kVCT data sets. As reported in Table 3-6, kVCT data sets of the CTMR, FSDs and FW applicators had 81%, 78% and 68% of CTPs meeting the ±2 mm criteria, respectively; on MVCT data sets, these percentages decreased to 67%, 73% and 65%, respectively. A two-proportion t-test determined that the percentage of CTPs meeting the 2 mm criteria in FSDs MVCT data sets was significantly less than the percentage of CTPs meeting the 2 mm criteria in CTMR kV data sets (78% vs. 85%, p=0.2). The percentage of CTPs meeting the 2 mm criteria in FW MVCT data sets was significantly less than the percentage of CTPs meeting the 2 mm criteria in CTMR kV data sets (73% vs. 85%, p=0.02).

Table 3-6: Surrogate bladder artifact region CTP-diff results by applicator and imaging modality.

CTP-diff Results: Surrogate Bladder Artifact Region									
		Number of points that differ by:				Percent of points that differ by:			
		[0-2mm]	[>2-5mm]	[>5-10mm]	[>10-15mm]	[0-2mm]	[>2-5mm]	[>5-10mm]	[>10-15mm]
CTMR	kV	51	12	0	0	81%	19%	0%	0%
	MV	41	21	1	0	65%	33%	2%	0%
FSDs	kV	49	14	0	0	78%	22%	0%	0%
	MV	47	16	0	0	75%	25%	0%	0%
FW	kV	42	17	4	0	67%	27%	6%	0%
	MV	42	21	0	0	67%	33%	0%	0%

Table 3-7 summarizes the statistical characteristics of the CTP-diff results for the surrogate bladder artifact region for all six data sets. The mean CTP-diff for all samples sets was within the ±2 mm

criteria. As determined by the paired t-test the mean CTP-diff for the FSDs MVCT was not significantly different than the mean CTP-diff for the CTMR kVCT (-0.1 mm vs. 0.2 mm, p=0.6). The mean CTP-diff for the FW MVCT was not significantly different than the mean CTP-diff for the CTMR kVCT (0.1 mm vs. 0.2 mm, p=0.3). This suggests that surrogate bladder organ segmentation performed within the artifact region on MVCT data sets acquired of the shielded FSDs and FW applicators is as accurate as organ segmentation performed on kVCT data sets of the unshielded CTMR applicator. This will be discussed further in subsection 3.3.1.4

Table 3-7: Summary of surrogate bladder artifact region CTP-diff results by applicator and imaging modality.

CTP-diff Results: Surrogate Bladder Artifact Region *distances in mm						
		n	**Mean**	**σ**	**95% CI**	**Range**
CTMR	**kV**	63	0.2	1.6	-0.2-0.6	8.6
	MV	63	0.9	1.8	0.3-1.2	10.2
FSDs	**kV**	63	-0.2	1.7	-0.5-0.3	7.5
	MV	63	0.2	1.9	-0.4-0.5	9.2
FW	**kV**	63	-0.8	2.4	-1.3- -0.1	12.2
	MV	63	0.1	2.2	-0.7-0.4	8.6

For 2D organ segmentation analyses of the surrogate rectum artifact regions, fewer CTP measurements met the ±2 mm criteria on MVCT data sets than on kVCT data sets for the CTMR applicator, while an increase was observed for the FSDs and FW applicators. As reported in Table 3-6, kVCT data sets of the CTMR, FSDs and FW applicators resulted in 77%, 60% and 58% of points meeting the ±2 mm criteria, respectively; whereas on MVCT data sets 65%, 73% and 73% met the ±2 mm criteria, respectively. A two-proportion t-test determined that the percentage of CTPs meeting the ±2 mm criteria in FSDs MVCT data sets was not significantly different than the percentage of CTPs meeting the 2 mm criteria in CTMR kV data sets (73% vs. 77%, p=0.3). The percentage of CTPs meeting the 2 mm criteria in FW MVCT data sets was also not significantly different than the percentage of CTPs meeting the 2 mm criteria in CTMR kV data sets (73% vs. 77%, p=0.3).

Table 3-8: Surrogate rectum artifact region CTP-diff results by applicator and imaging modality.

CTP-diff Results: Surrogate Rectum Artifact Region									
		Number of points that differ by:				Percent of points that differ by:			
		[0-2mm]	[>2-5mm]	[>5-10mm]	[>10-15mm]	[0-2mm]	[>2-5mm]	[>5-10mm]	[>10-15mm]
CTMR	kV	65	14	2	0	80%	17%	2%	0%
	MV	53	17	8	3	65%	21%	10%	4%
FSDs	kV	47	27	6	1	58%	33%	7%	1%
	MV	60	15	6	0	74%	19%	7%	0%
FW	kV	44	19	17	1	54%	23%	21%	1%
	MV	60	20	1	0	74%	25%	1%	0%

Table 3-9 summarizes the statistical characteristics of the CTP-diff results for the surrogate rectum artifact region for all six data sets. The mean CTP-diff for all samples sets was within the ±2 mm criteria. As determined by the paired t-test the mean CTP-diff for the FSDs MVCT was not significantly different than the mean CTP-diff for the CTMR kVCT (0.1 mm vs. 0.2 mm, p=0.8). The mean CTP-diff for the FW MVCT was not significantly different than the mean CTP-diff for the CTMR kVCT (0.05 mm vs. 0.2 mm, p=0.6). This suggests that surrogate rectum organ segmentation performed within the artifact region on MVCT data sets acquired of the shielded FSDs and FW applicators is as accurate as organ segmentation performed on kVCT data sets of the unshielded CTMR applicator. This will be discussed further in subsection 3.3.1.4

Table 3-9: Summary of surrogate rectum artifact region CTP-diff results by applicator and imaging modality.

CTP-diff Results: Surrogate Rectum Artifact Region *distances in mm						
		n	Mean	σ	95% CI	Range
CTMR	kV	81	0.7	1.8	0.3-1.1	10.3
	MV	81	1.8	3.0	1.2-2.5	15.4
FSDs	kV	81	0.6	3.1	-0.1-1.2	16.9
	MV	81	1.5	2.3	1.0-2.0	11.3
FW	kV	81	0.3	3.9	-0.6-1.1	18.8
	MV	81	1.2	1.7	0.8-1.5	8.0

When analyzing the CT artifact region, it was observed that, as distance increases within a CT slice from high Z objects, the metal artifact visually decreases (see Figure 3-5). To determine the impact, if any, this might have, the rectum artifact region was separated into two parts—the anterior region and posterior region. The anterior region contains CTP measurements for angles 0, 40, 80, 120, and 160 degrees. The posterior region contains angles 200, 240, 280, and 320. Bladder results were not broken down by anterior and posterior results due to the bladder orientation relative to the artifact region, leading to few angles in each slice actually being found in the artifact region (see Figure 3-6). Rectum anterior and posterior artifact region results are found in Table 3-10.

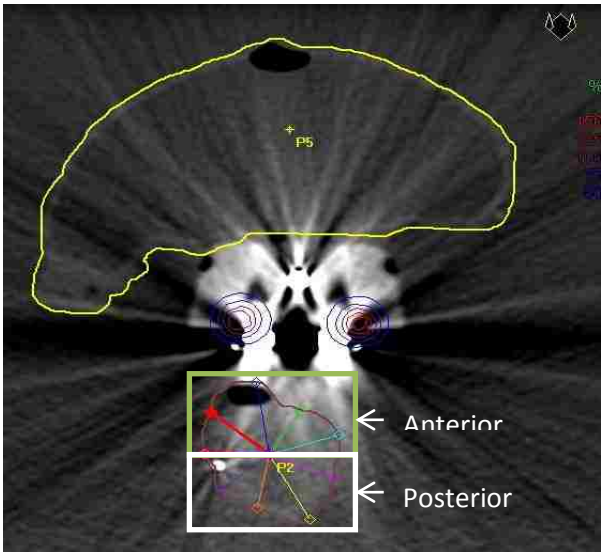

Figure 3-5: Axial CT slice of the FW shielded ovoids demonstrating the anterior and posterior artifact regions as well as the decrease in metal artifact with distance from the high Z objects.

For 2D organ segmentation analyses of the surrogate rectum anterior artifact regions, fewer CTP measurements met the ±2 mm criteria on MVCT data sets than on kVCT data sets for the CTMR applicator, while more CTPs met the criteria for the FSDs and FW applicators. As reported in Table 3-10, kVCT data sets of the CTMR, FSDs and FW applicators resulted in 71%, 47% and 40% of points meeting the ±2 mm criteria, respectively; on MVCT data sets 64%, 73% and 73% met the ±2 mm criteria, respectively. A two-proportion t-test determined that the percentage of CTPs meeting the 2 mm criteria in FSDs MVCT data sets was not significantly different than the percentage of CTPs meeting the ±2 mm

criteria in CTMR kV data sets (73% vs. 71%, p=0.6). The percentage of CTPs meeting the ±2 mm criteria in FW MVCT data sets was also not significantly different than the percentage of CTPs meeting the ±2 mm criteria in CTMR kV data sets (73% vs. 71%, p=0.6).

Figure 3-6: Sagittal CT slice of the FW applicator demonstrating the location of the artifact region relative to measurements made within the sagittal slice. Note that only 2 of 9 CTP measures are included within the artifact region negating the values of an anterior/posterior-type artifact region analysis.

Table 3-10: Surrogate rectum anterior and posterior artifact region CTP-diff results by applicator and imaging modality.

CTP-diff Results: Surrogate Rectum Anterior & Posterior Artifact Region									
		Number of points that differ by:				Percent of points that differ by:			
		[0-2mm]	[>2-5mm]	[>5-10mm]	[>10-15mm]	[0-2mm]	[>2-5mm]	[>5-10mm]	[>10-15mm]
CTMR-kV	**ant.**	33	11	1	0	73%	24%	2%	0%
	post.	32	3	1	0	89%	8%	3%	0%
CTMR-MV	**ant.**	29	8	6	2	64%	18%	13%	4%
	post.	24	9	2	1	67%	25%	6%	3%
FSDs-kV	**ant.**	20	19	5	1	44%	42%	11%	2%
	post.	27	8	1	0	75%	22%	3%	0%
FSDs-MV	**ant.**	33	7	5	0	73%	16%	11%	0%
	post.	27	8	1	0	75%	22%	3%	0%
FW-kV	**ant.**	16	15	14	0	36%	33%	31%	0%
	post.	28	4	3	1	78%	11%	8%	3%
FW-MV	**ant.**	34	11	0	0	76%	24%	0%	0%
	post.	26	9	1	0	72%	25%	3%	0%

Table 3-11 summarizes the sample characteristics of the CTP measures for the surrogate rectum artifact region for all six data sets. The mean CTP-diff for all samples sets was within the ±2 mm criteria. As determined by the paired t-test the mean CTP-diff for the FSDs MVCT was significantly different than the mean CTP-diff for the CTMR kVCT (1.7 mm vs. 0.8 mm, p=0.02). The mean CTP-diff for the FW MVCT was not significantly different than the mean CTP-diff for the CTMR kVCT (1.2 mm vs. 0.8 mm, p=0.5). This suggests that surrogate rectum organ segmentation performed within the anterior artifact region on MVCT data sets acquired of the shielded FSDs and FW applicators is as accurate as organ segmentation performed on kVCT data sets of the unshielded CTMR applicator. This will be discussed further in subsection 3.3.1.4

Table 3-11: Summary of surrogate rectum anterior artifact region CTP-diff results by applicator and imaging modality

CTP-diff Results: Surrogate Rectum Anterior Artifact Region *distances in mm						
		n	**Mean**	**σ**	**95% CI**	**Range**
CTMR	**kV**	45	0.8	1.9	0.2-1.3	10.2
	MV	45	1.8	3.4	0.8-2.8	15.4
FSDs	**kV**	45	0.5	3.8	-0.6-1.6	16.9
	MV	45	1.7	2.6	1.0-2.5	11.1
FW	**kV**	45	0.2	4.6	-1.1-1.6	18.1
	MV	45	1.2	1.5	0.8-1.7	6.4

For 2D organ segmentation analyses of the surrogate rectum posterior artifact regions fewer CTP measurements met the ±2 mm criteria on MVCT data sets than on kVCT data. As reported in Table 3-10, kVCT data sets of the CTMR, FSDs and FW applicators resulted in 83%, 78% and 81% of points meeting the ±2 mm criteria, respectively; on MVCT data sets 67%, 72% and 72% met the ±2 mm criteria, respectively. A two-proportion t-test determined that the percentage of CTPs meeting the ±2 mm criteria in FSDs MVCT data sets was not significantly different than the percentage of CTPs meeting the 2 mm criteria in CTMR kV data sets (72% vs. 83%, p=0.1). The percentage of CTPs meeting the 2 mm criteria in FW MVCT data sets was also not significantly different than the percentage of CTPs meeting

the 2 mm criteria in CTMR kV data sets (72% vs. 83%, p=0.1). This suggests that MVCT data sets of the shielded FSDs and FW applicators result in organ segmentation as accurate as kVCT data sets of the unshielded CTMR applicator in the posterior artifact region but may be trending towards significant differences.

Table 3-12 summarizes the sample characteristics of the CTP measures for the surrogate rectum artifact region for all six data sets. The mean CTP-diff for all samples sets was within the ±2 mm criteria. As determined by the paired t-test the mean CTP-diff for the FSDs MVCT was not significantly different than the mean CTP-diff for the CTMR kVCT (1.3 mm vs. 0.7 mm, p=0.1). The mean CTP-diff for the FW MVCT was not significantly different than the mean CTP-diff for the CTMR kVCT (1.0 mm vs. 0.7 mm, p=0.9). This suggests that surrogate rectum organ segmentation performed within the posterior artifact region on MVCT data sets acquired of the shielded FSDs and FW applicators is as accurate as organ segmentation performed on kVCT data sets of the unshielded CTMR applicator. This will be discussed further in subsection 3.3.1.4

Table 3-12: Summary of surrogate rectum posterior artifact region CTP-diff results by applicator and imaging modality

CTP-diff Results: Surrogate Rectum Posterior Artifact Region *distances in mm						
		n	**Mean**	**σ**	**95% CI**	**Range**
CTMR	**kV**	36	0.7	1.6	0.2-1.2	9.5
	MV	36	1.9	2.6	1.0-2.8	12.8
FSDs	**kV**	36	0.6	1.8	0.1-1.2	8.6
	MV	36	1.3	1.9	0.6-1.9	9.2
FW	**kV**	36	0.3	3.0	-0.7-1.3	16.7
	MV	36	1.1	2.0	0.4-1.7	8.0

3.3.1.4 CTP Results Discussion

Data sets imaged with MVCT had higher mean CTP-diff values compared with the same sets imaged with kVCT. However, MVCT results within the artifact region for the shielded FSDs and FW applicators were consistently comparable to those achieved with the artifact-free CTMR compatible

applicator. All t-test results for the anterior rectal region indicate that there is no significant difference between CTMR kVCT organ segmentation and FW or FSDs MVCT organ segmentation in this region. This is valuable as the anterior rectal area is the region receiving the highest dose due to ICBT (inverse-square falloff). The option to utilize shielded T&O ICBT applicators without sacrificing the ability to accurately segment the rectum is significant. Further studies could explore the ability of MVCT to mitigate metal artifact in the regions of the bladder closest to the ovoids.

Also of significance is the fact that, while the percentage of CTP-diffs meeting the ±2 mm hypothesis criteria decreased when utilizing MVCT (most cases), the percentage of CTP-diffs within ±2 mm for the shielded applicators was consistently comparable to that of the CTMR MVCT data sets. Previous studies have concluded that TomoTherapy's MVCT scanner is capable of yielding CT data sets with sufficient contrast and quality to facilitate segmentation of a number of soft tissues in the absence of metal artifact (Ruchala, et al., 1999) (Meeks, et al., 2005) (Korol, et al., 2010). Thus, in conjunction with the findings of these studies, the results of this study would indicate that MVCT data sets of the FSDs and FW applicators exhibit sufficient artifact reduction to facilitate patient organ segmentation when high Z objects are in close proximity (<20 mm). Clinical implementation of this methodology deserves further consideration.

Though statistical testing indicated a significant difference between CTMR kVCT and FW MVCT CTP-diff results for the surrogate rectum structure, the mean values and standard deviations differed by only 0.3 mm and 0.1 mm, respectively. These results are well within the mechanical uncertainty of the treatment delivery system (±1 mm). A means of determining the practical significance of results rather than statistical significance would yield different conclusions in some instances.

3.3.2 Volume Comparison Results

Three-dimensional organ segmentation analyses were based off a comparison of participants' TPS reconstructed volume with the control volume measured via water displacement (VOL-diff). As the

positioning of the surrogate bladder and rectum structures differed from one another as well as variations in physical characteristics (shape, wall thickness, etc.), results for bladder and rectum structures are analyzed separately. Results for all image sets containing T&O applicators are contained in Table 3-13 through Table 3-16.

3.3.2.1 Volume Comparison: Bladder Results

The overall organ segmentation results for the bladder structure are found in Table 3-13. Among all three applicators, reconstructed volume accuracy decreased on MVCT data sets. A two-proportion t-test determined that the percent of VOL-diff measures meeting the 15 cc criteria on FSDs MVCT data sets was significantly less than the percent of VOL-diff measures meeting the 15 cc criteria on CTMR kVCT data sets (22% vs78%, p=0.01). The percent of VOL-diff measures meeting the 15 cc criteria on FW MVCT data sets was trending towards significantly less than the percent of VOL-diff measures meeting the 15 cc criteria for CTMR kVCT data sets (44% vs. 78%,p=0.07).

Table 3-13: Organ segmentation results for segmented volumes: absolute volume results for the bladder structure.

VOL-diff Results: Reconstructed Bladder									
		Number that differ by:				Percent that differ by:			
		[0-15cc]	[>15-20cc]	[>20-25cc]	[>25cc]	[0-15cc]	[>15-20cc]	[>20-25cc]	[>25cc]
CTMR	**kV**	7	1	0	1	78%	11%	0%	11%
	MV	3	1	1	4	33%	11%	11%	44%
FSDs	**kV**	6	2	1	0	67%	22%	11%	0%
	MV	2	3	2	2	22%	33%	22%	22%
FW	**kV**	7	2	0	0	78%	22%	0%	0%
	MV	3	2	3	1	33%	22%	33%	11%

Table 3-14 presents the sample characteristics of the reconstructed surrogate bladder volume for all six data sets. Among all the data sets, the mean reconstructed volumes averaged from 8.1 cc to 20.9 cc from the control surrogate bladder volume. A paired t-test found that mean values of VOL-diff

on FSDs MVCT data sets were not significantly more different from control volumes than mean values of VOL-diff on CTMR kVCT data sets (18.9 cc vs. 11.1 cc, p=0.002). Mean values of VOL-diff on FW MVCT data sets were significantly more different from control volumes than mean values of VOL-diff on CTMR kVCT data sets (17.0 cc vs. 11.1 cc, p=0.3). This suggests that participants were able to produce similar quality of organ segmentation for FW MVCT and CTMR kVCT data sets where the quality worsened for FSDs kVCT data sets. It was also observed the for all MVCT data sets, the 95% confidence interval and range both grew, indicating MVCT yields poorer results than kVCT.

Table 3-14: Volume Comparison bladder results**.**

VOL-diff Results: Reconstructed Bladder (*volumes in cc)						
		n	**Mean**	**σ**	**95% CI**	**Range**
CTMR	**kV**	9	11.0	9.4	4.5 - 17.5	33.9
	MV	9	21.6	11.0	14.0 - 29.2	33.3
FSDs	**kV**	9	9.4	8.7	3.4 - 15.5	25.7
	MV	9	19.7	13.3	10.5 - 28.9	42.5
FW	**kV**	9	8.3	6.2	4.0 - 12.6	18.9
	MV	9	18.0	11.4	10.1 - 25.9	41.0

3.3.2.2 Volume Comparison: Rectum Results

Overall organ segmentation results for the rectum structures are shown in Table 3-15. The percent of VOL-diff measures meeting the 15 cc criteria was 89% for all applicators for both imaging modalities. This yields a p-value of 0.5 using a two-proportion t-test. Applying the same two-proportion t-test to a ±10 cc criteria shows that the percent of VOL-diff measures meeting the 10 cc criteria on FSDs MVCT are not significantly different than the percent of VOL-diff measures meeting the 10 cc criteria on CTMR kVCT (67% vs. 78%, p=0.3). The percent of VOL-diff measures meeting the 10 cc criteria on FW MVCT are not significantly different than the percent of VOL-diff measures meeting the 10 cc criteria on CTMR kVCT, however, they may be trending towards being significantly less accurate than CTMR kVCT VOL-diffs (56% vs. 78%, p=0.15).

Table 3-15: Organ segmentation results for segmented volumes: absolute volume results for rectum structures.

VOL-diff Results: Reconstructed Rectums									
		Number that differ by:				Percent that differ by:			
		[0-15cc]	[>15-20cc]	[>20-25cc]	[>25cc]	[0-15cc]	[>15-20cc]	[>20-25cc]	[>25cc]
CTMR	**kV**	8	0	1	0	89%	0%	11%	0%
	MV	8	0	1	0	89%	0%	11%	0%
FSDs	**kV**	7	2	0	0	78%	22%	0%	0%
	MV	8	1	0	0	89%	11%	0%	0%
FW	**kV**	8	1	0	0	89%	11%	0%	0%
	MV	8	0	1	0	89%	0%	11%	0%

Table 3-16 summarizes the sample characteristics for all six sample groups for VOL-diff measurements. The average VOL-diff for all sample sets ranged from -6.8 cc to 18.9 cc. A paired t-test found that the mean VOL-diff on FSDs MVCT data sets were significantly less than the mean VOL-diff on CTMR kVCT data sets (-1.2 cc vs. -6.8 cc, p=0.003). The mean VOL-diff on FW MVCT data sets was not significantly different than the mean VOL-diff on CTMR kVCT data sets (-1.3 cc vs. -6.8 cc, p=0.2). Removal of an outlier from the FW MVCT data (VOL-diff=21.6 cc) changes the FW MVCT mean VOL-diff to -4.1 cc with p=0.3. This suggests that participants were able to segment the rectum structure on FW MVCT data sets with similar accuracy as that achieved for CTMR kVCT data sets. It was also observed that for the shielded FSDs and FW applicators, MVCT imaging improved the 95% confidence interval however the range of participant VOL-diffs increased.

Table 3-16: Volume Comparison bladder results**.**

VOL-diff Results: Reconstructed Rectum (*volumes in cc)						
		n	Mean	σ	95% CI	Range
CTMR	**kV**	9	-6.8	9.0	-13 - -0.6	32.1
	MV	9	-0.3	10.6	-7.7 - 7.0	35.0
FSDs	**kV**	9	-8.4	8.7	-14.4 - -2.4	27.6
	MV	9	-1.9	9.0	-8.2 - 4.3	29.0
FW	**kV**	9	-8.7	5.8	-12.8 - -4.7	21.1
	MV	9	-1.3	10.7	-8.7 - 6.2	33.1

3.3.2.3 Volume Comparison Discussion

Overall, the MVCT data sets containing the FSDs and FW applicators lead toward opposing conclusions regarding shielded applicators. Although the FSDs applicator shields exhibit less artifact than the FW applicator, results indicated participants were actually able to generate more accurate surrogate structure organ segmentation for the MVCT data sets containing the FW applicator. The observations of this portion of the study are limited to less than ten degrees of freedom, meaning results possibly exceed the limitations of the statistical tests utilized in this study. It would be of benefit to repeat this volume comparison portion of the study with either a larger number of participants (>20) or more CT data sets on which participants could perform organ segmentation.

In all but the CTMR kV surrogate bladder and rectum data sets, a greater percentage of VOL-diffs fell within the 15 cc criteria for surrogate rectum segmentation than for surrogate bladder segmentation, regardless of imaging energy or type of applicator (c.f Table 3-17). In other words, the participant reconstructed rectum volumes were closer to control volumes than participant-reconstructed bladder volumes, suggesting that the surrogate bladder was more difficult to segment than the surrogate rectum structures. This could be due to structure wall shape and thickness: bladder walls were thinner in which case they suffered from poorer MVCT imaging contrast. Although the bladder and rectum structures varied from one another, it is still worth analyzing, as typical patient anatomies vary, resulting in varying responses to different imaging modalities.

Table 3-17: VOL-diff comparison of bladder and rectum

VOL-diff Results: Bladder versus Rectum (*volumes in cc)									
		Mean		**Max**		**Min**		**±15cc Criteria**	
		Blad.	**Rec.**	**Blad.**	**Rec.**	**Blad.**	**Rec.**	**Blad.**	**Rec.**
CTMR	**kV**	11.3	9.7	32.4	23.9	1.5	1.1	77.8%	88.9%
	MV	21.6	9.7	37.1	23.5	3.8	2.7	33.3%	88.9%
FSDs	**kV**	10.0	9.5	23.2	19.6	1.0	3.2	77.8%	77.8%
	MV	19.7	5.7	44.8	18.4	2.3	0.1	33.3%	88.9%
FW	**kV**	8.3	10.1	19.7	18.1	0.8	3.0	66.7%	88.9%
	MV	18.3	8.6	39.8	21.6	1.2	0.3	22.2%	88.9%

For all MVCT data sets, the surrogate rectum had smaller mean VOL-diffs and more VOL-diffs meeting the 15 cc criteria than the surrogate bladder structures (see Table 3-17). Rectum results suggest participants were able to segment this structure with more accuracy than the bladder structure on kVCT and MVCT data sets. These surrogate rectum results are consistent with other studies demonstrating the viability of TomoTherapy's MV scanner for organ segmentation (Ruchala, et al., 1999) (Meeks, et al., 2005). While previous studies have not incorporated shielded HDR tandem and ovoid applicators, they have utilized unshielded CT/MR compatible applicators for which MV scans yielded sufficient contrast to segment the bladder, rectum and small bowel (Korol, et al., 2010). Results by Wagner *et al.* also indicate that MVCT scans of the shielded Fletcher-Suit-Delclos applicator yield acceptable CT data sets for 3D, MVCT-based treatment planning. This suggests that the surrogate rectum structures more closely approximated an actual rectum than the surrogate bladder approximated an actual bladder. However, additional studies with larger sample sizes would be needed to draw these conclusions.

Another indication of physical differences between surrogate bladder and rectum structures is whether a structure volume was over- or underestimated. The over- and underestimations were recorded for both the kV and MV energies (see Table 3-18). These results show for kV image sets that the participants tended to overestimate bladder structures (=89%) and to underestimate rectum structure (=89%). For MV image sets the majority of participants continued to overestimate the surrogate bladder volume (=93%) while the over- and underestimations were more evenly distributed for the surrogate rectum structure (41% and 59%).

Table 3-18: Comparison of over-and underestimations between kV and MV imaging modalities for surrogate bladder and rectum structures.

VOL-diff Results: Over- vs. Underestimation					
		Bladder	% of Volumes	Rectum	% of Volumes
kV	Under	2	7.4%	24	88.9%
	Over	25	92.6%	3	11.1%
MV	Under	1	3.7%	16	59.3%
	Over	26	96.3%	11	40.7%

3.3.3 Catheter Reconstruction Results

3.3.3.1 Investigator Catheter Reconstruction via Oncentra's Applicator Modeling Plugin

A part of this study was to validate the use of Nucletron's AMp for catheter reconstruction. To accomplish this purpose the results of the AMp will be reported with and tested statistically against participant's catheter reconstruction results in the following section. Basic analyses are included in this section.

As shown in Table 3-19, all but three AMp-defined distal dwell positions yielded marker-to-dwell differences (MD-diffs) within the ±2 mm hypothesis criteria. The mean deviation from the control values for all applicators was 1.0 mm ± 0.7 mm with a maximum deviation of 2.3mm. Of the 36 AMp-defined dwell positions, 50% were within ±1 mm of the control values which is within the mechanical tolerance of the treatment delivery system (afterloader, applicators, etc.). Of the three points differing by more than 2mm from control values, 1 was on kVCT data sets and 2 were on MVCT data sets.

Table 3-19: Applicator Modeling plugin results for Nucletron's CT/MR compatible applicator and shielded Fletcher-Williamson applicator. Results in green, yellow and red indicate values that are less than 1.0 mm from the control values, less than or equal to 2.0 mm from the control value and greater than 2.0 mm from the control values, respectively. The "Rectum-#" label refers to the bladder/rectum arrangement utilized for the given CT data set. The uncertainty in kV and MV images are ±1.3 mm and ±1.6 mm, respectively

Applicator Modeling Plugin: Raw Results				
*distances in mm		R. Ovoid	L. Ovoid	Tandem
CTMR kV	Rectum 1	1.1	-0.3	0.7
	Rectum 2	1.4	0.5	0.0
	Rectum 3	1.4	-0.7	-0.1
CTMR MV	Rectum 1	-0.1	-1.3	0.0
	Rectum 2	1.3	-0.4	-1.7
	Rectum 3	0.2	-1.6	0.3
FW kV	Rectum 1	1.3	0.1	-1.1
	Rectum 2	2.3	-1.0	-1.6
	Rectum 3	1.3	-0.6	-1.0
FW MV	Rectum 1	0.9	-2.2	-2.3
	Rectum 2	0.9	-1.2	0.1
	Rectum 3	1.9	-1.4	-1.5

3.3.3.2 Participant Catheter Reconstruction MD-diff Results

As shown in Table 3-20, the percentage of MD-diffs that were within the 2 mm criteria for the CTMR, FSDs and FW applicator kVCT data sets were 96%, 85% and 52%, respectively. The percentage of MD-diffs that were within the 2 mm criteria for MVCT data sets were 93%, 96% and 93%. All CTMR-AMp kVCT and MVCT dwells were within the 2 mm criteria whereas the FW-AMp kVCT and MVCT data sets resulted in 78% and 83% of dwells being within the 2 mm criteria, respectively. A two-proportion t-test showed that the percentage of MD-diffs meeting the 2 mm criteria for FSDs MVCT data sets was not significantly different from the percentage of MD-diffs meeting the 2 mm criteria for CTMR kVCT data sets (96% vs. 96%, p=0.4). The percentage of MD-diffs meeting the 2 mm criteria for FW MVCT data sets was not significantly different from CTMR kVCT data sets (93% vs. 96%, p=0.3). This suggests that, for all distal dwell positions of the shielded FSDs and FW applicators, MVCT data sets provide sufficient visibility to accurately place distal source dwells within the TPS.

Table 3-20: MD-diff results for all applicators for all catheter tubes combined. AMp MD-diff results were included as an alternate method of catheter reconstruction.

MD-diff Results: All Catheter Tubes Combined									
		Number of points differing by:				Percent of points differing by:			
		[0-2mm]	[>2-5mm]	[>5-10mm]	[>10-15mm]	[0-2mm]	[>2-5mm]	[>5-10mm]	[>10-15mm]
CTMR	kV	26	1	0	0	96%	4%	0%	0%
	MV	26	1	0	0	96%	4%	0%	0%
FSDs	kV	23	4	0	0	85%	15%	0%	0%
	MV	26	1	0	0	96%	4%	0%	0%
FW	kV	14	11	2	0	52%	41%	7%	0%
	MV	25	2	0	0	93%	7%	0%	0%
CTMR-AMp	kV	9	0	0	0	100%	0%	0%	0%
	MV	9	0	0	0	100%	0%	0%	0%
FW-AMp	kV	8	1	0	0	89%	11%	0%	0%
	MV	7	2	0	0	78%	22%	0%	0%

Table 3-21 summarizes the sample characteristics of the MD-diff measures for all catheters for all six data sets plus four AMp data sets. The mean MD-diff for all image sets was within the 2 mm criteria. As determined by an unpaired t-test, the mean MD-diff for the FSDs MVCT data sets was

significantly better than the mean MD-diff for the CTMR kVCT data sets (0.5 mm vs. 1.0 mm, p=0.05). The mean MD-diff for the FW MVCT was significantly better than the mean MD-diff for the CTMR kVCT (-0.3 mm vs. 1.0 mm, p=0.00003). For the CTMR kVCT and MVCT data sets, the mean AMp MD-diffs varied significantly for kV and insignificantly for MV from mean participant-generated MD-diffs (kV: 0.4 mm vs. 1.0 mm, p=0.04; MV: -0.4 mm vs. 0.3 mm, p=0.07). For FW kVCT and MCT data sets, the mean AMp MD-diffs varied insignificantly from mean participant-generated MD-diffs (kV: 0.0 mm vs. -1.1 mm,p=0.24; MV: -1.0 mm vs. -0.3 mm, p=0.6).

Table 3-21: MD-diff results for all catheter tubes combined.

MD-diff Results: All Catheter Tubes Combined						
***distances in mm**		**n**	**Mean**	**σ**	**95% CI**	**Range**
CTMR	**kV**	27	0.9	0.6	0.7-1.2	2.9
	MV	27	0.2	0.9	-0.1-0.5	3.4
FSDs	**kV**	27	0.1	1.4	-0.4-0.7	5.6
	MV	27	0.3	1.0	-0.1-0.7	3.8
FW	**kV**	27	-0.5	2.7	-1.5- 0.5	9.8
	MV	27	-0.4	1.3	-0.9-0.1	5.9
CTMR-AMp	**kV**	9	0.4	0.8	-0.1-1.0	2.1
	MV	9	-0.4	1.0	-1-0.3	3
FW-AMp	**kV**	9	0.0	1.4	-1.0-0.9	3.9
	MV	9	-1.0	1.5	-2.0-0.5	4.2

3.3.3.3 Ovoid Catheter Tubes

As shown in Table 3-22, the percentage of MD-diffs that were within the 2 mm criteria for the CTMR, FSDs and FW applicator kVCT data sets were 94%, 83% and 28%, respectively. The percentage of MD-diffs that were within the 2 mm criteria for MVCT data sets were 89%, 94% and 94%. All CTMR-AMp kVCT and MVCT dwells were within the 2 mm criteria whereas the FW-AMp kVCT and MVCT data sets resulted in 83% of dwells being within the 2 mm criteria, respectively. A two-proportion t-test showed that the percentage of MD-diffs meeting the 2 mm criteria for FSDs MVCT data sets was not significantly different from the percentage of MD-diffs meeting the 2 mm criteria for CTMR kVCT data sets (94% vs.

94%, p=0.4). The percentage of MD-diffs meeting the 2 mm criteria for FW MVCT data sets was not significantly different from CTMR kVCT data sets (94% vs. 94%, p=0.3).

Table 3-22: MD-diff results for all applicators for ovoid catheter tubes.

MD-diff Results: Ovoid Catheter Tubes									
		Number of points differing by:				Percent of points differing by:			
		[0-2mm]	[>2-5mm]	[>5-10mm]	[>10-15mm]	[0-2mm]	[>2-5mm]	[>5-10mm]	[>10-15mm]
CTMR	**kV**	17	1	0	0	94%	6%	0%	0%
	MV	17	1	0	0	94%	6%	0%	0%
FSDs	**kV**	15	3	0	0	83%	17%	0%	0%
	MV	17	1	0	0	94%	6%	0%	0%
FW	**kV**	5	11	2	0	28%	61%	11%	0%
	MV	17	1	0	0	94%	6%	0%	0%
CTMR-AMp	**kV**	6	0	0	0	100%	0%	0%	0%
	MV	6	0	0	0	100%	0%	0%	0%
FW-AMp	**kV**	5	1	0	0	83%	17%	0%	0%
	MV	5	1	0	0	83%	17%	0%	0%

Table 3-23 summarizes the sample characteristics of the MD-diff measures for ovoid catheters for all six data sets plus four AMp data sets. The mean MD-diff for all sample sets was within the 2 mm criteria. As determined by an unpaired t-test, the mean MD-diff for the FSDs MVCT was not significantly better than the mean MD-diff for the CTMR kVCT (0.7 mm vs. 1.0 mm, p=0.3). The mean MD-diff for the FW MVCT was significantly better than the mean MD-diff for the CTMR kVCT (-0.3 mm vs. 1.0 mm, p=0.00003). For the CTMR kVCT and MVCT data sets, the mean AMp MD-diffs varied insignificantly from mean participant-generated MD-diffs (kV: 0.6 mm vs. 1.0 mm, p=0.2; MV: -0.3 mm vs. 0.4 mm, p=0.2). For FW kVCT and MCT data sets, the mean AMp MD-diffs varied insignificantly from mean participant-generated MD-diffs (kV: -0.6 mm vs. -1.4 mm, p=0.1; MV: -0.3 mm vs. -0.3 mm, p=0.8). This suggests that, for distal ovoid dwell positions of the shielded FSDs and FW applicators, MVCT data sets provide sufficient visibility to accurately place distal source dwells within the TPS.

Table 3-23: MD-diff results for ovoid catheter tubes.

MD-diff Results: Ovoid Catheter Tubes						
*distances in mm		n	Mean	σ	95% CI	Range
CTMR	kV	18	1.0	0.7	0.6-1.3	2.9
	MV	18	0.2	1.0	-0.3-0.6	3.4
FSDs	kV	18	0.3	1.3	-0.3-1.0	5.6
	MV	18	0.5	0.9	0.1-0.9	3.0
FW	kV	18	-0.6	3.1	-2.0 -0.9	9.8
	MV	18	-0.5	1.0	-1.0-0.0	3.9
CTMR-AMp	kV	6	0.6	0.9	-.2-1.3	2.1
	MV	6	-0.3	1.1	-1.2-0.6	3
FW-AMp	kV	6	0.6	1.3	-0.6-1.7	3.3
	MV	6	-0.2	1.6	-1.6-1.2	4.1

3.3.3.4 Tandem Catheter Tubes

As shown in Table 3-24, the percentages of MD-diffs that were within the 2 mm criteria for the CTMR, FSDs and FW applicator kVCT data sets were 100%, 78% and 100%, respectively. The percentage of MD-diffs that were within the 2 mm criteria for MVCT data sets were 100%, 100% and 89%. All AMp-defined dwells were within the 2 mm criteria except for the FW MVCT which had 67% of dwells within the 2 mm criteria. A two-proportion t-test showed that the percentage of MD-diffs meeting the 2 mm criteria for FSDs MVCT data sets was not significantly different from the percentage of MD-diffs meeting the 2 mm criteria for CTMR kVCT data sets (94% vs. 94%, p=0.4). The percentage of MD-diffs meeting the 2 mm criteria for FW MVCT data sets was not significantly different from CTMR kVCT data sets (94% vs. 94%, p=0.3).

Table 3-24: MD-diff results for tandem catheter tubes. Applicator modeling plugin results were included as an alternate method of catheter reconstruction.

Catheter Reconstruction Results: Tandem Catheter Tubes									
		Number of points differing by:				Percent of points differing by:			
		[0-2mm]	[>2-5mm]	[>5-10mm]	[>10-15mm]	[0-2mm]	[>2-5mm]	[>5-10mm]	[>10-15mm]
CTMR	**kV**	9	0	0	0	100%	0%	0%	0%
	MV	9	0	0	0	100%	0%	0%	0%
FSDs	**kV**	8	1	0	0	89%	11%	0%	0%
	MV	9	0	0	0	100%	0%	0%	0%
FW	**kV**	9	0	0	0	100%	0%	0%	0%
	MV	8	1	0	0	89%	11%	0%	0%
CTMR-AMp	**kV**	3	0	0	0	100%	0%	0%	0%
	MV	3	0	0	0	100%	0%	0%	0%
FW-AMp	**kV**	3	0	0	0	100%	0%	0%	0%
	MV	2	1	0	0	67%	33%	0%	0%

Table 3-25 summarizes the sample characteristics of the MD-diff measures for tandem catheters for all six data sets plus four AMp data sets. The mean MD-diff for all sample sets was within the 2 mm criteria. As determined by an unpaired t-test, the mean MD-diff for the FSDs MVCT was not significantly better than the mean MD-diff for the CTMR kVCT (0.1 mm vs. 0.9 mm, p=0.08). The mean MD-diff for the FW MVCT was not significantly different than the mean MD-diff for the CTMR kVCT (-0.2 mm vs. -0.9 mm, p=0.1). No statistical tests were applied to AMp-defined tandem catheter dwells as the sample size was too small. This suggests that, for distal tandem dwell positions of the shielded FSDs and FW applicators, MVCT data sets provide sufficient visibility to accurately place distal source dwells within the TPS.

Table 3-25: MD-diff results for tandem catheter tubes.

MD-diff Results: Tandem Catheter Tubes						
*distances in mm		n	Mean	σ	95% CI	Range
CTMR	kV	9	0.9	0.4	0.7-1.2	1.1
	MV	9	0.3	0.6	-0.1-0.7	2.0
FSDs	kV	9	-0.3	1.7	-1.4-0.9	4.5
	MV	9	0.1	1.3	0.8-1.0	3.4
FW	kV	9	-0.4	1.7	-1.5-0.8	4.4
	MV	9	-0.2	1.9	-1.5-1.1	5.9
CTMR-AMp	kV	3	0.2	0.9	-0.4-0.8	0.8
	MV	3	-0.5	1.1	-2.0-1.0	2
FW-AMp	kV	3	-1.2	1.3	-1.7- -0.8	0.6
	MV	3	-1.2	1.6	-2.9-0.5	2.4

3.3.3.5 Catheter Reconstruction Results Discussion

A summary of catheter reconstruction results is given in Table 3-26. For all MVCT data sets, participant-defined MD-diff results either remained the same as or improved upon kVCT results, with the exception of one outlier for the FW MVCT tandem distal dwell location (=-2.3). Utilization of CT/MR compatible applicators with kVCT imaging is current clinical practice at many institutions. This suggests that MVCT imaging of shielded applicators could possibly be implemented as clinical practice with no reduction in quality compared to CT/MR compatible applicators with kVCT..

Table 3-26: Summary of MD-diff results for all catheter tubes, tandem tubes and ovoid tubes.

Summary of MD-diff Measures Meeting ±2 mm Criteria				
		All	Tandem	Ovoids
CTMR	kV	96%	100%	94%
	MV	93%	100%	89%
FSDs	kV	85%	89%	83%
	MV	96%	100%	94%
FW	kV	52%	100%	28%
	MV	93%	89%	94%
CTMR-AMp	kV	100%	100%	100%
	MV	100%	100%	100%
FW-AMp	kV	89%	100%	83%
	MV	78%	67%	83%

Table 3-26 shows the advantage of MVCT when utilizing shielded T&O applicators. Both shielded T&O applicators saw an improvement in terms of the number of MD-diff measures within 2 mm. Most noticeable is the improvement within the ovoid region where 28% of MD-diff measures on kVCT were within 2 mm of the control, which improved to 94% of MD-diff measures on MVCT being within 2 mm, a change of +66%.

Though no clinics are currently utilizing the AMp to facilitate catheter reconstruction for shielded applicators, these results indicate that further consideration should be given for clinical implementation of the AMp. It appears from these results that a combination of the AMp with MV imaging would allow for accurate catheter reconstruction of the distal dwell location. Limitations of these results include small sample sizes and only one participant performing organ segmentation.

Chapter 4 Conclusions

4.1 Summary of Results

This study demonstrated that MVCT is a feasible alternative for acquiring clinically viable CT data sets of shielded T&O-type applicators, specifically Nucletron's tungsten-shielded Fletcher-Williamson applicator and Varian's stainless steel-shielded Fletcher-Suit-Delclos-style applicator. Results indicate that MVCT data sets acquired of the shielded FSDs and FW T&O applicators consistently display sufficient image quality to allow for accurate organ segmentation. The ability to accurately segment OARs in the artifact region is critical for correct DVH analysis, providing the best opportunity for early and late sequelae prevention. Catheter reconstruction quality for MVCT data sets of the shielded FSDs and FW applicators was comparable to the catheter reconstruction performed for kVCT data sets of the unshielded, artifact-free CTMR applicator. Overall, TomoTherapy's Hi Art II MVCT scanner yielded image sets displaying sufficient image quality to facilitate accurate and acceptable organ segmentation and catheter reconstruction. Utilization of Nucletron's AMp yielded catheter reconstruction quality comparable to that achieved by participants for kVCT and MVCT data sets.

4.2 Response to Hypothesis

In response to the hypothesis, neither kVCT nor MVCT yielded image sets of sufficient quality for all physicists to meet the hypothesis metrics for the criterion used in this study. While the criterion may not be realistic for day-to-day clinical standards, they did provide a sufficient metric to compare kVCT imaging of the CTMR applicator with MVCT imaging of the FW and FSDs applicators. MVCT imaging of shielded FW and FSDs applicators was sufficiently comparably to the current, clinical standard that further consideration need be given to include MVCT as proper procedure for the imaging of cervical cancer patients treated using shielded tandem and ovoid applicators.

4.3 Future Work

For both 2D and 3D organ segmentation methods, the bladder consistently had fewer CTP-diffs and reconstructed volumes meeting the hypothesis criteria. A new method of developing surrogate bladder structures should be explored to allow consistency of results throughout the experiment.. This could be done by first making a rigid structure around which the bladder could mold rather than around an inflated balloon which is prone to stretching the hot aquaplast. Another possible solution could be to purchase or develop a rigid pelvic phantom designed specifically for the T&O applicators being explored, possibly utilizing technology offered commercially.

A number of parameters in this study, such as slice thickness, could be better controlled to mitigate errors arising from differences in kV and MV image acquisition. Though the SFOV would not physically change much, it could potentially reduce any bias towards either kVCT or MVCT imaging. Also, matched slice thicknesses would potentially reduce TPS volume reconstruction errors due to interpolating over larger volumes on MVCT data sets than kVCT data sets.

Regarding catheter reconstruction, the method used in this study was only capable of validating the most distal dwell position of each applicator tube. Another strategy could be investigated, allowing for the accuracy of all dwell locations to be validated. A possible idea would be to rigidly attach two fiducial markers in line with each other and in the same sagittal plane as the catheter tube dwell positions. This would facilitate distance and angle measures between the fiducial markers and each of the catheter's dwell locations. The clinical commissioning procedure would, in theory, work for determining control values for a study of this nature.

The use of Nucletron's AMp for catheter reconstruction in this study approached the accuracy of the participant-defined catheter reconstruction. This catheter reconstruction was solely performed by the investigator. To validate the AMp for clinical use, the next step should be to increase the sample size as well as the number of medical physicists participating in the study.

References

Aubin, M., 2006. The use of megavoltage cone-beam CT to compliment CT for target definition in pelvic radiotherapy in the presence of hip replacement. *The British Institute of Radiology,* Volume 79, pp. 918-921.

Awschalom, M., 1983. *About Phanta for Clinical Neutron Dosimetry, Fermilab.* [Online]
Available at: lss.fnal.gov
[Accessed November 2011].

Bentel, G. C., 1996. *Radiation Therapy Planning.* s.l.:McGraw-Hill Professional.

Elert, G., Sutherland, K. & M., M., 2004. *Density of Steel.* [Online]
Available at: http://hypertextbook.com/facts/2004/KarenSutherland.shtml
[Accessed 18 April 2012].

Glover, G. H. & Pelc, N. J., 1981. An algorithm for the reduction of metal clip artifacts in CT reconstructions. *The International Journal of Medical Physics Research and Practice,* 8(6), pp. 799-807.

Hansen, E. K. et al., 2006. Image-Guided Radiotherapy using megavoltage cone-beam computed tomography for treatment of paraspinous tumors in the presence of orthopedic hardware. *The International Journal of Radiation Oncology Biology Physics,* 66(2), pp. 323-326.

Horton, J., Lawyer, A. & Mourtada, F., 2005. *The American Association of Physics in Medicine.* [Online]
Available at: http://www.aapm.org/meetings/05SS/program/LDR_PDR_Afterloaders_Horton.pdf
[Accessed May 2011].

Hsieh, J., 1998. Adaptive streak artifact reduction in computed tomography resulting from excessive x-ray photon noise. *The International Journal of Medical Physics Research and Practice,* pp. 2139-2147.

Jameson, M. G. et al., 2010. A review of methods of analysis in contouring studies for radiation oncology. *Journal of Medical Imaging and Radiation Oncology,* Volume 54, pp. 401-410.

Kalendar, W., Hebel, R. & Ebersberger, J., 1987. Reduction of CT Artifacts Caused by Metallic Implants. *Radiology,* pp. 576-577.

Kapp, K. S. et al., 1997. Carcinoma of the cervix: analysis of complications after primary external beam radiation and Ir-192 HDR brachytherapy. *Radiotherapy and Oncology,* pp. 143-153.

Korol, R. M. et al., 2010. Three-dimensional image-based planning for cervix brachytherapy with bilateral hip prostheses: A solution using MVCT with helical tomotherapy. *Brachytherapy,* Volume 9, pp. 278-281.

Krishnan, K. H., 2011. *The Anatomy of Rectum.* [Online]
Available at: http://www.slideshare.net/visprod/anatomy-of-rectum
[Accessed 12 April 2012].

Meeks, S. L. et al., 2005. Performance characterization of megavoltage computed tomography imaging on a helical tomotherapy unit. *The International Journal of Medical Physics Research and Practice,* 32(8), pp. 2673-2681.

National Cancer Institute, N., 2011. *Surveillance Epidemiology and End Results.* [Online]
Available at: http://www.seer.cancer.gov/statistics/
[Accessed 12 April 2011].

Naydenov, S. V. & Ryzhikov, V. D., 2005. *Direct reconstruction of the effective atomic number of materials by the method of multi-energy radiography,* Livermore: Lawrence Livermore National Laboratory.

Noll, C. & Stanton, F. D., 2011. [Online]
Available at: http://www.hemorrhoid.net/anatomy.php

Pokhrel, D. et al., 2011. Localizing intracavitary brachytherapy applicators from cone-beam CT x-ray projections via a novel iterative forward projection matching algortihm. *The International Journal of Medical Physics Research and Practice,* pp. 1070-1079.

Price, M. J., 2008. *The Imaging and Dosimetric Capabilities of a CT/MR-suitable, Anatomically Adaptive, Shielded Intracavitary Brachytherapy Applicator for the Treatment of Cervical Cancer,* s.l.: s.n.

Price, M. J., 2008. *The imaging and dosimetric capabilities of a novel, CT/MR-suitable, anatomically adaptive, shielded HDR/PDR ICBT applicator for the treatment of cervical cancer,* s.l.: s.n.

Price, M. J. et al., 2009. Monte Carlo model for a prototype CT-compatible, anatomically adaptive, shielded intracavitary brachytherapy applicator for the treatment of cervical cancer. *Medical Physics,* pp. 4147-4155.

Roeske, J. C. et al., 2003. Reduction of computed tomography metal artifacts due to the Fletcher-Suit applicator in gynecology patients receiving intracavitary brachytherapy. *Brachytherapy,* pp. 207-214.

RPD, I., 2011. *Radiation Products Design, INC.* [Online]
Available at: www.rpdinc.com
[Accessed November 2011].

Ruchala, K. J., Olivera, G. H., Schloesser, E. A. & Mackie, T. R., 1999. Megavoltage CT on a Tomotherapy System. *Physics in Medicine and Biology,* Volume 44, pp. 2597-2621.

Saibishkumar, E. P., Patel, F. D. & Sharma, S. C., 2005. Results of radiotherapy alone in the treatment of carcinoma of uterine cervix: a retrospective analysis of 1069 patients. *International Journal of Gynecological Cancer,* pp. 890-897.

Shaw, D., 2001. *Volume of a Human Bladder.* [Online]
Available at: http://hypertextbook.com/facts/2001/DanielShaw.shtml
[Accessed January 2012].

Varian Medical Systems, 2009. *Varian Brachytherapy Products: Applicators and Accessories.* s.l.:Varian Medical Systems.

Verellen, D. et al., 1994. On the determination of the effective transmission factor for stainless steel ovoid shielding segments and estimation of their shielding efficacy for the clinical situation. *The International Journal of Medical Physics Research and Practice,* pp. 1677-1684.

Viswanathan, A. N., Petereit, D. G. & Devlin, P. M., 2007. *Brachytherapy: Applications and Technique.* Philadelphia: Lippincott Williams & WIlkins.

Viswanathan, A. N. et al., 2011. *American Brachytherapy Society Cervical Cancer Brachytherapy Task Group.* [Online]
Available at: http://www.americanbrachytherapy.org/guidelines/cervical_cancer_taskgroup.pdf
[Accessed 1 November 2011].

Wagner, T. et al., 2009. Megavoltage computed tomography image-gased low-dose rate intracavitary brachytherapy planning for cervical carcinoma. *Technology in Cancer Research and Treatment,* 8(2), pp. 123-130.

Weeks, K. J. & Montana, G. S., 1997. Three-dimensional applicator system for carcinoma of the uterine cervix. *International Journal of Radiation Oncology Biology Physics,* 37(2), pp. 455-463.

Williamson, J. F., 1990. Dose calculations about shielded gynecological colpostats. *International Journal of Radiation Oncologoy Biology Physics,* pp. 167-178.

Williamson, J. F. et al., 2002. Prospects for quantitative computed tomography imaging in the presence of foreign metal bodies using statistical image reconstruction. *The International Journal of Medical Physics Research and Practice,* pp. 2404-2418.

Yank, C. et al., 2010. Utility of Megavoltage Fan-Beam CT for Treatment Planning in a Head-And-Neck Cancer Patient with Extensive Dental Fillings Undergoing Helical Tomotherapy. *Medical Dosimetry,* pp. 108-114.

Yazdia, M., Gingras, L. & Beaulieu, L., 2005. An adaptive approach to metal artifact reduction in helical computed tomography for radiation therapy treatment planning: experimental and clinical studies. *The International Journal of Radiation Oncology Biology Physics,* pp. 1224-1231.

Yorke, E. D. et al., 1987. Using measured dose distribution data of the Fletcher-Suit-Delclos colpostat in brachytherapy treatment planning. *International Journal of Radiation Oncology Biology Physics,* pp. 1413-1419.

Appendix A: Surrogate Structures-Contrast Agent vs. Aquaplast

The use of contrast agent was explored as an aid in organ segmentation for MVCT scans. ICRU report 38 specifies the use of a bladder Foley catheter filled with 7 ml of contrast to aid in the localization of ICRU-defined bladder point. The percentage of actual contrast to saline is up to individual clinics to decide what suits them best. At MBPCC, a 7% solution of Omnipaque 300 mgI/ml mixed with a normal saline is typically used. This was tested with the MVCT scanner and determined undistinguishable when compared with surrounding water for most center and width values. The amount of contrast was increased to 10%. Visual inspection of the 10% contrast scans yielded what were thought to be acceptable results however a comparison of contours generated from the kVCT and MVCT scans for the CTMR applicator (no artifact present) showed that the MVCT structure had a volume 15.1% smaller than that of the kVCT. It was concluded that 10% contrast also provided insufficient contrast. Higher contrast amounts were explored however it was observed that, as contrast levels increased, streaking artifacts were introduced into the kVCT scans due to the high effective atomic number of iodinated contrast (≈54). At a 50% contrast agent to saline mixture, the rectum structure contrast was acceptable on MVCT scans and also lacked streaking artifact making this a desirable setup if one is solely using MVCT. Due to the streaking artifact issues along with the bladder and rectum structure rigidity issues, an alternative was sought to deformed condoms filled with contrast agent and thus, aquaplast became the material of choice. It is still possible that clinically acceptable results may be achieved with the use of a high percentage contrast to saline mixture however accurate comparisons between kVCT and MVCT are not feasible due to streaking artifact. Meeks et al determined that MVCT provides sufficient contrast to contour the bladder and rectum therefore it would be feasible to conduct a future experiment using high percentages of contrast agent in a Foley balloon catheter for MVCT treatment planning scans. (Meeks, et al., 2005)

The use of air, a negative contrast agent, was also explored. A positive contrast agent has a higher attenuation coefficient than surround materials whereas a negative contrast agent as a lower attenuation coefficient than surrounding tissues. Iodinated contrast is an example of a positive contrast agent and air is an example of a negative contrast agent. Negative contrast agents can be used effectively on kVCT and MVCT scans. Korol *et al.* used air as a Foley catheter contrast agent for MVCT treatment planning scans of cervical cancer patients with bilateral hip prostheses treated with a Varian CT/MR compatible tandem and ovoid applicator. (Korol, et al., 2010) Air is also commonly used in GI radiographs for procedures such as Barium-air enemas. Reconstruction algorithms can compensate for air heterogeneities resulting in no artifact from contrast agents. I observed that for both kVCT and MVCT, distinguishing between air and soft tissue is a trivial matter. Several drawbacks prevented the use of air. First, is that a Foley catheter is no longer used to calculate dose to the ICRU-defined bladder point; rather, dose is calculated to the hottest 2CC of bladder tissue using DVH analysis. Second, there are no current, clinical methods for filling the bladder and rectum organs with air so it is clinically irrelevant. Third, it has already been shown that MVCT scans provide sufficient contrast to delineate the bladder, rectum and sigmoid colon in the absence of metal artifact. (Meeks, et al., 2005) This means that if MVCT can reduce the shielded T&O applicator induced metal artifact, then there is the possibility that adequate contrast will be present in the CT scan to segment the bladder, rectum and sigmoid colon.

Appendix B: Participation Instructions

Purpose of research:

The purpose of this research is to compare the quality of organ segmentation and catheter reconstruction for HDR cervical brachytherapy administered using 3 different tandem and ovoid (T&O) applicators: Nucletron's shielded CT/MR compatible, Nucletron's shielded Fletcher-Williamson, and Varian's shielded Fletcher-Suit-Delclos-style. The quality of plans will be determined by organ segmentation and catheter reconstruction accuracy. A water phantom, containing only a bladder surrogate, a rectum surrogate and HDR T&O applicator is used to facilitate these measurements. KVCT and MVCT imaging modalities have been used to acquire the image sets you will use for treatment planning.

Participant's Responsibility:

For the 7 image sets, you are asked to segment the bladder and rectum structures in the pelvic water phantom. To minimize confusion there are only four constituents to the phantom: a bladder surrogate, a rectum surrogate, water and one of 3 HDR T&O applicators. The bladder is the anterior structure; the rectum is the posterior structure. You will see fiducial markers on the bladder and rectum surrogates. Any time these markers appear, do your best to ignore them.

You are also asked to perform catheter reconstruction for the tandem and ovoids in image sets where an applicator is visible.

Several guidelines are given for TPS setup, Organ Segmentation, and Catheter reconstruction. Please follow the specified guidelines. For all other TPS settings, follow your clinical protocol.

*__Please provide a copy of your clinical protocol for HDR cervical brachytherapy__.

Order of Events:

1. For the image sets, follow the numerical order for organ segmentation and catheter reconstruction. DO NOT VIEW THE NEXT IMAGE SET UNTIL ORGAN SEGMENTATION AND CATHETER RECONSTRUCTION IS COMPLETE. Doing so could compromise the integrity of your results.

2. While performing organ segmentation and catheter reconstruction, fill out the corresponding image set instructions/information sheet.

3. Once completed, export the image sets with the plan and structure information. Please place the image sets in folders with the same number but add the label *completed*. For example, you receive a folder labeled: *1*. When you are finished, you create a new folder labeled: *1-completed*.

Oncentra Masterplan Settings:

1. Change Image Smoothing to Lanczos window:

   Tools menu → Options → General → Image Smoothing

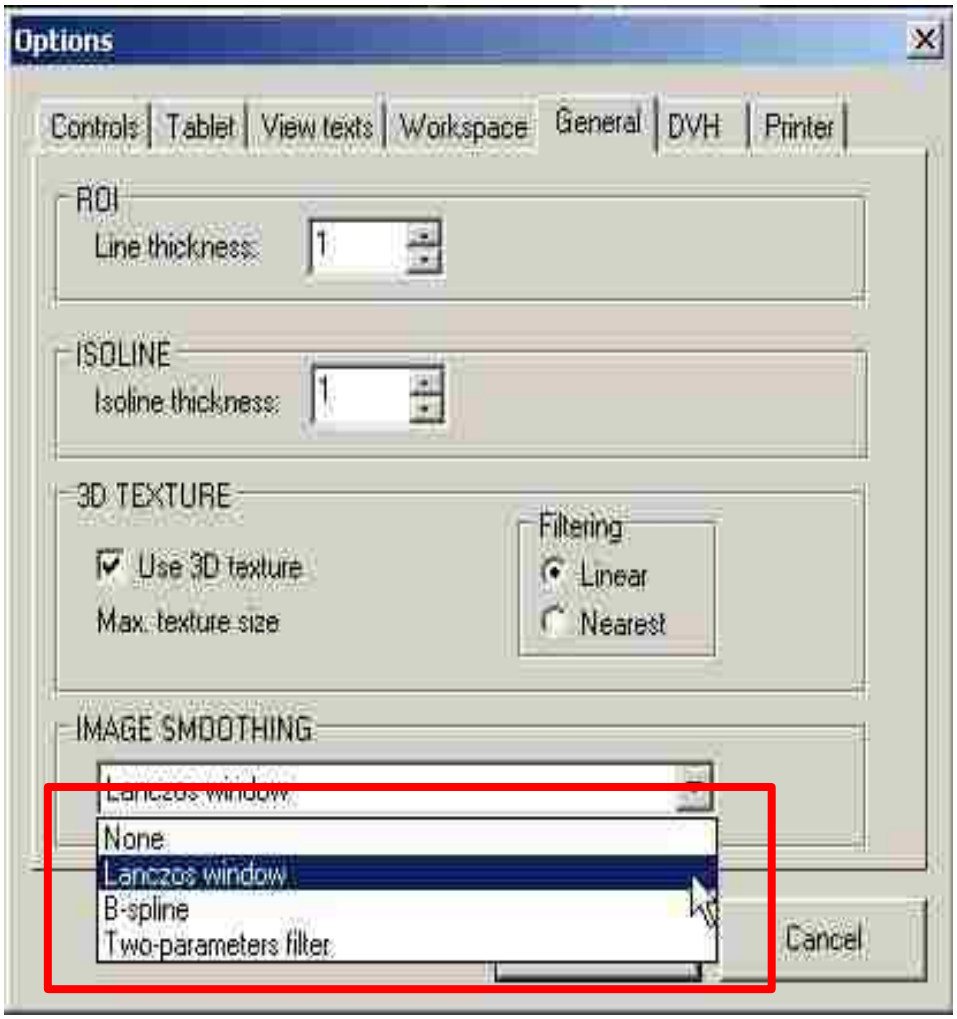

2. Verify ROI voxel size is 2 mm

ROI menu → Manage ROI Catalog… → ROI Catalog (choose ROI name *i.e.* Bladder) → edit → deselect Automatic Voxel Size (if already selected) → Change voxel size to 2 mm

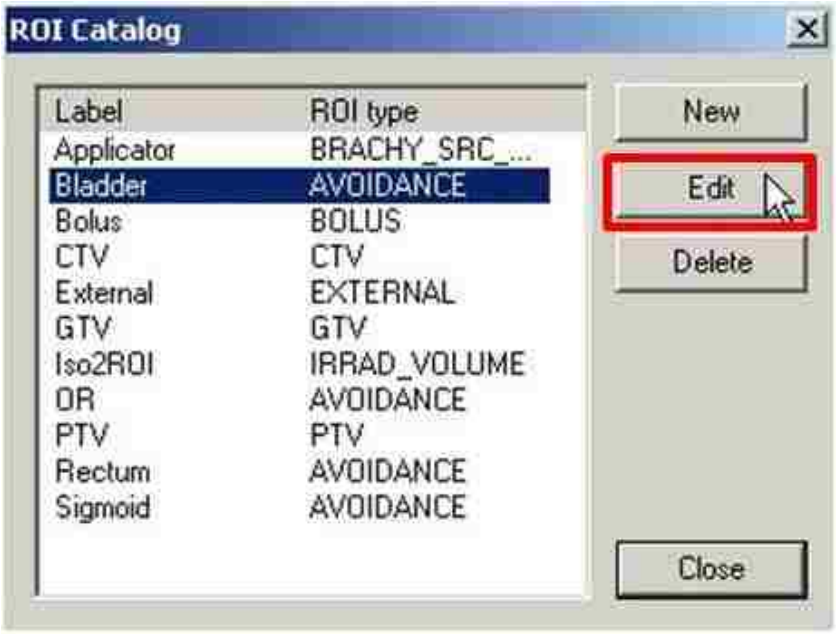

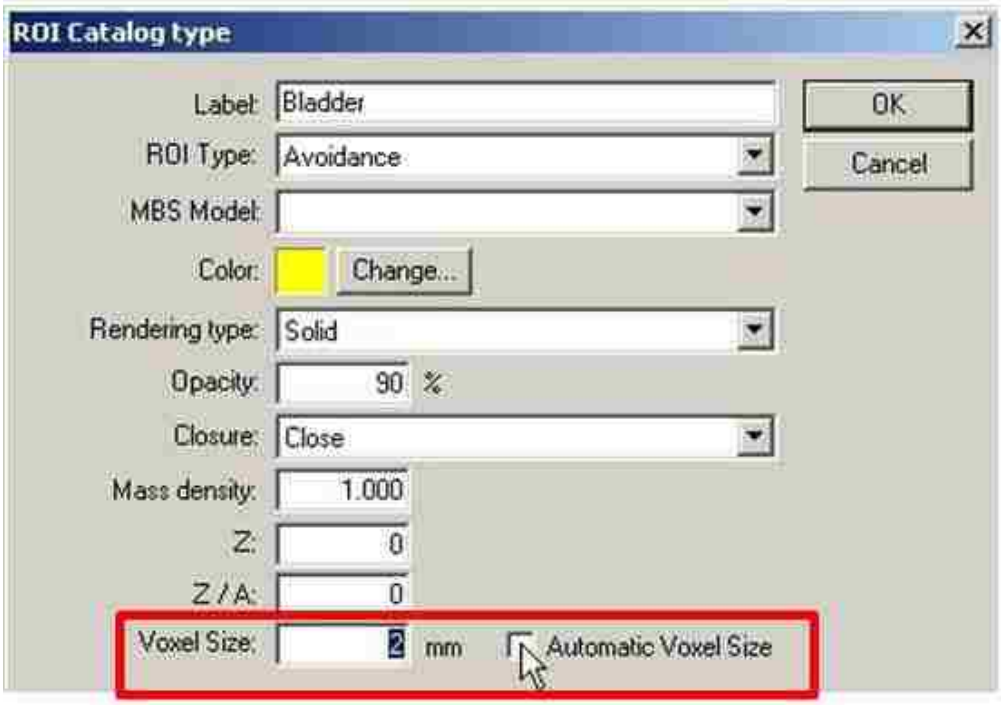

Organ Segmentation Instructions:

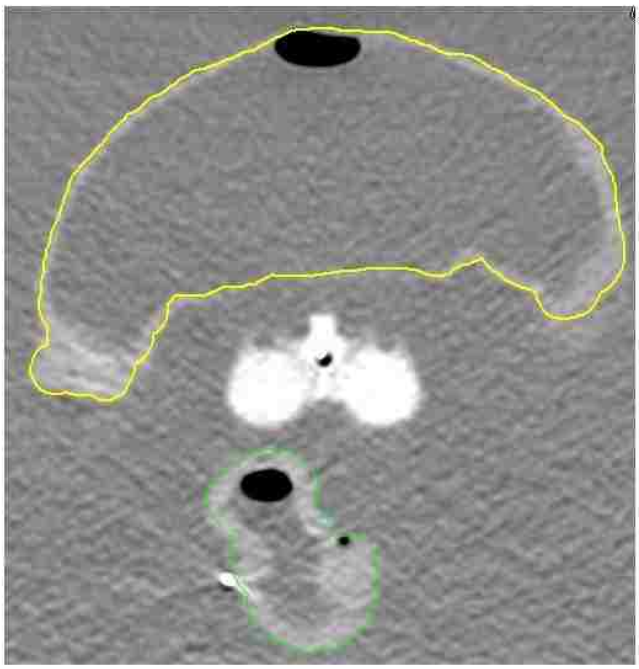

Right

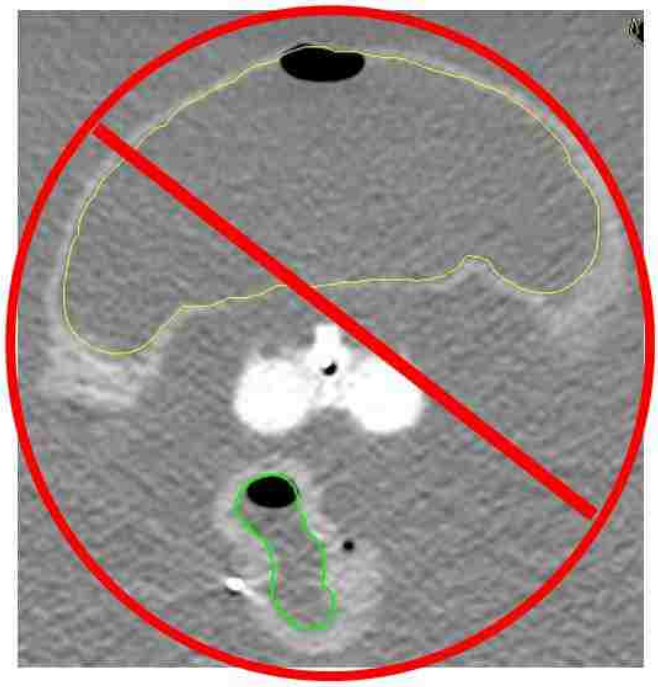

Wrong

1. This is an example of what you will see-yellow is the bladder, green is the rectum.
    a. Segment to the outer edge of the tissue wall
    b. Ignore fiducial markers. They lie directly on the surface of the structures so assume the tissue continues directly inside the markers.
    c. When image artifact is present, do the best guesswork you can.
    d. <u>Record Window/Level presets or values that were used</u>

Because you are contouring a phantom, you need to be aware of two things:

1. The bladder immobilization arm can inhibit segmentation. In the image series below you can see where it begins to come off the bladder. Slice numbers will be given were this approximation should be made (see the instructions for each image set). Using your best approximation, follow the example in the images below.

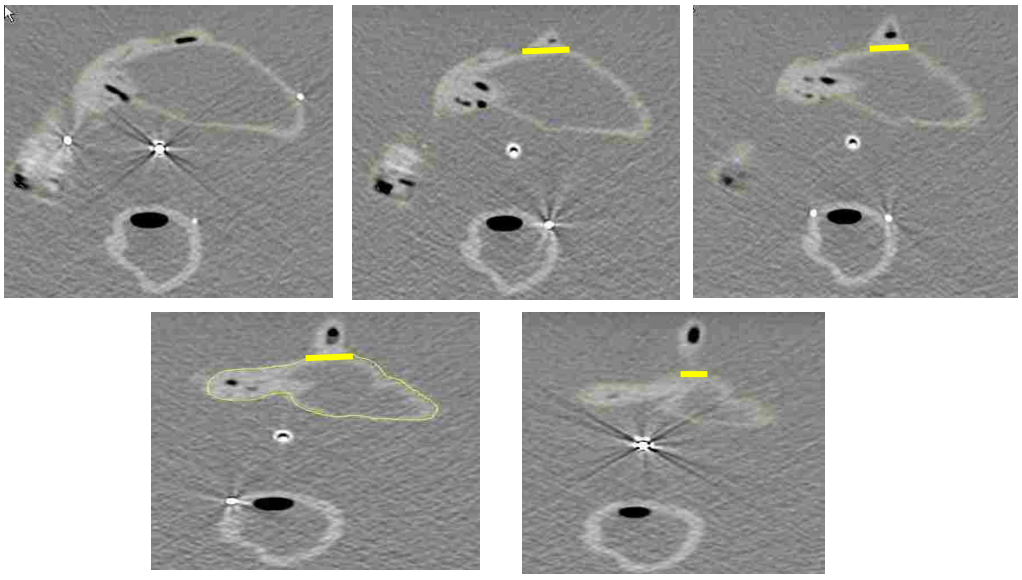

2. Unlike a true rectum, the surrogate rectums have defined start and end points. An example of a starting point is shown below. Please contour all parts of the rectum visible in each CT slice.

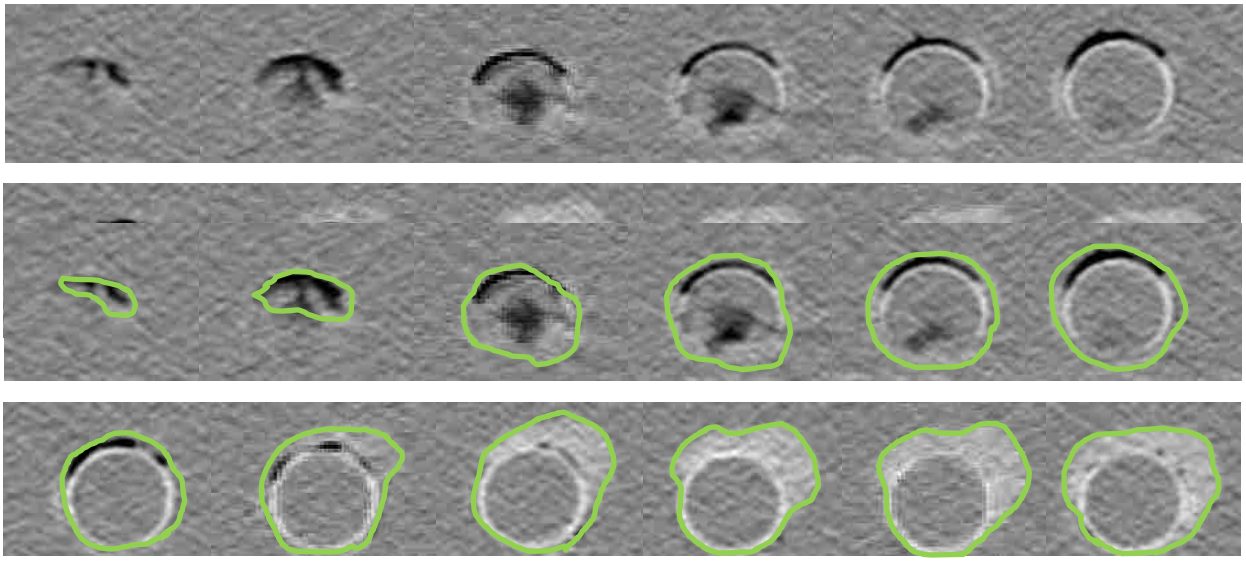

Catheter Reconstruction:

If source position markers are visible, plan off those. Source position markers will not be visible for the shielded T&O applicators in which case you are expected to follow your current, clinical protocol for catheter reconstruction of shielded T&O applicators (*e.g. at Mary Bird Perkins Cancer Center and MD Anderson, the first dwell position is chosen by placing the center of the source in the center of the tube 7 mm from the ovoid tip*)

Within Oncentra, please use the following settings for catheter reconstruction:

1. Under preferences, choose “No Sequencing”
2. Under Catheters, choose 3 for the number of catheters
3. Under Applicator Properties, choose:
    a. 5.0 mm source step
    b. Start at **Tip End**

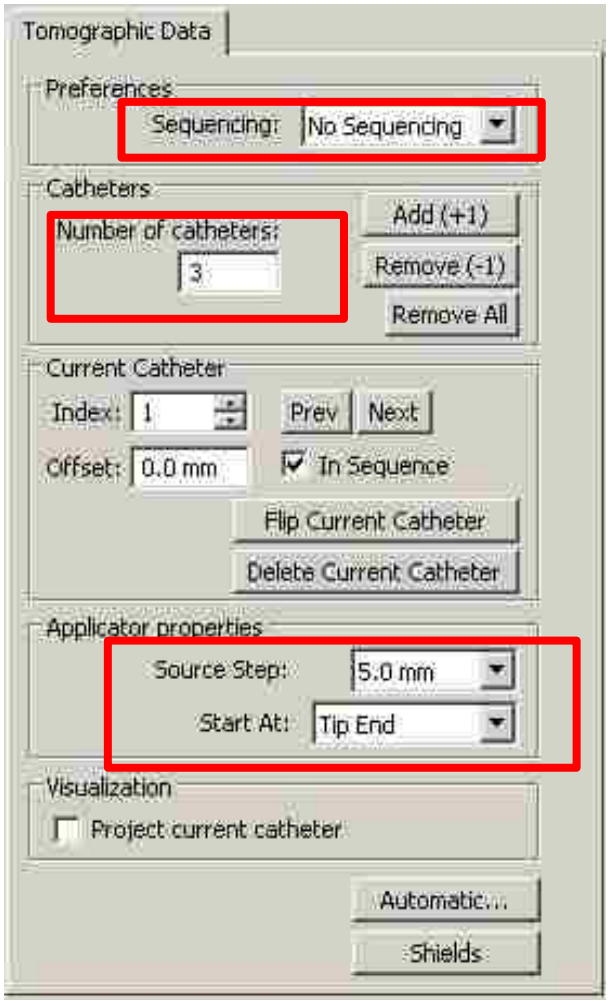

*Also, be aware when performing catheter reconstruction for the applicator(s) with source position markers visible that a fiducial marker has been placed on the tandem and it should not be confused with the source position markers for catheter reconstruction. See image below.

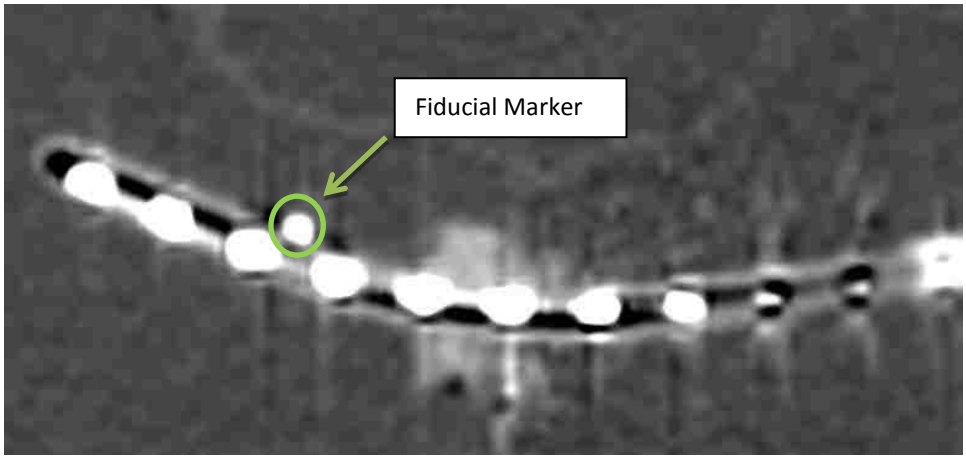

Export Instructions (for those at institutions other than Mary Bird Perkins):
After performing organ segmentation and catheter reconstruction, you will need to export your plan information.

1. Be sure to save the current plan (under File tab).
2. Click the Export tab:

3. This will then give you the option of what you want to export. At this point, you just need to choose the "RT Plan". This will contain all the organ segmentation and catheter reconstruction information.

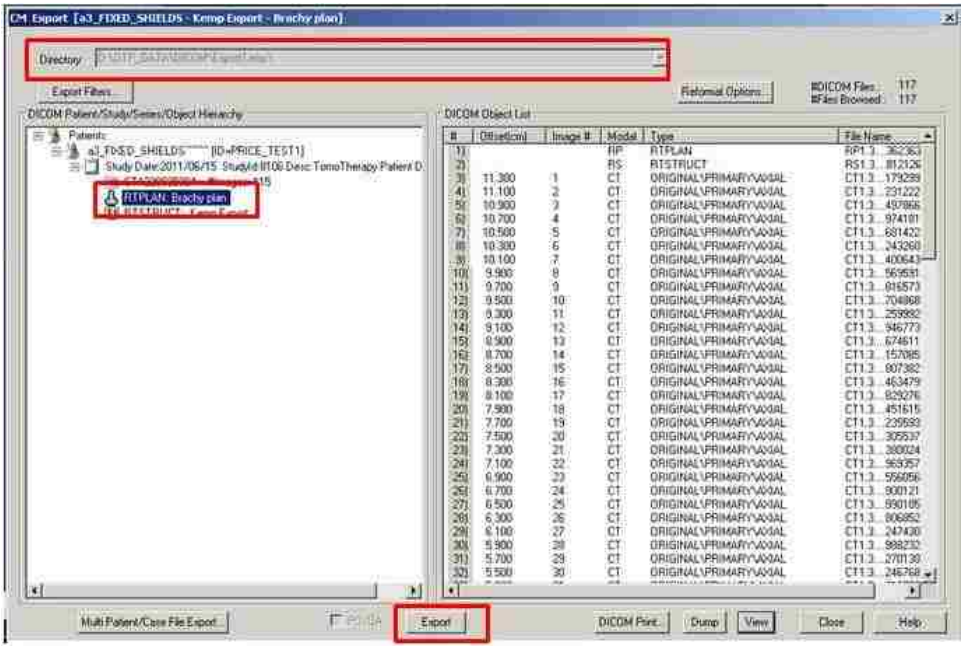

4. Next, click export on the bottom of the window.

5. Now, you will want to go to the location listed in the "Directory" spot above. In this case it is: D:\OTP_DATA\DICOM\ExportTemp\. From here, you can just copy all the files into a folder and label it in the style mentioned above (*i.e.* image set 1 is labeled *1-Completed*).

6. Lastly, organize all of your image sets, zip them (conserve space and save time), and upload them to the amazon cloud server.

Appendix C: Participant's Raw Results

The results for the participants of this study are reported in following subsections. An analysis and discussion of these results is given in Section 3.3.1. For all raw results, values highlighted in red differed by more than the hypothesized metric values. In the case of two-dimensional organ segmentation analysis, values highlighted in yellow signify values that met the hypothesis metric of ±2 mm but differed by more than 1 mm from the control value. For catheter reconstruction accuracy, values highlighted in yellow signify value that met the hypothesis metric of ±2 mm however were outside the mechanical tolerance of the treatment delivery system (±1 mm).

Physicist 1

Table C-1: Results from two-dimensional CTP organ segmentation measurements for surrogate rectum structures. Color coding for columns displaying differences from control values is as follows: No coloring signifies results within 1 mm of control values, yellow coloring signifies results differing from the control values by 1-2 mm, light red signifies results differing from control values by 2-5 mm and dark red signifies results differing from control values by more than 5 mm. Clear and yellow results met the hypothesis criteria of ±2 mm. The terms "sup", "mid", and "inf" refer to locations relative to the artifact region. Sup=superior, inf=inferior and mid=middle.

CTP: Rectum Results

*distances in mm		Measured values									Absolute difference from control values								
	angle:	**0**	**40**	**80**	**120**	**160**	**200**	**240**	**280**	**320**	**0**	**40**	**80**	**120**	**160**	**200**	**240**	**280**	**320**
CTMR kV 2	**sup**	10.7	10.1	13.4	19.1	19.7	20.9	23.6	24	17.9	0.9	1	0.5	1.2	0.1	0.4	0.7	0.2	1.3
	mid	30.6	26.6	18.9	16.6	21.4	22.9	16.1	16.3	22.9	1.8	2.7	0.4	1.9	0.6	1.1	0.1	2	1.5
	inf	18.3	18.4	16.7	16.5	15.3	17.1	16.8	17.9	18.1	0	0.7	0.6	0.2	0.9	1.6	0.7	0.1	0.1
CTMR MV 3	**sup**	13.6	13.1	12.8	14.1	19.3	25	26.9	19.6	16.2	0.8	1	0.4	0.3	0.5	0.6	2.2	1	0.5
	mid	13.1	21	24.3	16.3	17.4	17.5	17.6	14.8	12.5	0.4	0.2	0.7	4.8	**6.8**	2.1	0.8	1.3	0.1
	inf	16.6	16.1	16.5	17.4	20.6	20.5	19.9	21.2	20.3	0.8	1.1	0.4	0.7	0.2	1.1	1.4	0.4	0.8
FW kV 3	**sup**	14.1	13	12.7	15	21.4	24.8	25.8	19.6	16.5	1.3	0.9	0.3	0.6	1.6	0.4	1.1	1	0.2
	mid	13.3	18.8	21.2	18.6	15.4	15.9	17.5	14.8	12.1	0.6	2.4	2.4	**7.1**	4.8	0.5	0.9	1.3	0.3
	inf	16.6	15.4	16.2	17.2	20.7	20.7	18.6	20.3	19.8	0.8	0.4	0.1	0.5	0.3	1.3	0.1	0.5	0.3
FW MV 1	**sup**	18.2	13.8	14.5	15.8	23.2	17.6	15.1	13.3	18.2	2.3	0.2	1.3	0	3.3	1.5	0.6	2.3	1.7
	mid	11.5	16.9	23.9	17.9	16.4	16.8	19.3	18.9	15.1	4.3	2	0.1	1.7	2.1	2	0.9	3.5	**5.4**
	inf	23.5	13	14	19.1	14.3	14.1	19.3	23.2	26	3.2	1	1.6	1.9	1.2	1.5	0.5	1.1	0.3
FSDs kV 1	**sup**	15.5	13.1	12.6	15.5	20.4	16.9	17.6	15.5	17.1	0.4	0.5	0.6	0.3	0.5	0.8	1.9	0.1	0.6
	mid	13.7	18.9	18.3	17.1	15.2	16.8	19.9	15.9	15.3	**6.5**	4	**5.7**	0.9	0.9	2	1.5	0.5	**5.6**
	inf	21.2	12.5	13.3	16.7	13.8	12.8	17.9	22.7	25.7	0.9	0.5	0.9	0.5	0.7	0.2	0.9	1.6	0
FSDs MV 2	**sup**	11.5	10.7	14.6	19.1	21.2	21.8	23.4	24.1	16.3	1.7	1.6	1.7	1.2	1.6	0.5	0.5	0.3	0.3
	mid	28.5	24.1	18.4	18.6	21.5	21.6	17.5	15.9	21.2	0.3	0.2	0.1	0.1	0.5	0.2	1.3	1.6	0.2
	inf	17.4	19.4	16.5	16.5	15.5	17.8	18.1	19.2	18.2	0.9	0.3	0.4	0.2	1.1	2.3	2	1.4	0

Table C-2: Results from two-dimensional CTP organ segmentation measurements for surrogate bladder structures. Color coding for columns displaying differences from control values is as follows: No coloring signifies results within 1 mm of control values, yellow coloring signifies results differing from the control values by 1-2 mm, light red signifies results differing from control values by 2-5 mm and dark red signifies results differing from control values by more than 5 mm. Clear and yellow results met the hypothesis criteria of ±2 mm. The terms "rlat", "mid" and "llat" refer to locations relative to the artifact region. Rlat=right lateral, llat= left lateral and mid=middle.

CTP: Bladder Results

*distances in mm		Measured values									Absolute difference from control values								
	angle:	**0**	**40**	**80**	**120**	**160**	**200**	**240**	**280**	**320**	**0**	**40**	**80**	**120**	**160**	**200**	**240**	**280**	**320**
CTMR kV 2	**rlat**	15.2	17.9	19.1	20.6	19.1	18.2	24	21.7	15.8	0.9	0.6	0.5	4.4	3.1	1.3	0.3	0.8	0.4
	mid	29.2	32.6	37.2	28.2	24.9	24.8	26.7	32.1	33	1.8	2.8	1.5	0.4	0.3	0.3	0.9	0.9	0.8
	llat	16	13.8	14.6	18.5	19.3	18.4	18.6	15.5	15.4	0.4	0.1	1.3	0.6	1.2	2.3	2.8	0.1	1.7
CTMR MV 3	**rlat**	16.4	19.5	19.9	19.7	19.4	21.2	25.9	22.3	15.1	2.1	1	0.3	3.5	3.4	4.3	1.6	0.2	0.3
	mid	31.9	35.3	38.4	27.9	25.1	24	28.7	32.4	35.6	4.5	**5.5**	0.3	0.7	0.1	0.5	1.1	0.6	1.8
	llat	17.1	13.7	13.6	18.3	20.3	19.1	19.1	18.1	15.7	0.7	0	0.3	0.4	2.2	3	3.3	2.5	2
FW kV 3	**rlat**	14.8	18.4	17.7	17.9	17.9	20.5	24.1	19.8	15.5	0.5	0.1	1.9	1.7	1.9	3.6	0.2	2.7	0.1
	mid	28.3	32.1	38.9	28	25.4	24.1	26.2	31.8	35.3	0.9	2.3	0.2	0.6	0.2	0.4	1.4	1.2	1.5
	llat	16.8	14.3	14.6	18	18.5	17	17.7	17.1	15.1	0.4	0.6	1.3	0.1	0.4	0.9	1.9	1.5	1.4
FW MV 1	**rlat**	17.3	17	19.7	20.5	19.7	17.6	21.4	21.1	17.1	3	1.5	0.1	4.3	3.7	0.7	2.9	1.4	1.7
	mid	28.1	32.2	39.6	30.1	26.9	25.1	26.7	31.1	36.5	0.7	2.4	0.9	1.5	1.7	0.6	0.9	1.9	2.7
	llat	16.1	14	14.7	14.9	18.4	19.4	18.3	14.1	14.8	0.3	0.3	1.4	3	0.3	3.3	2.5	1.5	1.1
FSDs kV 1	**rlat**	16	19.6	20.1	19.3	16	18.6	21.9	21.7	15.5	1.7	1.1	0.5	3.1	0	1.7	2.4	0.8	0.1
	mid	29	32.6	38.5	29.2	24.9	22.3	27.1	32.5	33.9	1.6	2.8	0.2	0.6	0.3	2.2	0.5	0.5	0.1
	llat	16.4	14.5	13.7	18.1	18.4	17.4	17.2	15.5	15.4	0	0.8	0.4	0.2	0.3	1.3	1.4	0.1	1.7
FSDs MV 2	**rlat**	17.3	17.3	20.6	20	19.4	18.1	22.4	21.7	15.7	3	1.2	1	3.8	3.4	1.2	1.9	0.8	0.3
	mid	28.9	31.9	39.2	28.8	24.5	22.3	28.7	27.8	33.6	1.5	2.1	0.5	0.2	0.7	2.2	1.1	**5.2**	0.2
	llat	16.5	13.4	14.7	18.4	18	16.4	18.5	15.9	15.7	0.1	0.3	1.4	0.5	0.1	0.3	2.7	0.3	2

Table C-3: Results from three-dimensional reconstructed volume organ segmentation measurements. Color coding for columns displaying differences from control values is as follows: no coloring means the volume recorded was within the predetermined systematic error, red means the volume recorded exceeded the systematic error. The systematic error for the bladder, rectum 1, rectum 2 and rectum 3 was ±17.7cc, ±21.0cc, ±16.1cc and ±29.6cc, respectively. Values within 15cc of control values met the hypothesis criteria of ±15cc.

Volume Comparison Results				
*volume in cc	Bladder	Difference	Rectum	Difference
CTMR kV 2	271.4	24.4	124.3	1.1
CTMR MV 3	290.5	43.5	172.9	11.4
FSDs kV 1	271.2	24.2	153.1	7.3
FSDs MV 2	278.6	31.6	123.2	2.2
FW kV 3	273.2	26.2	166.3	18.1
FW MV 1	283.8	36.8	160.6	0.3

Table C-4: Results from catheter reconstruction for the procedurally defined, distal-most dwell position. "Distance" refers to the distance between the distal-most catheter tube dwell position and the applicator reference marker. The difference between TPS generated values and control values is in the "Δ" column. Color coding for the column displaying differences is as follows: no coloring signifies values within ±1 mm of control values, yellow signifies values between ±1-2 mm of control values (within hypothesis criteria of ±2 mm) and red signifies values differing by more than ±2 mm.

Catheter reconstruction results									
		Dwell Coordinates			Fiducial Marker Coordinates				
*distances in mm		x	y	z	x	y	z	Distance	Δ
CTMR kV 2	**R. Ovoid**	-13.5	24.3	-90.4	-11.8	9.5	-73.6	22.5	1.0
	L. Ovoid	12.7	23.3	-90.4	12.9	10.0	-77.2	18.7	2.0
	Tandem	-0.5	72.5	-71.2	1.1	51.0	-74.9	21.9	1.2
CTMR MV 3	**R. Ovoid**	-13.3	29.6	-96.8	-12.8	10.9	-81.2	24.4	0.9
	L. Ovoid	12.6	29.6	-95.1	12.1	12.5	-82.0	21.5	0.8
	Tandem	-3.7	75.8	-72.2	-1.5	53.6	-77.1	22.8	0.2
FSDs kV 1	**R. Ovoid**	-17.6	26.0	-78.6	-14.7	5.1	-65.3	24.9	0.2
	L. Ovoid	11.7	24.9	-79.5	11.1	6.1	-66.6	22.8	1.6
	Tandem	0.0	85.3	-47.5	-1.7	64.9	-52.2	21.0	2.7
FSDs MV 2	**R. Ovoid**	-15.4	22.9	-101.9	-13.4	3.0	-86.9	25.0	0.1
	L. Ovoid	13.4	23.6	-101.5	12.9	4.2	-87.1	24.2	0.3
	Tandem	0.2	84.3	-73.6	-1.3	62.9	-78.4	22.0	1.7
FW kV 3	**R. Ovoid**	-9.4	30.1	-85.6	-12.2	9.4	-69.4	26.4	4.8
	L. Ovoid	10.0	30.9	-84.9	13.7	10.2	-69.2	26.2	4.4
	Tandem	1.2	88.9	-52.3	0.4	66.0	-56.0	23.2	0.4
FW MV 1	**R. Ovoid**	-13.9	21.0	-93.4	-12.9	2.3	-82.1	21.9	0.2
	L. Ovoid	14.3	21.4	-94.5	12.8	1.7	-82.4	23.2	1.3
	Tandem	-0.4	74.0	-76.4	-1.0	49.3	-78.7	24.8	1.2

Physicist 2

Table C-5: Results from two-dimensional CTP organ segmentation measurements for surrogate rectum structures. Color coding for columns displaying differences from control values is as follows: No coloring signifies results within 1 mm of control values, yellow coloring signifies results differing from the control values by 1-2 mm, light red signifies results differing from control values by 2-5 mm and dark red signifies results differing from control values by more than 5 mm. Clear and yellow results met the hypothesis criteria of ±2 mm. The terms "sup", "mid", and "inf" refer to locations relative to the artifact region. Sup=superior, inf=inferior and mid=middle.

CTP: Rectum Results

*distances in mm		Measured values									Absolute difference from control values								
	angle:	**0**	**40**	**80**	**120**	**160**	**200**	**240**	**280**	**320**	**0**	**40**	**80**	**120**	**160**	**200**	**240**	**280**	**320**
CTMR kV 2	**sup**	9.5	9.1	12.1	17.3	20.5	22.3	22.6	23.4	15.6	0.3	0	0.8	0.6	0.9	1	0.3	0.4	1
	mid	30.1	24.4	16.9	16	20.4	20.4	14.5	14.7	20.7	1.3	0.5	1.6	2.5	1.6	1.4	1.7	0.4	0.7
	inf	18.6	19.5	16.7	16.2	16.7	17.5	17.5	18.5	17.1	0.3	0.4	0.6	0.5	2.3	2	1.4	0.7	1.1
CTMR MV 3	**sup**	13.6	13.6	13.4	15	20.5	26.1	27.4	20.3	18.6	0.8	1.5	1	0.6	0.7	1.7	2.7	1.7	1.9
	mid	10.6	21	23.8	13.7	16.1	18.1	19.1	18.1	14.8	2.1	0.2	0.2	2.2	**5.5**	2.7	0.7	2	2.4
	inf	16.7	16.5	17.7	18.9	21.8	20.2	20.7	20.5	19.1	0.9	1.5	1.6	2.2	1.4	0.8	2.2	0.3	0.4
FW kV 3	**sup**	14.1	12.9	13.1	15	20.6	26.2	25.3	19.9	15.9	1.3	0.8	0.7	0.6	0.8	1.8	0.6	1.3	0.8
	mid	12.6	17.6	24.8	18.1	14.4	12.8	13.9	16.1	12.3	0.1	3.6	1.2	**6.6**	3.8	2.6	4.5	0	0.1
	inf	16.9	15.5	16.7	18	21.5	20.7	19.6	21.7	21	1.1	0.5	0.6	1.3	1.1	1.3	1.1	0.9	1.5
FW MV 1	**sup**	15.3	15.8	15.1	16.7	19.7	18.2	15	13.1	17.5	0.6	2.2	1.9	0.9	0.2	2.1	0.7	2.5	1
	mid	10.9	14.2	23.5	17.3	16.2	17.3	19.9	18.8	14.1	3.7	0.7	0.5	1.1	1.9	2.5	1.5	3.4	4.4
	inf	22.2	13.4	13.3	19.8	13.8	14	18.2	21.5	23.6	1.9	1.4	0.9	2.6	0.7	1.4	0.6	2.8	2.1
FSDs kV 1	**sup**	14.9	13.4	14	15.8	22.1	18.5	10.9	9.6	13.8	1	0.2	0.8	0	2.2	2.4	4.8	**6**	2.7
	mid	11	17.8	22	17.8	15.1	16.3	21.4	15.4	12.1	3.8	2.9	2	1.6	0.8	1.5	3	0	2.4
	inf	21.2	13.2	13.7	17.9	13.3	13.7	19	22.2	26.5	0.9	1.2	1.3	0.7	0.2	1.1	0.2	2.1	0.8
FSDs MV 2	**sup**	9.6	9.2	13.4	16.8	20.5	20.7	23.2	23.9	16.2	0.2	0.1	0.5	1.1	0.9	0.6	0.3	0.1	0.4
	mid	30	23.5	20.1	20.2	21.1	23.4	15.3	14.1	20.5	1.2	0.4	1.6	1.7	0.9	1.6	0.9	0.2	0.9
	inf	18.8	18.3	15.4	15.8	16.6	18.8	19.1	18.6	19.1	0.5	0.8	0.7	0.9	2.2	3.3	3	0.8	0.9

Table C-6: Results from two-dimensional CTP organ segmentation measurements for surrogate bladder structures. Color coding for columns displaying differences from control values is as follows: No coloring signifies results within 1 mm of control values, yellow coloring signifies results differing from the control values by 1-2 mm, light red signifies results differing from control values by 2-5 mm and dark red signifies results differing from control values by more than 5 mm. Clear and yellow results met the hypothesis criteria of ±2 mm. The terms "rlat", "mid" and "llat" refer to locations relative to the artifact region. Rlat=right lateral, llat= left lateral and mid=middle.

CTP: Bladder Results

*distances in mm		Measured values									Absolute difference from control values								
	angle:	**0**	**40**	**80**	**120**	**160**	**200**	**240**	**280**	**320**	**0**	**40**	**80**	**120**	**160**	**200**	**240**	**280**	**320**
CTMR kV 2	**rlat**	14.5	17.1	18.7	20.1	19.3	18.9	22.7	20.3	14.7	0.2	1.4	0.9	3.9	3.3	2	1.6	2.2	0.7
	mid	29.5	32.1	37.4	28.3	24.6	23.8	26.3	31.7	33.6	2.1	2.3	1.3	0.3	0.6	0.7	1.3	1.3	0.2
	llat	16.8	15.2	13.6	19.7	19.6	18.7	18.9	16.4	14.5	0.4	1.5	0.3	1.8	1.5	2.6	3.1	0.8	0.8
CTMR MV 3	**rlat**	16.3	17	16.7	19.5	21.4	20.2	23.1	23.7	15.1	2	1.5	2.9	3.3	**5.4**	3.3	1.2	1.2	0.3
	mid	33.2	34.2	38.8	28.6	24.8	22.4	28.2	30.9	34.8	**5.8**	4.4	0.1	0	0.4	2.1	0.6	2.1	1
	llat	16.8	13.4	13.6	18.2	19.8	18.9	17.9	17.6	17.3	0.4	0.3	0.3	0.3	1.7	2.8	2.1	2	3.6
FW kV 3	**rlat**	14.4	18.2	18.8	19.4	17.7	22.8	17.7	17.1	15.5	0.1	0.3	0.8	3.2	1.7	**5.9**	**6.6**	**5.4**	0.1
	mid	30	33.3	37.8	28.1	24.6	22.1	26.3	33	30.6	2.6	3.5	0.9	0.5	0.6	2.4	1.3	0	3.2
	llat	17.2	14.1	14.3	19.6	18.5	16.8	17.5	16.7	17.1	0.8	0.4	1	1.7	0.4	0.7	1.7	1.1	3.4
FW MV 1	**rlat**	16	16.3	20.9	21	19.5	27.4	24.5	19.1	14.5	1.7	2.2	1.3	4.8	3.5	**10.5**	0.2	3.4	0.9
	mid	30.6	33.7	38	28.3	24.6	22.6	28.4	29.1	33.5	3.2	3.9	0.7	0.3	0.6	1.9	0.8	3.9	0.3
	llat	16.8	15.5	15.3	19.7	19.6	18.2	18.6	16.2	14.7	0.4	1.8	2	1.8	1.5	2.1	2.8	0.6	1
FSDs kV 1	**rlat**	15.2	19	19.4	18.2	18.2	20.9	22.9	21	16.2	0.9	0.5	0.2	2	2.2	4	1.4	1.5	0.8
	mid	30	32.2	38.6	28.2	24.1	23.1	27	32	35	2.6	2.4	0.1	0.4	1.1	1.4	0.6	1	1.2
	llat	16.6	14	13.7	19.2	18.3	17.7	17.8	16.2	15	0.2	0.3	0.4	1.3	0.2	1.6	2	0.6	1.3
FSDs MV 2	**rlat**	14.3	18	17.7	19.8	18.8	20.2	23.6	21.2	16.5	0	0.5	1.9	3.6	2.8	3.3	0.7	1.3	1.1
	mid	31.4	35.4	39.4	29.9	26	22.2	27.5	32.6	33.1	4	**5.6**	0.7	1.3	0.8	2.3	0.1	0.4	0.7
	llat	16.6	14.1	15.6	17.6	17.5	17.5	18.9	16.2	19.3	0.2	0.4	2.3	0.3	0.6	1.4	3.1	0.6	**5.6**

Table C-7: Results from three-dimensional reconstructed volume organ segmentation measurements. Color coding for columns displaying differences from control values is as follows: no coloring means the volume recorded was within the predetermined systematic error, red means the volume recorded exceeded the systematic error. The systematic error for the bladder, rectum 1, rectum 2 and rectum 3 was ±17.7cc, ±21.0cc, ±16.1cc and ±29.6cc, respectively. Values within 15cc of control values met the hypothesis criteria of ±15cc.

Volume Comparison Results

*volume in cc	Bladder	Difference	Rectum	Difference
CTMR kV 2	273.2	26.2	116.2	9.1
CTMR MV 3	290.5	43.5	176.7	7.7
FSDs kV 1	278.4	31.4	152.3	8.1
FSDs MV 2	283.7	36.7	125.2	0.1
FW kV 3	268.6	21.6	170.6	13.8
FW MV 1	281.6	34.6	153.9	6.5

Table C-8: Results from catheter reconstruction for the procedurally defined, distal-most dwell position. "Distance" refers to the distance between the distal-most catheter tube dwell position and the applicator reference marker. The difference between TPS generated values and control values is in the "Δ" column. Color coding for the column displaying differences is as follows: no coloring signifies values within ±1 mm of control values, yellow signifies values between ±1-2 mm of control values (within hypothesis criteria of ±2 mm) and red signifies values differing by more than ±2 mm.

Catheter reconstruction results

		Dwell Coordinates			Fiducial Marker Coordinates				
*distances in mm		x	y	z	x	y	z	Distance	Δ
CTMR kV 2	**R. Ovoid**	-13.8	23.8	-90.3	-11.8	9.5	-73.6	22.1	1.4
	L. Ovoid	13.0	22.9	-92.0	12.9	10.0	-77.2	19.6	1.1
	Tandem	-0.4	71.6	-70.9	1.1	51.0	-74.9	21.0	2.0
CTMR MV 3	**R. Ovoid**	-13.7	29.6	-96.3	-12.8	10.9	-81.2	24.1	0.6
	L. Ovoid	13.3	28.1	-95.4	12.1	12.5	-82.0	20.6	0.1
	Tandem	-3.9	76.2	-72.2	-1.5	53.6	-77.1	23.2	0.2
FSDs kV 1	**R. Ovoid**	-14.6	27.1	-82.6	-14.7	5.1	-65.3	28.0	2.9
	L. Ovoid	7.7	26.6	-82.8	11.1	6.1	-66.6	26.3	1.9
	Tandem	-0.1	87.5	-46.4	-1.7	64.9	-52.2	23.4	0.3
FSDs MV 2	**R. Ovoid**	-13.6	22.5	-102.5	-13.4	3.0	-86.9	25.0	0.1
	L. Ovoid	12.4	22.8	-101.7	12.9	4.2	-87.1	23.7	0.8
	Tandem	-0.3	86.5	-72.9	-1.3	62.9	-78.4	24.3	0.6
FW kV 3	**R. Ovoid**	-10.9	25.5	-86.9	-12.2	9.4	-69.4	23.8	2.2
	L. Ovoid	16.3	32.2	-85.7	13.7	10.2	-69.2	27.6	5.7
	Tandem	1.3	89.4	-51.4	0.4	66.0	-56.0	23.9	0.3
FW MV 1	**R. Ovoid**	-13.6	19.8	-96.3	-12.9	2.3	-82.1	22.5	0.9
	L. Ovoid	13.2	21.1	-97.2	12.8	1.7	-82.4	24.4	2.5
	Tandem	0.1	73.0	-76.7	-1.0	49.3	-78.7	23.8	0.2

Physicist 3

Table C-9: Results from two-dimensional CTP organ segmentation measurements for surrogate rectum structures. Color coding for columns displaying differences from control values is as follows: No coloring signifies results within 1 mm of control values, yellow coloring signifies results differing from the control values by 1-2 mm, light red signifies results differing from control values by 2-5 mm and dark red signifies results differing from control values by more than 5 mm. Clear and yellow results met the hypothesis criteria of ±2 mm. The terms "sup", "mid", and "inf" refer to locations relative to the artifact region. Sup=superior, inf=inferior and mid=middle.

CTP: Rectum Results

*distances in mm		Measured values									Absolute difference from control values								
	angle:	**0**	**40**	**80**	**120**	**160**	**200**	**240**	**280**	**320**	**0**	**40**	**80**	**120**	**160**	**200**	**240**	**280**	**320**
CTMR kV 2	**sup**	12.3	11.5	14.6	19.2	20.6	22.7	24.9	25.2	19.7	2.5	2.4	1.7	1.3	1	1.4	2	1.4	3.1
	mid	31.9	25.3	18.4	16.9	21.1	22.7	16.8	16.7	23.2	3.1	1.4	0.1	1.6	0.9	0.9	0.6	2.4	1.8
	inf	18.2	19.3	18	15.3	16.7	17.2	19.7	20.1	20.3	0.1	0.2	1.9	1.4	2.3	1.7	3.6	2.3	2.1
CTMR MV 3	**sup**	15	13.6	13.8	16	21.6	26.3	27.8	20.9	19.6	2.2	1.5	1.4	1.6	1.8	1.9	3.1	2.3	2.9
	mid	16.1	21.5	24.2	24	18.9	18.6	21.3	17.9	14.4	3.4	0.3	0.6	**12.5**	**8.3**	3.2	2.9	1.8	2
	inf	17.1	15.3	16.8	18.7	22.1	22.7	20.3	23.7	20.5	1.3	0.3	0.7	2	1.7	3.3	1.8	2.9	1
FW kV 3	**sup**	15.8	13.9	15.2	21.6	26.3	26.4	27	20.8	18.5	3	1.8	2.8	**7.2**	**6.5**	2	2.3	2.2	1.8
	mid	14.9	19.5	20.3	14.5	17.1	14.8	19.9	15.8	13.1	2.2	1.7	3.3	3	**6.5**	0.6	1.5	0.3	0.7
	inf	17.5	15.4	17.3	17.8	22.6	22.1	20.3	22.5	21.3	1.7	0.4	1.2	1.1	2.2	2.7	1.8	1.7	1.8
FW MV 1	**sup**	18.1	15.3	15.6	18.9	22.5	18.3	18.1	16.4	20.4	2.2	1.7	2.4	3.1	2.6	2.2	2.4	0.8	3.9
	mid	11.4	19.8	23.6	18.1	17.4	19	21.8	19.8	13.1	4.2	4.9	0.4	1.9	3.1	4.2	3.4	4.4	3.4
	inf	27.4	14.7	14.8	20.4	15.2	16.2	20.8	23.6	27.1	**7.1**	2.7	2.4	3.2	2.1	3.6	2	0.7	1.4
FSDs kV 1	**sup**	16.6	14.2	15	16.3	20	21.6	17.9	16.6	18.4	0.7	0.6	1.8	0.5	0.1	**5.5**	2.2	1	1.9
	mid	9.8	17.9	24	16.1	16	16.2	20.9	18.9	11.9	2.6	3	0	0.1	1.7	1.4	2.5	3.5	2.2
	inf	23	13.5	15.2	19.3	13.9	14.4	19.7	23.6	25.9	2.7	1.5	2.8	2.1	0.8	1.8	0.9	0.7	0.2
FSDs MV 2	**sup**	11.6	10	14.5	20.5	22.8	24	24.8	25.1	17.8	1.8	0.9	1.6	2.6	3.2	2.7	1.9	1.3	1.2
	mid	30.2	23.7	17.9	18	20.8	23.4	17.5	18.2	24	1.4	0.2	0.6	0.5	1.2	1.6	1.3	3.9	2.6
	inf	17.7	19.4	15.8	17.3	17.3	19	19.3	20.3	18.9	0.6	0.3	0.3	0.6	2.9	3.5	3.2	2.5	0.7

Table C-10: Results from two-dimensional CTP organ segmentation measurements for surrogate bladder structures. Color coding for columns displaying differences from control values is as follows: No coloring signifies results within 1 mm of control values, yellow coloring signifies results differing from the control values by 1-2 mm, light red signifies results differing from control values by 2-5 mm and dark red signifies results differing from control values by more than 5 mm. Clear and yellow results met the hypothesis criteria of ±2 mm. The terms "rlat", "mid" and "llat" refer to locations relative to the artifact region. Rlat=right lateral, llat= left lateral and mid=middle.

CTP: Bladder Results

*distances in mm		Measured values									Absolute difference from control values								
	angle:	**0**	**40**	**80**	**120**	**160**	**200**	**240**	**280**	**320**	**0**	**40**	**80**	**120**	**160**	**200**	**240**	**280**	**320**
CTMR kV 2	**rlat**	15.4	20.3	19.9	20.7	20.1	19.3	26.9	22.9	15.5	1.1	1.8	0.3	4.5	4.1	2.4	2.6	0.4	0.1
	mid	29.2	33	37.8	29.1	25.5	26.6	27	31.6	34.4	1.8	3.2	0.9	0.5	0.3	2.1	0.6	1.4	0.6
	llat	16.3	16.3	20.3	20.1	18.4	18.7	18.5	17.5	17	0.1	2.6	**7**	2.2	0.3	2.6	2.7	1.9	3.3
CTMR MV 3	**rlat**	14.3	19.3	20.6	18.7	20.5	20.8	23.4	22.9	14.4	0	0.8	1	2.5	4.5	3.9	0.9	0.4	1
	mid	30.2	32.6	38.6	29.9	24.2	24	28.9	32	34.8	2.8	2.8	0.1	1.3	1	0.5	1.3	1	1
	llat	18.9	15.7	14.6	21.7	20.5	18	19.5	17.8	15.6	2.5	2	1.3	3.8	2.4	1.9	3.7	2.2	1.9
FW kV 3	**rlat**	16.1	18.7	19.7	19.9	17.9	32	22.1	21.1	15.6	1.8	0.2	0.1	3.7	1.9	**15.1**	2.2	1.4	0.2
	mid	28.1	32.7	39.3	28.5	24.5	24	26.9	32.6	34.7	0.7	2.9	0.6	0.1	0.7	0.5	0.7	0.4	0.9
	llat	17.7	15.6	15.1	20	19.4	18.3	17.3	16.9	17.3	1.3	1.9	1.8	2.1	1.3	2.2	1.5	1.3	3.6
FW MV 1	**rlat**	17.3	19.6	20.6	21.9	20.2	19.2	21.3	21.8	15.5	3	1.1	1	**5.7**	4.2	2.3	3	0.7	0.1
	mid	30.3	33.6	42	31.8	24.3	23.3	28.4	33.6	34.6	2.9	3.8	3.3	3.2	0.9	1.2	0.8	0.6	0.8
	llat	16.6	14.2	15.7	18.4	19.7	19.4	19.3	17.6	17.1	0.2	0.5	2.4	0.5	1.6	3.3	3.5	2	3.4
FSDs kV 1	**rlat**	16.5	20.1	19.6	19.5	18.1	20.1	24.9	21.9	16	2.2	1.6	0	3.3	2.1	3.2	0.6	0.6	0.6
	mid	29.4	33.2	38.4	28.9	24.3	23.2	27.8	33.1	34.5	2	3.4	0.3	0.3	0.9	1.3	0.2	0.1	0.7
	llat	17.6	15	16.3	19.8	19.3	18.1	17.6	17.2	16.4	1.2	1.3	3	1.9	1.2	2	1.8	1.6	2.7
FSDs MV 2	**rlat**	15.8	19.8	20.8	21.3	21.4	21.8	23.7	23.5	14.8	1.5	1.3	1.2	**5.1**	**5.4**	4.9	0.6	1	0.6
	mid	29.2	35.1	41.5	30.1	25.4	22.3	28.5	33.2	34.4	1.8	**5.3**	2.8	1.5	0.2	2.2	0.9	0.2	0.6
	llat	17.3	15.2	16.5	20	19.7	19	19.5	18	17.1	0.9	1.5	3.2	2.1	1.6	2.9	3.7	2.4	3.4

Table C-11: Results from three-dimensional reconstructed volume organ segmentation measurements. Color coding for columns displaying differences from control values is as follows: no coloring means the volume recorded was within the predetermined systematic error, red means the volume recorded exceeded the systematic error. The systematic error for the bladder, rectum 1, rectum 2 and rectum 3 was ±17.7cc, ±21.0cc, ±16.1cc and ±29.6cc, respectively. Values within 15cc of control values met the hypothesis criteria of ±15cc.

Volume Comparison Results

*volume in cc	Bladder	Difference	Rectum	Difference
CTMR kV 2	295.9	48.9	133.5	8.2
CTMR MV 3	297.8	50.8	192.2	7.9
FSDs kV 1	286.7	39.7	168.3	8.0
FSDs MV 2	308.3	61.3	135.9	10.6
FW kV 3	283.2	36.2	187.3	3.0
FW MV 1	303.3	56.3	181.9	21.6

Table C-12: Results from catheter reconstruction for the procedurally defined, distal-most dwell position. "Distance" refers to the distance between the distal-most catheter tube dwell position and the applicator reference marker. The difference between TPS generated values and control values is in the "Δ" column. Color coding for the column displaying differences is as follows: no coloring signifies values within ±1 mm of control values, yellow signifies values between ±1-2 mm of control values (within hypothesis criteria of ±2 mm) and red signifies values differing by more than ±2 mm.

Catheter reconstruction results

		Dwell Coordinates			Fiducial Marker Coordinates				
*distances in mm		x	y	z	x	y	z	Distance	Δ
CTMR kV 2	**R. Ovoid**	-12.8	24.1	-90.6	-11.8	9.5	-73.6	22.4	1.0
	L. Ovoid	13.1	23.4	-92.0	12.9	10.0	-77.2	20.0	0.7
	Tandem	-0.2	72.4	-71.1	1.1	51.0	-74.9	21.8	1.3
CTMR MV 3	**R. Ovoid**	-13.5	28.3	-96.6	-12.8	10.9	-81.2	23.2	0.2
	L. Ovoid	12.8	27.9	-95.7	12.1	12.5	-82.0	20.6	0.1
	Tandem	-4.1	75.4	-71.9	-1.5	53.6	-77.1	22.6	0.5
FSDs kV 1	**R. Ovoid**	-17.3	25.5	-79.9	-14.7	5.1	-65.3	25.2	0.1
	L. Ovoid	11.9	24.9	-80.3	11.1	6.1	-66.6	23.3	1.2
	Tandem	0.3	87.3	-46.5	-1.7	64.9	-52.2	23.2	0.5
FSDs MV 2	**R. Ovoid**	-15.8	21.9	-101.1	-13.4	3.0	-86.9	23.8	1.3
	L. Ovoid	14.1	22.3	-100.4	12.9	4.2	-87.1	22.5	1.9
	Tandem	-0.3	84.7	-73.3	-1.3	62.9	-78.4	22.4	1.3
FW kV 3	**R. Ovoid**	-13.0	27.1	-78.1	-12.2	9.4	-69.4	19.7	1.9
	L. Ovoid	16.1	27.2	-79.0	13.7	10.2	-69.2	19.8	2.1
	Tandem	0.9	89.1	-51.4	0.4	66.0	-56.0	23.6	0.0
FW MV 1	**R. Ovoid**	-13.5	19.0	-93.3	-12.9	2.3	-82.1	20.1	1.5
	L. Ovoid	14.9	19.6	-95.4	12.8	1.7	-82.4	22.2	0.3
	Tandem	-0.2	76.8	-75.3	-1.0	49.3	-78.7	27.7	4.2

Physicist 4

Table C-13: Results from two-dimensional CTP organ segmentation measurements for surrogate rectum structures. Color coding for columns displaying differences from control values is as follows: No coloring signifies results within 1 mm of control values, yellow coloring signifies results differing from the control values by 1-2 mm, light red signifies results differing from control values by 2-5 mm and dark red signifies results differing from control values by more than 5 mm. Clear and yellow results met the hypothesis criteria of ±2 mm. The terms "sup", "mid", and "inf" refer to locations relative to the artifact region. Sup=superior, inf=inferior and mid=middle.

CTP: Rectum Results

*distances in mm		Measured values									Absolute difference from control values								
	angle:	**0**	**40**	**80**	**120**	**160**	**200**	**240**	**280**	**320**	**0**	**40**	**80**	**120**	**160**	**200**	**240**	**280**	**320**
FW kV 2	**rlat**	10.7	10.1	13.4	19.1	19.7	20.9	23.6	24	17.9	0.9	1	0.5	1.2	0.1	0.4	0.7	0.2	1.3
	mid	30.6	26.6	18.9	16.6	21.4	22.9	16.1	16.3	22.9	1.8	2.7	0.4	1.9	0.6	1.1	0.1	2	1.5
	llat	18.3	18.4	16.7	16.5	15.3	17.1	16.8	17.9	18.1	0	0.7	0.6	0.2	0.9	1.6	0.7	0.1	0.1
FW MV 3	**rlat**	13.6	13.1	12.8	14.1	19.3	25	26.9	19.6	16.2	0.8	1	0.4	0.3	0.5	0.6	2.2	1	0.5
	mid	13.1	21	24.3	16.3	17.4	17.5	17.6	14.8	12.5	0.4	0.2	0.7	4.8	**6.8**	2.1	0.8	1.3	0.1
	llat	16.6	16.1	16.5	17.4	20.6	20.5	19.9	21.2	20.3	0.8	1.1	0.4	0.7	0.2	1.1	1.4	0.4	0.8
FSDs kV 3	**rlat**	14.1	13	12.7	15	21.4	24.8	25.8	19.6	16.5	1.3	0.9	0.3	0.6	1.6	0.4	1.1	1	0.2
	mid	13.3	18.8	21.2	18.6	15.4	15.9	17.5	14.8	12.1	0.6	2.4	2.4	**7.1**	4.8	0.5	0.9	1.3	0.3
	llat	16.6	15.4	16.2	17.2	20.7	20.7	18.6	20.3	19.8	0.8	0.4	0.1	0.5	0.3	1.3	0.1	0.5	0.3
FSDs MV 1	**rlat**	18.2	13.8	14.5	15.8	23.2	17.6	15.1	13.3	18.2	2.3	0.2	1.3	0	3.3	1.5	0.6	2.3	1.7
	mid	11.5	16.9	23.9	17.9	16.4	16.8	19.3	18.9	15.1	4.3	2	0.1	1.7	2.1	2	0.9	3.5	**5.4**
	llat	23.5	13	14	19.1	14.3	14.1	19.3	23.2	26	3.2	1	1.6	1.9	1.2	1.5	0.5	1.1	0.3
CTMR kV 1	**rlat**	15.5	13.1	12.6	15.5	20.4	16.9	17.6	15.5	17.1	0.4	0.5	0.6	0.3	0.5	0.8	1.9	0.1	0.6
	mid	13.7	18.9	18.3	17.1	15.2	16.8	19.9	15.9	15.3	**6.5**	4	**5.7**	0.9	0.9	2	1.5	0.5	**5.6**
	llat	21.2	12.5	13.3	16.7	13.8	12.8	17.9	22.7	25.7	0.9	0.5	0.9	0.5	0.7	0.2	0.9	1.6	0
CTMR MV 2	**rlat**	11.5	10.7	14.6	19.1	21.2	21.8	23.4	24.1	16.3	1.7	1.6	1.7	1.2	1.6	0.5	0.5	0.3	0.3
	mid	28.5	24.1	18.4	18.6	21.5	21.6	17.5	15.9	21.2	0.3	0.2	0.1	0.1	0.5	0.2	1.3	1.6	0.2
	llat	17.4	19.4	16.5	16.5	15.5	17.8	18.1	19.2	18.2	0.9	0.3	0.4	0.2	1.1	2.3	2	1.4	0

Table C-14: Results from two-dimensional CTP organ segmentation measurements for surrogate bladder structures. Color coding for columns displaying differences from control values is as follows: No coloring signifies results within 1 mm of control values, yellow coloring signifies results differing from the control values by 1-2 mm, light red signifies results differing from control values by 2-5 mm and dark red signifies results differing from control values by more than 5 mm. Clear and yellow results met the hypothesis criteria of ±2 mm. The terms "rlat", "mid" and "llat" refer to locations relative to the artifact region. Rlat=right lateral, llat= left lateral and mid=middle.

CTP: Bladder Results

*distances in mm		Measured values									Absolute difference from control values								
	angle:	**0**	**40**	**80**	**120**	**160**	**200**	**240**	**280**	**320**	**0**	**40**	**80**	**120**	**160**	**200**	**240**	**280**	**320**
FW kV 2	**rlat**	15.2	17.9	19.1	20.6	19.1	18.2	24	21.7	15.8	0.9	0.6	0.5	4.4	3.1	1.3	0.3	0.8	0.4
	mid	29.2	32.6	37.2	28.2	24.9	24.8	26.7	32.1	33	1.8	2.8	1.5	0.4	0.3	0.3	0.9	0.9	0.8
	llat	16	13.8	14.6	18.5	19.3	18.4	18.6	15.5	15.4	0.4	0.1	1.3	0.6	1.2	2.3	2.8	0.1	1.7
FW MV 3	**rlat**	16.4	19.5	19.9	19.7	19.4	21.2	25.9	22.3	15.1	2.1	1	0.3	3.5	3.4	4.3	1.6	0.2	0.3
	mid	31.9	35.3	38.4	27.9	25.1	24	28.7	32.4	35.6	4.5	**5.5**	0.3	0.7	0.1	0.5	1.1	0.6	1.8
	llat	17.1	13.7	13.6	18.3	20.3	19.1	19.1	18.1	15.7	0.7	0	0.3	0.4	2.2	3	3.3	2.5	2
FSDs kV 3	**rlat**	14.8	18.4	17.7	17.9	17.9	20.5	24.1	19.8	15.5	0.5	0.1	1.9	1.7	1.9	3.6	0.2	2.7	0.1
	mid	28.3	32.1	38.9	28	25.4	24.1	26.2	31.8	35.3	0.9	2.3	0.2	0.6	0.2	0.4	1.4	1.2	1.5
	llat	16.8	14.3	14.6	18	18.5	17	17.7	17.1	15.1	0.4	0.6	1.3	0.1	0.4	0.9	1.9	1.5	1.4
FSDs MV 1	**rlat**	17.3	17	19.7	20.5	19.7	17.6	21.4	21.1	17.1	3	1.5	0.1	4.3	3.7	0.7	2.9	1.4	1.7
	mid	28.1	32.2	39.6	30.1	26.9	25.1	26.7	31.1	36.5	0.7	2.4	0.9	1.5	1.7	0.6	0.9	1.9	2.7
	llat	16.1	14	14.7	14.9	18.4	19.4	18.3	14.1	14.8	0.3	0.3	1.4	3	0.3	3.3	2.5	1.5	1.1
CTMR kV 1	**rlat**	16	19.6	20.1	19.3	16	18.6	21.9	21.7	15.5	1.7	1.1	0.5	3.1	0	1.7	2.4	0.8	0.1
	mid	29	32.6	38.5	29.2	24.9	22.3	27.1	32.5	33.9	1.6	2.8	0.2	0.6	0.3	2.2	0.5	0.5	0.1
	llat	16.4	14.5	13.7	18.1	18.4	17.4	17.2	15.5	15.4	0	0.8	0.4	0.2	0.3	1.3	1.4	0.1	1.7
CTMR MV 2	**rlat**	17.3	17.3	20.6	20	19.4	18.1	22.4	21.7	15.7	3	1.2	1	3.8	3.4	1.2	1.9	0.8	0.3
	mid	28.9	31.9	39.2	28.8	24.5	22.3	28.7	27.8	33.6	1.5	2.1	0.5	0.2	0.7	2.2	1.1	**5.2**	0.2
	llat	16.5	13.4	14.7	18.4	18	16.4	18.5	15.9	15.7	0.1	0.3	1.4	0.5	0.1	0.3	2.7	0.3	2

Table C-15: Results from three-dimensional reconstructed volume organ segmentation measurements. Color coding for columns displaying differences from control values is as follows: no coloring means the volume recorded was within the predetermined systematic error, red means the volume recorded exceeded the systematic error. The systematic error for the bladder, rectum 1, rectum 2 and rectum 3 was ±17.7cc, ±21.0cc, ±16.1cc and ±29.6cc, respectively. Values within 15cc of control values met the hypothesis criteria of ±15cc.

Volume Comparison Results

*volume in cc	Bladder	Difference	Rectum	Difference
CTMR kV 1	271.4	24.4	124.3	1.1
CTMR MV 2	290.5	43.5	172.9	11.4
FSDs kV 3	271.2	24.2	153.1	7.3
FSDs MV 1	278.6	31.6	123.2	2.2
FW kV 2	273.2	26.2	166.3	18.1
FW MV 3	283.8	36.8	160.6	0.3

Table C-16: Results from catheter reconstruction for the procedurally defined, distal-most dwell position. "Distance" refers to the distance between the distal-most catheter tube dwell position and the applicator reference marker. The difference between TPS generated values and control values is in the "Δ" column. Color coding for the column displaying differences is as follows: no coloring signifies values within ±1 mm of control values, yellow signifies values between ±1-2 mm of control values (within hypothesis criteria of ±2 mm) and red signifies values differing by more than ±2 mm.

Catheter reconstruction results

		Dwell Coordinates			Fiducial Marker Coordinates				
*distances in mm		x	y	z	x	y	z	Distance	Δ
CTMR kV 1	**R. Ovoid**	-13.5	24.3	-90.4	-11.8	9.5	-73.6	22.5	1.0
	L. Ovoid	12.7	23.3	-90.4	12.9	10.0	-77.2	18.7	2.0
	Tandem	-0.5	72.5	-71.2	1.1	51.0	-74.9	21.9	1.2
CTMR MV 2	**R. Ovoid**	-13.3	29.6	-96.8	-12.8	10.9	-81.2	24.4	0.9
	L. Ovoid	12.6	29.6	-95.1	12.1	12.5	-82.0	21.5	0.8
	Tandem	-3.7	75.8	-72.2	-1.5	53.6	-77.1	22.8	0.2
FSDs kV 3	**R. Ovoid**	-17.6	26.0	-78.6	-14.7	5.1	-65.3	24.9	0.2
	L. Ovoid	11.7	24.9	-79.5	11.1	6.1	-66.6	22.8	1.6
	Tandem	0.0	85.3	-47.5	-1.7	64.9	-52.2	21.0	2.7
FSDs MV 1	**R. Ovoid**	-15.4	22.9	-101.9	-13.4	3.0	-86.9	25.0	0.1
	L. Ovoid	13.4	23.6	-101.5	12.9	4.2	-87.1	24.2	0.3
	Tandem	0.2	84.3	-73.6	-1.3	62.9	-78.4	22.0	1.7
FW kV 2	**R. Ovoid**	-9.4	30.1	-85.6	-12.2	9.4	-69.4	26.4	4.8
	L. Ovoid	10.0	30.9	-84.9	13.7	10.2	-69.2	26.2	4.4
	Tandem	1.2	88.9	-52.3	0.4	66.0	-56.0	23.2	0.4
FW MV 3	**R. Ovoid**	-13.9	21.0	-93.4	-12.9	2.3	-82.1	21.9	0.2
	L. Ovoid	14.3	21.4	-94.5	12.8	1.7	-82.4	23.2	1.3
	Tandem	-0.4	74.0	-76.4	-1.0	49.3	-78.7	24.8	1.2

Physicist 5

Table C-17: Results from two-dimensional CTP organ segmentation measurements for surrogate rectum structures. Color coding for columns displaying differences from control values is as follows: No coloring signifies results within 1 mm of control values, yellow coloring signifies results differing from the control values by 1-2 mm, light red signifies results differing from control values by 2-5 mm and dark red signifies results differing from control values by more than 5 mm. Clear and yellow results met the hypothesis criteria of ±2 mm. The terms "sup", "mid", and "inf" refer to locations relative to the artifact region. Sup=superior, inf=inferior and mid=middle.

CTP: Rectum Results

*distances in mm		Measured values									Absolute difference from control values								
	angle:	**0**	**40**	**80**	**120**	**160**	**200**	**240**	**280**	**320**	**0**	**40**	**80**	**120**	**160**	**200**	**240**	**280**	**320**
FW kV 2	**rlat**	10.6	9.9	12.5	18.7	20.1	21.9	23.9	23.8	15.8	0.8	0.8	0.4	0.8	0.5	0.6	1	0	0.8
	mid	26.8	23	20.2	21.2	23.4	20.8	15.1	13.6	21.4	2	0.9	1.7	2.7	1.4	1	1.1	0.7	0
	llat	17.8	18	16.2	16.4	16.7	16	18.3	17.2	17.2	0.5	1.1	0.1	0.3	2.3	0.5	2.2	0.6	1
FW MV 3	**rlat**	12.3	10.8	11.9	14.3	19.9	24.5	25	17.1	16.5	0.5	1.3	0.5	0.1	0.1	0.1	0.3	1.5	0.2
	mid	11.2	21.8	25.9	13.4	13.8	15.8	18.5	16	11.2	1.5	0.6	2.3	1.9	3.2	0.4	0.1	0.1	1.2
	llat	16.3	14.3	16.2	18	20.8	21.9	21.8	21	20	0.5	0.7	0.1	1.3	0.4	2.5	3.3	0.2	0.5
FSDs kV 3	**rlat**	12.9	11.3	11.7	13.2	20.8	24.7	26.5	19	17.9	0.1	0.8	0.7	1.2	1	0.3	1.8	0.4	1.2
	mid	14	21.1	24.8	20.8	15.5	15.2	18.6	14.7	13	1.3	0.1	1.2	**9.3**	4.9	0.2	0.2	1.4	0.6
	llat	16	15.5	16.1	17.9	21.1	20.9	20.2	21.8	20.2	0.2	0.5	0	1.2	0.7	1.5	1.7	1	0.7
FSDs MV 1	**rlat**	16.1	13.8	14.7	17.6	22.1	18.5	18.1	16.1	19.2	0.2	0.2	1.5	1.8	2.2	2.4	2.4	0.5	2.7
	mid	15.7	22	23.7	17.5	15.6	16.8	18.2	18.4	17.5	**8.5**	**7.1**	0.3	1.3	1.3	2	0.2	3	**7.8**
	llat	21.8	14.3	15.4	18	14.3	14.7	20.5	23.6	26.4	1.5	2.3	3	0.8	1.2	2.1	1.7	0.7	0.7
CTMR kV 1	**rlat**	16.9	13.6	12.6	16.2	20.7	18.3	18	16.8	16.1	1	0	0.6	0.4	0.8	2.2	2.3	1.2	0.4
	mid	14.9	18.3	23.1	16.8	16.3	15.6	20.9	14.9	17.5	**7.7**	3.4	0.9	0.6	2	0.8	2.5	0.5	**7.8**
	llat	20.4	12.4	12.8	17.5	13.4	14.1	18.6	22.5	24.3	0.1	0.4	0.4	0.3	0.3	1.5	0.2	1.8	1.4
CTMR MV 2	**rlat**	11	9.3	12.5	19.1	21.7	22.6	24.6	24.6	17.7	1.2	0.2	0.4	1.2	2.1	1.3	1.7	0.8	1.1
	mid	29.5	24.5	16.5	17.5	23.4	22.4	16.9	15.7	22.6	0.7	0.6	2	1	1.4	0.6	0.7	1.4	1.2
	llat	18.4	18.4	15.8	17.1	15.4	16.7	18.5	17	16.9	0.1	0.7	0.3	0.4	1	1.2	2.4	0.8	1.3

Table C-18: Results from two-dimensional CTP organ segmentation measurements for surrogate bladder structures. Color coding for columns displaying differences from control values is as follows: No coloring signifies results within 1 mm of control values, yellow coloring signifies results differing from the control values by 1-2 mm, light red signifies results differing from control values by 2-5 mm and dark red signifies results differing from control values by more than 5 mm. Clear and yellow results met the hypothesis criteria of ±2 mm. The terms "rlat", "mid" and "llat" refer to locations relative to the artifact region. Rlat=right lateral, llat= left lateral and mid=middle.

CTP: Bladder Results

*distances in mm		Measured values									Absolute difference from control values								
	angle:	**0**	**40**	**80**	**120**	**160**	**200**	**240**	**280**	**320**	**0**	**40**	**80**	**120**	**160**	**200**	**240**	**280**	**320**
FW kV 2	**rlat**	15.4	19.6	19.9	19.5	18.7	17.6	25.1	18.2	15.5	1.1	1.1	0.3	3.3	2.7	0.7	0.8	4.3	0.1
	mid	28.8	31.1	37.9	28.7	24.9	23.2	28.9	33.9	33.3	1.4	1.3	0.8	0.1	0.3	1.3	1.3	0.9	0.5
	llat	16.9	14	13.6	17.8	19.3	17.4	18.2	14.6	14.2	0.5	0.3	0.3	0.1	1.2	1.3	2.4	1	0.5
FW MV 3	**rlat**	14.8	17.4	19.1	16.1	18.7	22.3	20.2	21.5	15.9	0.5	1.1	0.5	0.1	2.7	**5.4**	4.1	1	0.5
	mid	29.2	31.9	38.4	29.6	23.7	21.3	27.6	33.6	32	1.8	2.1	0.3	1	1.5	3.2	0	0.6	1.8
	llat	16.5	13.1	13.1	17.8	18.6	17	18.3	16.4	14	0.1	0.6	0.2	0.1	0.5	0.9	2.5	0.8	0.3
FSDs kV 3	**rlat**	14.4	17.3	19.4	18.7	18.8	17.3	23.4	20.4	16.4	0.1	1.2	0.2	2.5	2.8	0.4	0.9	2.1	1
	mid	28.9	31.3	38.4	28.5	23.6	22.2	28.1	34.6	32.9	1.5	1.5	0.3	0.1	1.6	2.3	0.5	1.6	0.9
	llat	16.5	13.6	13.8	17.6	18.4	16.7	15.1	16.1	15	0.1	0.1	0.5	0.3	0.3	0.6	0.7	0.5	1.3
FSDs MV 1	**rlat**	14.7	19.3	18.1	20.3	20.1	20.9	20.8	20.2	17.4	0.4	0.8	1.5	4.1	4.1	4	3.5	2.3	2
	mid	29.6	34.1	40	28.2	25.1	25.3	27.2	31	32.9	2.2	4.3	1.3	0.4	0.1	0.8	0.4	2	0.9
	llat	16.9	15.1	14.6	18.3	17.6	16.7	17.7	17.1	17.2	0.5	1.4	1.3	0.4	0.5	0.6	1.9	1.5	3.5
CTMR kV 1	**rlat**	14.5	18.4	19.3	20.3	16.5	19.2	24.1	21.6	15.2	0.2	0.1	0.3	4.1	0.5	2.3	0.2	0.9	0.2
	mid	29.2	31.6	36.9	27.7	24.4	24.2	26.9	33	34.4	1.8	1.8	1.8	0.9	0.8	0.3	0.7	0	0.6
	llat	17.2	15.3	14.6	19.1	17.8	15.8	17.2	16.3	15.3	0.8	1.6	1.3	1.2	0.3	0.3	1.4	0.7	1.6
CTMR MV 2	**rlat**	16.4	19.6	17.9	19.9	21.9	16.8	23.3	22.1	17	2.1	1.1	1.7	3.7	**5.9**	0.1	1	0.4	1.6
	mid	30	33.2	39.4	30.5	26	25.4	28.5	33.6	34.5	2.6	3.4	0.7	1.9	0.8	0.9	0.9	0.6	0.7
	llat	15.6	14.9	12.6	17.7	17.4	16.2	18.7	20.6	16.7	0.8	1.2	0.7	0.2	0.7	0.1	2.9	5	3

Table C-19: Results from three-dimensional reconstructed volume organ segmentation measurements. Color coding for columns displaying differences from control values is as follows: no coloring means the volume recorded was within the predetermined systematic error, red means the volume recorded exceeded the systematic error. The systematic error for the bladder, rectum 1, rectum 2 and rectum 3 was ±17.7cc, ±21.0cc, ±16.1cc and ±29.6cc, respectively. Values within 15cc of control values met the hypothesis criteria of ±15cc.

Volume Comparison Results

*volume in cc	Bladder	Difference	Rectum	Difference
CTMR kV 1	272.3	25.3	157.6	2.7
CTMR MV 2	280.7	33.7	123.2	2.1
FSDs kV 3	264.5	17.5	170.5	13.8
FSDs MV 1	279.8	32.8	165.5	5.2
FW kV 2	270.2	23.2	117.8	7.5
FW MV 3	276.4	29.4	173.9	10.4

Table C-20: Results from catheter reconstruction for the procedurally defined, distal-most dwell position. "Distance" refers to the distance between the distal-most catheter tube dwell position and the applicator reference marker. The difference between TPS generated values and control values is in the "Δ" column. Color coding for the column displaying differences is as follows: no coloring signifies values within ±1 mm of control values, yellow signifies values between ±1-2 mm of control values (within hypothesis criteria of ±2 mm) and red signifies values differing by more than ±2 mm.

Catheter reconstruction results

		Dwell Coordinates			Fiducial Marker Coordinates				
*distances in mm		x	y	z	x	y	z	Distance	Δ
CTMR kV 1	**R. Ovoid**	-11.4	24.5	-84.1	-10.4	8.7	-68.5	22.2	1.2
	L. Ovoid	14.4	24.5	-84.7	15.0	9.8	-69.8	20.9	0.2
	Tandem	-0.4	71.7	-61.0	1.6	50.3	-65.9	22.0	1.0
CTMR MV 2	**R. Ovoid**	-12.9	24.7	-101.6	-12.3	9.9	-86.5	21.2	2.3
	L. Ovoid	12.8	24.3	-102.2	13.1	10.9	-88.8	19.0	1.8
	Tandem	-1.5	73.0	-82.0	0.5	50.5	-84.9	22.8	0.3
FSDs kV 3	**R. Ovoid**	-13.5	31.7	-79.6	-11.7	11.7	-66.0	24.3	0.9
	L. Ovoid	15.3	31.4	-79.6	13.0	12.0	-66.2	23.7	0.8
	Tandem	0.1	93.0	-52.7	0.2	69.9	-58.5	23.8	0.1
FSDs MV 1	**R. Ovoid**	-16.7	23.2	-91.9	-12.6	4.2	-78.7	23.5	1.6
	L. Ovoid	13.2	23.7	-93.2	12.3	5.0	-79.4	23.3	1.2
	Tandem	1.9	86.9	-65.6	0.5	64.3	-70.6	23.2	0.5
FW kV 2	**R. Ovoid**	-11.0	30.2	-94.3	-14.0	10.2	-76.9	26.7	5.0
	L. Ovoid	8.6	29.2	-92.4	11.6	10.2	-76.8	24.8	2.9
	Tandem	-1.4	79.3	-68.2	-2.2	56.3	-71.7	23.3	0.3
FW MV 3	**R. Ovoid**	-14.8	33.2	-94.8	-13.4	15.0	-83.0	21.7	0.1
	L. Ovoid	14.7	33.6	-93.9	12.2	14.8	-82.8	22.0	0.1
	Tandem	-1.0	93.6	-63.6	-1.4	69.9	-68.6	24.2	0.7

Physicist 6

Table C-21: Results from two-dimensional CTP organ segmentation measurements for surrogate rectum structures. Color coding for columns displaying differences from control values is as follows: No coloring signifies results within 1 mm of control values, yellow coloring signifies results differing from the control values by 1-2 mm, light red signifies results differing from control values by 2-5 mm and dark red signifies results differing from control values by more than 5 mm. Clear and yellow results met the hypothesis criteria of ±2 mm. The terms "sup", "mid", and "inf" refer to locations relative to the artifact region. Sup=superior, inf=inferior and mid=middle.

CTP: Rectum Results

*distances in mm		Measured values									Absolute difference from control values								
	angle:	**0**	**40**	**80**	**120**	**160**	**200**	**240**	**280**	**320**	**0**	**40**	**80**	**120**	**160**	**200**	**240**	**280**	**320**
FW kV 2	**rlat**	11.2	10.4	14.5	18.5	20.2	21.2	22.7	23.8	17.1	1.4	1.3	1.6	0.6	0.6	0.1	0.2	0	0.5
	mid	29.8	18.1	11.4	11.2	16.3	19.6	16.2	15.8	23.4	1	**5.8**	**7.1**	**7.3**	**5.7**	2.2	0	1.5	2
	llat	19.1	20	17.2	15.8	14.7	17	17.4	16.9	19.9	0.8	0.9	1.1	0.9	0.3	1.5	1.3	0.9	1.7
FW MV 3	**rlat**	13.9	12.6	11.9	14.1	20.4	24	26.3	18.4	15.2	1.1	0.5	0.5	0.3	0.6	0.4	1.6	0.2	1.5
	mid	13.1	20.9	24.5	13.8	11.4	13.7	17.6	16.5	13.6	0.4	0.3	0.9	2.3	0.8	1.7	0.8	0.4	1.2
	llat	17.2	15.8	15.8	17.1	20.8	20	18.6	22.9	19.8	1.4	0.8	0.3	0.4	0.4	0.6	0.1	2.1	0.3
FSDs kV 3	**rlat**	13.9	11.6	12.6	13.1	19.3	24	26	19.2	17.6	1.1	0.5	0.2	1.3	0.5	0.4	1.3	0.6	0.9
	mid	15.1	19.7	19	14.3	11.9	12.4	18	16.5	13.8	2.4	1.5	4.6	2.8	1.3	3	0.4	0.4	1.4
	llat	16.6	15.7	16.2	17.1	19.2	20.6	20	21.8	20.8	0.8	0.7	0.1	0.4	1.2	1.2	1.5	1	1.3
FSDs MV 1	**rlat**	16.1	14.9	14	16.2	21.6	18.2	18.4	17.1	17	0.2	1.3	0.8	0.4	1.7	2.1	2.7	1.5	0.5
	mid	9.7	19	23.8	17.4	15.1	16.9	17.8	16	10.9	2.5	4.1	0.2	1.2	0.8	2.1	0.6	0.6	1.2
	llat	22.7	13.9	15	19	14.5	14	20	23.3	26.4	2.4	1.9	2.6	1.8	1.4	1.4	1.2	1	0.7
CTMR kV 1	**rlat**	16.3	12.9	14.7	16.8	20.5	17.6	18	17.3	17.9	0.4	0.7	1.5	1	0.6	1.5	2.3	1.7	1.4
	mid	10	17.2	23.3	15.5	15.2	15.5	18.6	17.9	10.5	2.8	2.3	0.7	0.7	0.9	0.7	0.2	2.5	0.8
	llat	20.6	12.6	12.9	19	12.8	14.4	18.9	22.2	24.3	0.3	0.6	0.5	1.8	0.3	1.8	0.1	2.1	1.4
CTMR MV 2	**rlat**	10.9	10.9	14.6	18.7	20.4	21.3	23	23	17.2	1.1	1.8	1.7	0.8	0.8	0	0.1	0.8	0.6
	mid	27.3	24.4	15.6	16	22.4	25.4	17.3	14.4	22.6	1.5	0.5	2.9	2.5	0.4	3.6	1.1	0.1	1.2
	llat	18.4	16.9	16.3	17.3	15.3	14.9	17.2	15.2	16.7	0.1	2.2	0.2	0.6	0.9	0.6	1.1	2.6	1.5

Table C-22: Results from two-dimensional CTP organ segmentation measurements for surrogate bladder structures. Color coding for columns displaying differences from control values is as follows: No coloring signifies results within 1 mm of control values, yellow coloring signifies results differing from the control values by 1-2 mm, light red signifies results differing from control values by 2-5 mm and dark red signifies results differing from control values by more than 5 mm. Clear and yellow results met the hypothesis criteria of ±2 mm. The terms "rlat", "mid" and "llat" refer to locations relative to the artifact region. Rlat=right lateral, llat= left lateral and mid=middle.

CTP: Bladder Results

*distances in mm		Measured values									Absolute difference from control values								
	angle:	**0**	**40**	**80**	**120**	**160**	**200**	**240**	**280**	**320**	**0**	**40**	**80**	**120**	**160**	**200**	**240**	**280**	**320**
FW kV 2	**rlat**	14.7	19.7	20.3	19.2	18.2	20	25.2	19.7	15.4	0.4	1.2	0.7	3	2.2	3.1	0.9	2.8	0
	mid	27.5	33.3	28.2	29.3	24.7	23.5	27	33.9	33	0.1	3.5	**10.5**	0.7	0.5	1	0.6	0.9	0.8
	llat	16.9	14.6	13.7	18.6	19.8	17.7	17.7	17.9	15.9	0.5	0.9	0.4	0.7	1.7	1.6	1.9	2.3	2.2
FW MV 3	**rlat**	15.1	17.5	20.1	19.4	21.2	21.3	23.7	21.4	16.1	0.8	1	0.5	3.2	**5.2**	4.4	0.6	1.1	0.7
	mid	30	33.4	40	28.4	24.3	21.6	27.5	28.7	35.7	2.6	3.6	1.3	0.2	0.9	2.9	0.1	4.3	1.9
	llat	19.4	15.7	14.2	16.7	19.9	15.4	18.1	17.8	15.3	3	2	0.9	1.2	1.8	0.7	2.3	2.2	1.6
FSDs kV 3	**rlat**	15.2	18.8	20.3	18.4	17.8	19.4	23	21.8	15.8	0.9	0.3	0.7	2.2	1.8	2.5	1.3	0.7	0.4
	mid	29.5	31.3	38.2	29.4	24.8	24.3	26.6	34	36.5	2.1	1.5	0.5	0.8	0.4	0.2	1	1	2.7
	llat	17.8	14.2	13.1	18.2	19.6	17.5	17.8	16.8	15.8	1.4	0.5	0.2	0.3	1.5	1.4	2	1.2	2.1
FSDs MV 1	**rlat**	14.8	19.3	20.1	20.7	18.6	21.4	26.1	23.1	16	0.5	0.8	0.5	4.5	2.6	4.5	1.8	0.6	0.6
	mid	29.3	33.7	38.1	31.2	25.9	23.2	27.3	29	34.4	1.9	3.9	0.6	2.6	0.7	1.3	0.3	4	0.6
	llat	16.4	16.3	15.4	19.5	20.4	17	17.8	16.8	18.5	0	2.6	2.1	1.6	2.3	0.9	2	1.2	4.8
CTMR kV 1	**rlat**	14.6	17.3	19.1	19.7	20.1	20.4	22.6	21.5	15.2	0.3	1.2	0.5	3.5	4.1	3.5	1.7	1	0.2
	mid	28.5	32.1	37.2	28.5	24.2	25.3	27.3	32.8	35.5	1.1	2.3	1.5	0.1	1	0.8	0.3	0.2	1.7
	llat	16.3	14.3	14.5	17.7	18.7	16.5	17.1	16.8	16.6	0.1	0.6	1.2	0.2	0.6	0.4	1.3	1.2	2.9
CTMR MV 2	**rlat**	17.4	18.9	19.6	18.5	18.4	21.3	23.9	22.4	18.8	3.1	0.4	0	2.3	2.4	4.4	0.4	0.1	3.4
	mid	27.3	32.4	37.3	31.3	23.2	21.5	28.7	27.6	36.2	0.1	2.6	1.4	2.7	2	3	1.1	**5.4**	2.4
	llat	17.1	15.2	14.3	18	19	16.3	18	18.4	14.8	0.7	1.5	1	0.1	0.9	0.2	2.2	2.8	1.1

Table C-23: Results from three-dimensional reconstructed volume organ segmentation measurements. Color coding for columns displaying differences from control values is as follows: no coloring means the volume recorded was within the predetermined systematic error, red means the volume recorded exceeded the systematic error. The systematic error for the bladder, rectum 1, rectum 2 and rectum 3 was ±17.7cc, ±21.0cc, ±16.1cc and ±29.6cc, respectively. Values within 15cc of control values met the hypothesis criteria of ±15cc.

Volume Comparison Results

*volume in cc	Bladder	Difference	Rectum	Difference
CTMR kV 1	274.9	27.9	151.9	8.4
CTMR MV 2	276.4	29.4	120.3	5.0
FSDs kV 3	279.5	32.5	164.7	19.6
FSDs MV 1	282.3	35.3	161.3	1.0
FW kV 2	279.4	32.4	118.6	6.7
FW MV 3	282.4	35.4	172.8	11.5

Table C-24: Results from catheter reconstruction for the procedurally defined, distal-most dwell position. "Distance" refers to the distance between the distal-most catheter tube dwell position and the applicator reference marker. The difference between TPS generated values and control values is in the "Δ" column. Color coding for the column displaying differences is as follows: no coloring signifies values within ±1 mm of control values, yellow signifies values between ±1-2 mm of control values (within hypothesis criteria of ±2 mm) and red signifies values differing by more than ±2 mm.

Catheter reconstruction results

		Dwell Coordinates			Fiducial Marker Coordinates				
*distances in mm		x	y	z	x	y	z	Distance	Δ
CTMR kV 1	**R. Ovoid**	-10.2	23.9	-84.4	-10.4	8.7	-68.5	22.0	1.5
	L. Ovoid	13.8	23.5	-84.8	15.0	9.8	-69.8	20.4	0.4
	Tandem	1.7	71.7	-60.8	1.6	50.3	-65.9	22.0	1.0
CTMR MV 2	**R. Ovoid**	-12.6	24.6	-102.9	-12.3	9.9	-86.5	22.0	1.4
	L. Ovoid	13.7	24.6	-103.0	13.1	10.9	-88.8	19.7	1.0
	Tandem	-1.1	73.7	-80.8	0.5	50.5	-84.9	23.6	0.6
FSDs kV 3	**R. Ovoid**	-13.8	36.0	-79.0	-11.7	11.7	-66.0	27.6	2.5
	L. Ovoid	15.1	36.0	-78.7	13.0	12.0	-66.2	27.1	2.7
	Tandem	0.2	94.6	-51.5	0.2	69.9	-58.5	25.7	2.0
FSDs MV 1	**R. Ovoid**	-15.7	28.0	-88.9	-12.6	4.2	-78.7	26.1	1.0
	L. Ovoid	13.6	28.4	-89.2	12.3	5.0	-79.4	25.4	1.0
	Tandem	1.3	87.5	-65.2	0.5	64.3	-70.6	23.8	0.1
FW kV 2	**R. Ovoid**	-15.3	30.6	-89.2	-14.0	10.2	-76.9	23.9	2.2
	L. Ovoid	14.0	29.0	-90.1	11.6	10.2	-76.8	23.2	1.3
	Tandem	-0.6	80.2	-68.3	-2.2	56.3	-71.7	24.2	0.6
FW MV 3	**R. Ovoid**	-14.5	34.2	-88.1	-13.4	15.0	-83.0	19.9	1.8
	L. Ovoid	15.4	34.7	-87.2	12.2	14.8	-82.8	20.6	1.2
	Tandem	-1.4	93.9	-63.9	-1.4	69.9	-68.6	24.5	0.9

Physicist 7

Table C-25: Results from two-dimensional CTP organ segmentation measurements for surrogate rectum structures. Color coding for columns displaying differences from control values is as follows: No coloring signifies results within 1 mm of control values, yellow coloring signifies results differing from the control values by 1-2 mm, light red signifies results differing from control values by 2-5 mm and dark red signifies results differing from control values by more than 5 mm. Clear and yellow results met the hypothesis criteria of ±2 mm. The terms "sup", "mid", and "inf" refer to locations relative to the artifact region. Sup=superior, inf=inferior and mid=middle.

CTP: Rectum Results

*distances in mm		Measured values									Absolute difference from control values								
	angle:	**0**	**40**	**80**	**120**	**160**	**200**	**240**	**280**	**320**	**0**	**40**	**80**	**120**	**160**	**200**	**240**	**280**	**320**
FSDs kV 2	**sup**	9.9	9.6	13.3	19.1	20.2	21.3	22.7	23.6	15.3	0.1	0.5	0.4	1.2	0.6	0	0.2	0.2	1.3
	mid	24.8	17.8	15	16.8	21.1	21.5	15.6	14.2	20.6	4	**6.1**	3.5	1.7	0.9	0.3	0.6	0.1	0.8
	inf	18.1	18.7	17.4	17.4	16.7	16.7	16.7	17.7	18.2	0.2	0.4	1.3	0.7	2.3	1.2	0.6	0.1	0
FSDs MV 3	**sup**	12.8	13.2	13.1	14.7	19.4	24.2	25.5	19.3	14.9	0	1.1	0.7	0.3	0.4	0.2	0.8	0.7	1.8
	mid	13.1	20.7	24.8	13.3	16	17.7	17.2	14.7	13.5	0.4	0.5	1.2	1.8	**5.4**	2.3	1.2	1.4	1.1
	inf	16.1	16.6	17.4	17.8	20.6	17.8	17.2	21	19.1	0.3	1.6	1.3	1.1	0.2	1.6	1.3	0.2	0.4
CTMR kV 3	**sup**	12.5	11.7	11.7	13.2	19	24.7	25.5	18.5	15.6	0.3	0.4	0.7	1.2	0.8	0.3	0.8	0.1	1.1
	mid	12	20.6	23.1	12.2	12.7	14.9	17.5	16	12	0.7	0.6	0.5	0.7	2.1	0.5	0.9	0.1	0.4
	inf	15.5	14.9	16.4	17.2	21.3	20.2	18.7	21.3	18.5	0.3	0.1	0.3	0.5	0.9	0.8	0.2	0.5	1
CTMR MV 1	**sup**	16.6	15.5	15.3	17.6	19.5	17.4	17.4	16.8	16.9	0.7	1.9	2.1	1.8	0.4	1.3	1.7	1.2	0.4
	mid	14.2	19.8	23.7	15.7	14.4	14.6	20.4	17.9	15.1	**7**	4.9	0.3	0.5	0.1	0.2	2	2.5	**5.4**
	inf	22.4	14.5	14.3	19.1	11.9	14.1	17.8	21.4	25.8	2.1	2.5	1.9	1.9	1.2	1.5	1	2.9	0.1
FW kV 1	**sup**	16.1	13.1	13.6	16.6	20.7	16.3	12.2	14.5	16.5	0.2	0.5	0.4	0.8	0.8	0.2	3.5	1.1	0
	mid	15.4	21.2	21.7	14.7	14.3	15	18.4	16.6	14.8	**8.2**	**6.3**	2.3	1.5	0	0.2	0	1.2	**5.1**
	inf	20	11.9	12.7	17.2	13.1	13.9	18.2	22.4	25.2	0.3	0.1	0.3	0	0	1.3	0.6	1.9	0.5
FW MV 2	**sup**	11.4	11.9	15.1	19	21.4	22.7	24.1	24.8	16.5	1.6	2.8	2.2	1.1	1.8	1.4	1.2	1	0.1
	mid	29	24.2	18.2	18.9	24.4	20.6	13.6	13.3	20.1	0.2	0.3	0.3	0.4	2.4	1.2	2.6	1	1.3
	inf	17.3	18.6	16.6	16.9	16.5	16.7	17.5	17.5	16.8	1	0.5	0.5	0.2	2.1	1.2	1.4	0.3	1.4

Table C-26: Results from two-dimensional CTP organ segmentation measurements for surrogate bladder structures. Color coding for columns displaying differences from control values is as follows: No coloring signifies results within 1 mm of control values, yellow coloring signifies results differing from the control values by 1-2 mm, light red signifies results differing from control values by 2-5 mm and dark red signifies results differing from control values by more than 5 mm. Clear and yellow results met the hypothesis criteria of ±2 mm. The terms "rlat", "mid" and "llat" refer to locations relative to the artifact region. Rlat=right lateral, llat= left lateral and mid=middle.

CTP: Bladder Results

*distances in mm		Measured values									Absolute difference from control values								
	angle:	**0**	**40**	**80**	**120**	**160**	**200**	**240**	**280**	**320**	**0**	**40**	**80**	**120**	**160**	**200**	**240**	**280**	**320**
FSDs kV 2	**rlat**	14.3	16.2	19.2	17.7	16.3	19.3	20.5	19	15.1	0	2.3	0.4	1.5	0.3	2.4	3.8	3.5	0.3
	mid	26.8	34.8	37.1	29	24.1	23.2	26.7	34.8	33.7	0.6	5	1.6	0.4	1.1	1.3	0.9	1.8	0.1
	llat	17.3	13.9	13.4	18.8	17.9	16.6	17.4	16.4	15.4	0.9	0.2	0.1	0.9	0.2	0.5	1.6	0.8	1.7
FSDs MV 3	**rlat**	15.3	18.1	21.6	18.3	16.1	18.6	22.6	21.3	15.2	1	0.4	2	2.1	0.1	1.7	1.7	1.2	0.2
	mid	27.4	31.4	40	28.4	23.2	19.5	27.2	29.7	34.9	0	1.6	1.3	0.2	2	5	0.4	3.3	1.1
	llat	17.2	13.8	13.2	18.5	19.2	17.3	16.7	16.5	16.3	0.8	0.1	0.1	0.6	1.1	1.2	0.9	0.9	2.6
CTMR kV 3	**rlat**	15.2	17.6	19.3	16.7	16.1	18.1	21.7	22.1	15.3	0.9	0.9	0.3	0.5	0.1	1.2	2.6	0.4	0.1
	mid	28.8	31.8	37.5	27.1	24.9	25.1	26.7	32.4	32.9	1.4	2	1.2	1.5	0.3	0.6	0.9	0.6	0.9
	llat	15.8	13.6	12.9	18.4	19.1	17.7	17.3	14.7	15	0.6	0.1	0.4	0.5	1	1.6	1.5	0.9	1.3
CTMR MV 1	**rlat**	15.4	17.5	19.3	19.2	15.2	18	23.8	22	15.8	1.1	1	0.3	3	0.8	1.1	0.5	0.5	0.4
	mid	30.6	34.1	38.3	29.7	23.9	24.9	27.9	32.1	34.7	3.2	4.3	0.4	1.1	1.3	0.4	0.3	0.9	0.9
	llat	15.3	12.9	14.1	17.7	20.9	19.5	19.4	16.2	15.4	1.1	0.8	0.8	0.2	2.8	3.4	3.6	0.6	1.7
FW kV 1	**rlat**	15.5	18.8	19.8	17.5	16.8	18.3	19.4	18.7	14.6	1.2	0.3	0.2	1.3	0.8	1.4	4.9	3.8	0.8
	mid	29	32.6	38.7	28.7	24	21.9	26.3	31.9	31.4	1.6	2.8	0	0.1	1.2	2.6	1.3	1.1	2.4
	llat	17	14.9	14.4	18.1	17.8	16	17.4	17	15.8	0.6	1.2	1.1	0.2	0.3	0.1	1.6	1.4	2.1
FW MV 2	**rlat**	13.7	14.7	17.2	15.8	16.2	16.9	21	21.2	15.4	0.6	3.8	2.4	0.4	0.2	0	3.3	1.3	0
	mid	27.3	34	39	28.3	22.4	21.2	26.5	32.1	33.7	0.1	4.2	0.3	0.3	2.8	3.3	1.1	0.9	0.1
	llat	16.1	12.9	12.7	17.6	18.6	18	17.4	18.2	15.6	0.3	0.8	0.6	0.3	0.5	1.9	1.6	2.6	1.9

Table C-27: Results from three-dimensional reconstructed volume organ segmentation measurements. Color coding for columns displaying differences from control values is as follows: no coloring means the volume recorded was within the predetermined systematic error, red means the volume recorded exceeded the systematic error. The systematic error for the bladder, rectum 1, rectum 2 and rectum 3 was ±17.7cc, ±21.0cc, ±16.1cc and ±29.6cc, respectively. Values within 15cc of control values met the hypothesis criteria of ±15cc.

Volume Comparison Results

*volume in cc	Bladder	Difference	Rectum	Difference
CTMR kV 3	262.0	15.0	160.4	23.9
CTMR MV 1	275.2	28.2	163.0	2.7
FSDs kV 2	261.0	14.0	114.2	11.1
FSDs MV 3	267.2	20.2	165.9	18.4
FW kV 1	265.0	18.0	149.7	10.6
FW MV 2	262.3	15.3	121.5	3.8

Table C-28: Results from catheter reconstruction for the procedurally defined, distal-most dwell position. "Distance" refers to the distance between the distal-most catheter tube dwell position and the applicator reference marker. The difference between TPS generated values and control values is in the "Δ" column. Color coding for the column displaying differences is as follows: no coloring signifies values within ±1 mm of control values, yellow signifies values between ±1-2 mm of control values (within hypothesis criteria of ±2 mm) and red signifies values differing by more than ±2 mm.

Catheter reconstruction results

		Dwell Coordinates			Fiducial Marker Coordinates				
*distances in mm		x	y	z	x	y	z	Distance	Δ
CTMR kV 3	**R. Ovoid**	-11.0	23.1	-83.1	-11.4	8.7	-67.8	21.0	2.5
	L. Ovoid	14.6	23.6	-82.8	14.0	9.8	-68.2	20.1	0.6
	Tandem	-1.3	71.5	-60.3	0.9	49.9	-65.0	22.2	0.8
CTMR MV 1	**R. Ovoid**	-14.8	26.9	-93.9	-13.3	11.7	-78.5	21.7	1.8
	L. Ovoid	11.8	26.6	-96.6	12.0	12.9	-81.5	20.4	0.3
	Tandem	-2.4	76.3	-74.6	-0.5	53.7	-78.5	23.0	0.0
FSDs kV 2	**R. Ovoid**	-16.7	27.9	-89.1	-13.3	9.9	-72.8	24.5	0.6
	L. Ovoid	12.9	29.1	-87.7	11.1	10.4	-73.0	23.9	0.6
	Tandem	-0.3	92.2	-58.7	-1.1	70.3	-62.6	22.3	1.4
FSDs MV 3	**R. Ovoid**	-16.4	31.3	-92.0	-14.2	12.5	-79.4	22.7	2.4
	L. Ovoid	13.2	31.7	-91.1	11.1	12.8	-78.9	22.6	1.8
	Tandem	-4.0	92.9	-64.4	-3.7	70.1	-70.1	23.5	0.2
FW kV 1	**R. Ovoid**	-14.0	23.0	-78.5	-13.1	5.6	-68.8	19.9	3.8
	L. Ovoid	12.5	23.0	-76.3	12.4	5.3	-69.7	18.9	3.0
	Tandem	0.1	75.3	-62.0	-0.5	52.2	-64.7	23.3	0.3
FW MV 2	**R. Ovoid**	-15.9	22.7	-101.2	-13.6	4.7	-88.6	22.1	0.4
	L. Ovoid	14.0	22.6	-102.4	11.6	5.4	-89.9	21.4	0.5
	Tandem	-1.3	75.4	-85.4	-1.6	52.8	-86.7	22.6	0.9

Physicist 8

Table C-29: Results from two-dimensional CTP organ segmentation measurements for surrogate rectum structures. Color coding for columns displaying differences from control values is as follows: No coloring signifies results within 1 mm of control values, yellow coloring signifies results differing from the control values by 1-2 mm, light red signifies results differing from control values by 2-5 mm and dark red signifies results differing from control values by more than 5 mm. Clear and yellow results met the hypothesis criteria of ±2 mm. The terms "sup", "mid", and "inf" refer to locations relative to the artifact region. Sup=superior, inf=inferior and mid=middle.

CTP: Rectum Results

*distances in mm		Measured values									Absolute difference from control values								
	angle:	**0**	**40**	**80**	**120**	**160**	**200**	**240**	**280**	**320**	**0**	**40**	**80**	**120**	**160**	**200**	**240**	**280**	**320**
FSDs kV 2	**sup**	11.2	9.9	12.9	17.9	20.5	21.8	24.6	23.4	15.5	1.4	0.8	0	0	0.9	0.5	1.7	0.4	1.1
	mid	24.6	19.4	14.3	15.6	17.6	19.2	15.3	15.5	20.9	4.2	4.5	4.2	2.9	4.4	2.6	0.9	1.2	0.5
	inf	18.2	20	14.4	16.8	16.2	15.3	17.3	18	19.2	0.1	0.9	1.7	0.1	1.8	0.2	1.2	0.2	1
FSDs MV 3	**sup**	14.6	13.8	13.2	15.7	20.2	25.1	27.8	20.2	17	1.8	1.7	0.8	1.3	0.4	0.7	3.1	1.6	0.3
	mid	14.1	21.7	24.6	21.4	19.5	20	18.3	17	13.3	1.4	0.5	1	**9.9**	**8.9**	4.6	0.1	0.9	0.9
	inf	18.7	15.4	17.2	18.7	21.2	20.3	20.2	21.4	20.3	2.9	0.4	1.1	2	0.8	0.9	1.7	0.6	0.8
CTMR kV 3	**sup**	12.9	11.7	12	13.9	20.9	25.2	26.7	20	16.7	0.1	0.4	0.4	0.5	1.1	0.8	2	1.4	0
	mid	11.9	20.9	24.4	14.7	12.5	15.6	19.3	16.1	13.3	0.8	0.3	0.8	3.2	1.9	0.2	0.9	0	0.9
	inf	16.2	15.5	17.3	17.9	21.2	20.6	20.2	19.9	18.7	0.4	0.5	1.2	1.2	0.8	1.2	1.7	0.9	0.8
CTMR MV 1	**sup**	18.2	15.5	16	18.5	21	20.7	18.9	17.5	18.2	2.3	1.9	2.8	2.7	1.1	4.6	3.2	1.9	1.7
	mid	17.3	22.2	24.1	17.3	14.6	14.6	19.7	20.3	21.2	**10.1**	**7.3**	0.1	1.1	0.3	0.2	1.3	4.9	**11.5**
	inf	24.3	16.2	15.9	19.6	15	14.4	20.1	22.5	29	4	4.2	3.5	2.4	1.9	1.8	1.3	1.8	3.3
FW kV 1	**sup**	15.8	13.9	12.4	16.7	20.9	16.4	12.8	12	15.2	0.1	0.3	0.8	0.9	1	0.3	2.9	3.6	1.3
	mid	16.6	21.5	15.8	13.9	13.5	14.3	18.8	15	18.2	**9.4**	**6.6**	**8.2**	2.3	0.8	0.5	0.4	0.4	**8.5**
	inf	21.4	12.3	12.6	16.7	13	13.4	18.5	23.9	26.3	1.1	0.3	0.2	0.5	0.1	0.8	0.3	0.4	0.6
FW MV 2	**sup**	12.3	11.3	15.3	20	22	22	24.2	25.7	18.6	2.5	2.2	2.4	2.1	2.4	0.7	1.3	1.9	2
	mid	28.7	24.4	20.2	19.5	21.8	20.9	16.3	15.7	20.9	0.1	0.5	1.7	1	0.2	0.9	0.1	1.4	0.5
	inf	19.1	19.3	18.8	18.1	16.5	18.5	17.7	18.1	18.7	0.8	0.2	2.7	1.4	2.1	3	1.6	0.3	0.5

Table C-30: Results from two-dimensional CTP organ segmentation measurements for surrogate bladder structures. Color coding for columns displaying differences from control values is as follows: No coloring signifies results within 1 mm of control values, yellow coloring signifies results differing from the control values by 1-2 mm, light red signifies results differing from control values by 2-5 mm and dark red signifies results differing from control values by more than 5 mm. Clear and yellow results met the hypothesis criteria of ±2 mm. The terms "rlat", "mid" and "llat" refer to locations relative to the artifact region. Rlat=right lateral, llat= left lateral and mid=middle.

CTP: Bladder Results

*distances in mm		Measured values									Absolute difference from control values								
	angle:	**0**	**40**	**80**	**120**	**160**	**200**	**240**	**280**	**320**	**0**	**40**	**80**	**120**	**160**	**200**	**240**	**280**	**320**
FSDs kV 2	**rlat**	15.9	18.8	20.4	20.4	20.1	20	22.8	21.4	15.4	1.6	0.3	0.8	4.2	4.1	3.1	1.5	1.1	0
	mid	28.3	32.1	37.1	28.8	25.4	23.8	28.1	35.5	32.9	0.9	2.3	1.6	0.2	0.2	0.7	0.5	2.5	0.9
	llat	17.7	14.4	13.8	17.5	18.4	17	17.7	18.1	15.4	1.3	0.7	0.5	0.4	0.3	0.9	1.9	2.5	1.7
FSDs MV 3	**rlat**	15	19.6	22.7	21.7	23.7	20.7	27.3	23.2	16.3	0.7	1.1	3.1	**5.5**	**7.7**	3.8	3	0.7	0.9
	mid	29.7	23.8	40.7	33.4	25.6	23.2	27.3	31.7	34	2.3	**6**	2	4.8	0.4	1.3	0.3	1.3	0.2
	llat	17.9	16.2	14.4	17.6	18.5	18.1	19.7	21.1	19.1	1.5	2.5	1.1	0.3	0.4	2	3.9	**5.5**	**5.4**
CTMR kV 3	**rlat**	16.7	18.6	19.7	20	18.3	20.3	21.6	22.9	16	2.4	0.1	0.1	3.8	2.3	3.4	2.7	0.4	0.6
	mid	29.4	32.3	37.9	28.1	24.1	23.7	27.7	34	34.2	2	2.5	0.8	0.5	1.1	0.8	0.1	1	0.4
	llat	17.8	14.4	17.4	14	13.2	19.8	19.5	17.4	18.2	1.4	0.7	4.1	3.9	4.9	3.7	3.7	1.8	4.5
CTMR MV 1	**rlat**	17.3	18.4	21.9	23	20.6	18.1	23.4	23.2	15.8	3	0.1	2.3	**6.8**	4.6	1.2	0.9	0.7	0.4
	mid	28.5	33.6	39.6	29.8	24	22.5	28.2	34.8	34.1	1.1	3.8	0.9	1.2	1.2	2	0.6	1.8	0.3
	llat	16.6	13.9	13.3	19.4	20.3	18.3	20.4	17.4	16.3	0.2	0.2	0	1.5	2.2	2.2	4.6	1.8	2.6
FW kV 1	**rlat**	16.3	19.3	19.8	20.6	19.4	18	22.6	21	15.5	2	0.8	0.2	4.4	3.4	1.1	1.7	1.5	0.1
	mid	28.7	32.7	38.4	29.1	24.1	23.7	27.2	31.9	25	1.3	2.9	0.3	0.5	1.1	0.8	0.4	1.1	**8.8**
	llat	17.5	14.5	13.2	16.6	17.2	16.5	17.5	17.4	16.2	1.1	0.8	0.1	1.3	0.9	0.4	1.7	1.8	2.5
FW MV 2	**rlat**	15.3	18.5	20.9	22.2	24	20	21.5	21.7	16.7	1	0	1.3	**6**	**8**	3.1	2.8	0.8	1.3
	mid	26.2	32.6	39	29.6	24.8	22.6	27.6	27.9	32.3	1.2	2.8	0.3	1	0.4	1.9	0	**5.1**	1.5
	llat	17	12.6	13.7	18.4	22	18.8	20	16.1	17.9	0.6	1.1	0.4	0.5	3.9	2.7	4.2	0.5	4.2

Table C-31: Results from three-dimensional reconstructed volume organ segmentation measurements. Color coding for columns displaying differences from control values is as follows: no coloring means the volume recorded was within the predetermined systematic error, red means the volume recorded exceeded the systematic error. The systematic error for the bladder, rectum 1, rectum 2 and rectum 3 was ±17.7cc, ±21.0cc, ±16.1cc and ±29.6cc, respectively. Values within 15cc of control values met the hypothesis criteria of ±15cc.

Volume Comparison Results

*volume in cc	Bladder	Difference	Rectum	Difference
CTMR kV 3	280.2	33.2	176.9	7.4
CTMR MV 1	300.6	53.6	183.9	23.5
FSDs kV 2	280.5	33.5	122.1	3.2
FSDs MV 3	296.4	49.4	186.2	1.9
FW kV 1	264.3	17.3	151.9	8.5
FW MV 2	287.1	40.1	133.5	8.1

Table C-32: Results from catheter reconstruction for the procedurally defined, distal-most dwell position. "Distance" refers to the distance between the distal-most catheter tube dwell position and the applicator reference marker. The difference between TPS generated values and control values is in the "Δ" column. Color coding for the column displaying differences is as follows: no coloring signifies values within ±1 mm of control values, yellow signifies values between ±1-2 mm of control values (within hypothesis criteria of ±2 mm) and red signifies values differing by more than ±2 mm.

Catheter reconstruction results

		Dwell Coordinates			Fiducial Marker Coordinates				
*distances in mm		x	y	z	x	y	z	Distance	Δ
CTMR kV 3	**R. Ovoid**	-11.2	24.4	-84.0	-11.4	8.7	-67.8	22.6	0.9
	L. Ovoid	14.6	24.1	-82.9	14.0	9.8	-68.2	20.5	0.2
	Tandem	-1.4	72.0	-60.5	0.9	49.9	-65.0	22.7	0.4
CTMR MV 1	**R. Ovoid**	-14.8	29.0	-95.8	-13.3	11.7	-78.5	24.5	1.0
	L. Ovoid	11.5	28.0	-96.4	12.0	12.9	-81.5	21.2	0.5
	Tandem	-2.5	76.9	-75.1	-0.5	53.7	-78.5	23.5	0.5
FSDs kV 2	**R. Ovoid**	-16.2	29.1	-90.8	-13.3	9.9	-72.8	26.5	1.4
	L. Ovoid	12.8	29.3	-88.3	11.1	10.4	-73.0	24.4	0.1
	Tandem	0.1	93.3	-58.3	-1.1	70.3	-62.6	23.4	0.3
FSDs MV 3	**R. Ovoid**	-16.6	33.4	-93.2	-14.2	12.5	-79.4	25.2	0.0
	L. Ovoid	13.3	34.3	-91.6	11.1	12.8	-78.9	25.1	0.6
	Tandem	-3.5	93.2	-63.9	-3.7	70.1	-70.1	23.9	0.2
FW kV 1	**R. Ovoid**	-14.0	24.2	-80.3	-13.1	5.6	-68.8	21.9	0.2
	L. Ovoid	13.3	24.2	-82.3	12.4	5.3	-69.7	22.7	0.9
	Tandem	0.7	75.2	-62.2	-0.5	52.2	-64.7	23.2	0.4
FW MV 2	**R. Ovoid**	-14.4	22.9	-101.5	-13.6	4.7	-88.6	22.3	0.7
	L. Ovoid	14.9	21.5	-102.1	11.6	5.4	-89.9	20.5	1.4
	Tandem	-0.6	75.6	-85.2	-1.6	52.8	-86.7	22.9	0.7

Physicist 9

Table C-33: Results from two-dimensional CTP organ segmentation measurements for surrogate rectum structures. Color coding for columns displaying differences from control values is as follows: No coloring signifies results within 1 mm of control values, yellow coloring signifies results differing from the control values by 1-2 mm, light red signifies results differing from control values by 2-5 mm and dark red signifies results differing from control values by more than 5 mm. Clear and yellow results met the hypothesis criteria of ±2 mm. The terms "sup", "mid", and "inf" refer to locations relative to the artifact region. Sup=superior, inf=inferior and mid=middle.

CTP: Rectum Results

*distances in mm		Measured values									Absolute difference from control values								
	angle:	**0**	**40**	**80**	**120**	**160**	**200**	**240**	**280**	**320**	**0**	**40**	**80**	**120**	**160**	**200**	**240**	**280**	**320**
FSDs kV 2	**sup**	10.7	10.1	13.4	19.1	19.7	20.9	23.6	24	17.9	0.9	1	0.5	1.2	0.1	0.4	0.7	0.2	1.3
	mid	30.6	26.6	18.9	16.6	21.4	22.9	16.1	16.3	22.9	1.8	2.7	0.4	1.9	0.6	1.1	0.1	2	1.5
	inf	18.3	18.4	16.7	16.5	15.3	17.1	16.8	17.9	18.1	0	0.7	0.6	0.2	0.9	1.6	0.7	0.1	0.1
FSDs MV 3	**sup**	13.6	13.1	12.8	14.1	19.3	25	26.9	19.6	16.2	0.8	1	0.4	0.3	0.5	0.6	2.2	1	0.5
	mid	13.1	21	24.3	16.3	17.4	17.5	17.6	14.8	12.5	0.4	0.2	0.7	4.8	**6.8**	2.1	0.8	1.3	0.1
	inf	16.6	16.1	16.5	17.4	20.6	20.5	19.9	21.2	20.3	0.8	1.1	0.4	0.7	0.2	1.1	1.4	0.4	0.8
CTMR kV 3	**sup**	14.1	13	12.7	15	21.4	24.8	25.8	19.6	16.5	1.3	0.9	0.3	0.6	1.6	0.4	1.1	1	0.2
	mid	13.3	18.8	21.2	18.6	15.4	15.9	17.5	14.8	12.1	0.6	2.4	2.4	**7.1**	4.8	0.5	0.9	1.3	0.3
	inf	16.6	15.4	16.2	17.2	20.7	20.7	18.6	20.3	19.8	0.8	0.4	0.1	0.5	0.3	1.3	0.1	0.5	0.3
CTMR MV 1	**sup**	18.2	13.8	14.5	15.8	23.2	17.6	15.1	13.3	18.2	2.3	0.2	1.3	0	3.3	1.5	0.6	2.3	1.7
	mid	11.5	16.9	23.9	17.9	16.4	16.8	19.3	18.9	15.1	4.3	2	0.1	1.7	2.1	2	0.9	3.5	**5.4**
	inf	23.5	13	14	19.1	14.3	14.1	19.3	23.2	26	3.2	1	1.6	1.9	1.2	1.5	0.5	1.1	0.3
FW kV 1	**sup**	15.5	13.1	12.6	15.5	20.4	16.9	17.6	15.5	17.1	0.4	0.5	0.6	0.3	0.5	0.8	1.9	0.1	0.6
	mid	13.7	18.9	18.3	17.1	15.2	16.8	19.9	15.9	15.3	**6.5**	4	**5.7**	0.9	0.9	2	1.5	0.5	**5.6**
	inf	21.2	12.5	13.3	16.7	13.8	12.8	17.9	22.7	25.7	0.9	0.5	0.9	0.5	0.7	0.2	0.9	1.6	0
FW MV 2	**sup**	11.5	10.7	14.6	19.1	21.2	21.8	23.4	24.1	16.3	1.7	1.6	1.7	1.2	1.6	0.5	0.5	0.3	0.3
	mid	28.5	24.1	18.4	18.6	21.5	21.6	17.5	15.9	21.2	0.3	0.2	0.1	0.1	0.5	0.2	1.3	1.6	0.2
	inf	17.4	19.4	16.5	16.5	15.5	17.8	18.1	19.2	18.2	0.9	0.3	0.4	0.2	1.1	2.3	2	1.4	0

Table C-34: Results from two-dimensional CTP organ segmentation measurements for surrogate bladder structures. Color coding for columns displaying differences from control values is as follows: no coloring signifies results within 1 mm of control values, yellow coloring signifies results differing from the control values by 1-2 mm, light red signifies results differing from control values by 2-5 mm and dark red signifies results differing from control values by more than 5 mm. Clear and yellow results met the hypothesis criteria of ±2 mm. The terms "rlat", "mid" and "llat" refer to locations relative to the artifact region. Rlat=right lateral, llat= left lateral and mid=middle.

CTP: Bladder Results

*distances in mm		Measured values									Absolute difference from control values								
	angle:	**0**	**40**	**80**	**120**	**160**	**200**	**240**	**280**	**320**	**0**	**40**	**80**	**120**	**160**	**200**	**240**	**280**	**320**
FSDs kV 2	**rlat**	15.2	17.9	19.1	20.6	19.1	18.2	24	21.7	15.8	0.9	0.6	0.5	4.4	3.1	1.3	0.3	0.8	0.4
	mid	29.2	32.6	37.2	28.2	24.9	24.8	26.7	32.1	33	1.8	2.8	1.5	0.4	0.3	0.3	0.9	0.9	0.8
	llat	16	13.8	14.6	18.5	19.3	18.4	18.6	15.5	15.4	0.4	0.1	1.3	0.6	1.2	2.3	2.8	0.1	1.7
FSDs MV 3	**rlat**	16.4	19.5	19.9	19.7	19.4	21.2	25.9	22.3	15.1	2.1	1	0.3	3.5	3.4	4.3	1.6	0.2	0.3
	mid	31.9	35.3	38.4	27.9	25.1	24	28.7	32.4	35.6	4.5	**5.5**	0.3	0.7	0.1	0.5	1.1	0.6	1.8
	llat	17.1	13.7	13.6	18.3	20.3	19.1	19.1	18.1	15.7	0.7	0	0.3	0.4	2.2	3	3.3	2.5	2
CTMR kV 3	**rlat**	14.8	18.4	17.7	17.9	17.9	20.5	24.1	19.8	15.5	0.5	0.1	1.9	1.7	1.9	3.6	0.2	2.7	0.1
	mid	28.3	32.1	38.9	28	25.4	24.1	26.2	31.8	35.3	0.9	2.3	0.2	0.6	0.2	0.4	1.4	1.2	1.5
	llat	16.8	14.3	14.6	18	18.5	17	17.7	17.1	15.1	0.4	0.6	1.3	0.1	0.4	0.9	1.9	1.5	1.4
CTMR MV 1	**rlat**	17.3	17	19.7	20.5	19.7	17.6	21.4	21.1	17.1	3	1.5	0.1	4.3	3.7	0.7	2.9	1.4	1.7
	mid	28.1	32.2	39.6	30.1	26.9	25.1	26.7	31.1	36.5	0.7	2.4	0.9	1.5	1.7	0.6	0.9	1.9	2.7
	llat	16.1	14	14.7	14.9	18.4	19.4	18.3	14.1	14.8	0.3	0.3	1.4	3	0.3	3.3	2.5	1.5	1.1
FW kV 1	**rlat**	16	19.6	20.1	19.3	16	18.6	21.9	21.7	15.5	1.7	1.1	0.5	3.1	0	1.7	2.4	0.8	0.1
	mid	29	32.6	38.5	29.2	24.9	22.3	27.1	32.5	33.9	1.6	2.8	0.2	0.6	0.3	2.2	0.5	0.5	0.1
	llat	16.4	14.5	13.7	18.1	18.4	17.4	17.2	15.5	15.4	0	0.8	0.4	0.2	0.3	1.3	1.4	0.1	1.7
FW MV 2	**rlat**	17.3	17.3	20.6	20	19.4	18.1	22.4	21.7	15.7	3	1.2	1	3.8	3.4	1.2	1.9	0.8	0.3
	mid	28.9	31.9	39.2	28.8	24.5	22.3	28.7	27.8	33.6	1.5	2.1	0.5	0.2	0.7	2.2	1.1	**5.2**	0.2
	llat	16.5	13.4	14.7	18.4	18	16.4	18.5	15.9	15.7	0.1	0.3	1.4	0.5	0.1	0.3	2.7	0.3	2

Table C-35: Results from three-dimensional reconstructed volume organ segmentation measurements. Color coding for columns displaying differences from control values is as follows: no coloring means the volume recorded was within the predetermined systematic error, red means the volume recorded exceeded the systematic error. The systematic error for the bladder, rectum 1, rectum 2 and rectum 3 was ±17.7cc, ±21.0cc, ±16.1cc and ±29.6cc, respectively. Values within 15cc of control values met the hypothesis criteria of ±15cc.

Volume Comparison Results

*volume in cc	Bladder	Difference	Rectum	Difference
CTMR kV 3	262.0	15.0	160.4	23.9
CTMR MV 1	275.2	28.2	163.0	2.7
FSDs kV 2	261.0	14.0	114.2	11.1
FSDs MV 3	267.2	20.2	165.9	18.4
FW kV 1	265.0	18.0	149.7	10.6
FW MV 2	262.3	15.3	121.5	3.8

Table C-36: Results from catheter reconstruction for the procedurally defined, distal-most dwell position. "Distance" refers to the distance between the distal-most catheter tube dwell position and the applicator reference marker. The difference between TPS generated values and control values is in the "Δ" column. Color coding for the column displaying differences is as follows: no coloring signifies values within ±1 mm of control values, yellow signifies values between ±1-2 mm of control values (within hypothesis criteria of ±2 mm) and red signifies values differing by more than ±2 mm.

Catheter reconstruction results

		Dwell Coordinates			Fiducial Marker Coordinates				
*distances in mm		x	y	z	x	y	z	Distance	Δ
CTMR kV 3	**R. Ovoid**	-11.0	23.1	-83.1	-11.4	8.7	-67.8	21.0	2.5
	L. Ovoid	14.6	23.6	-82.8	14.0	9.8	-68.2	20.1	0.6
	Tandem	-1.3	71.5	-60.3	0.9	49.9	-65.0	22.2	0.8
CTMR MV 1	**R. Ovoid**	-14.8	26.9	-93.9	-13.3	11.7	-78.5	21.7	1.8
	L. Ovoid	11.8	26.6	-96.6	12.0	12.9	-81.5	20.4	0.3
	Tandem	-2.4	76.3	-74.6	-0.5	53.7	-78.5	23.0	0.0
FSDs kV 2	**R. Ovoid**	-16.7	27.9	-89.1	-13.3	9.9	-72.8	24.5	0.6
	L. Ovoid	12.9	29.1	-87.7	11.1	10.4	-73.0	23.9	0.6
	Tandem	-0.3	92.2	-58.7	-1.1	70.3	-62.6	22.3	1.4
FSDs MV 3	**R. Ovoid**	-16.4	31.3	-92.0	-14.2	12.5	-79.4	22.7	2.4
	L. Ovoid	13.2	31.7	-91.1	11.1	12.8	-78.9	22.6	1.8
	Tandem	-4.0	92.9	-64.4	-3.7	70.1	-70.1	23.5	0.2
FW kV 1	**R. Ovoid**	-14.0	23.0	-78.5	-13.1	5.6	-68.8	19.9	3.8
	L. Ovoid	12.5	23.0	-76.3	12.4	5.3	-69.7	18.9	3.0
	Tandem	0.1	75.3	-62.0	-0.5	52.2	-64.7	23.3	0.3
FW MV 2	**R. Ovoid**	-15.9	22.7	-101.2	-13.6	4.7	-88.6	22.1	0.4
	L. Ovoid	14.0	22.6	-102.4	11.6	5.4	-89.9	21.4	0.5
	Tandem	-1.3	75.4	-85.4	-1.6	52.8	-86.7	22.6	0.9

Vita

Jeffrey Roger Kemp was born in Spokane, Washington to William Jesse Kemp and Janet Marie Janson Kemp. Prior to studying at Brigham Young University he spent two years on a church service mission in the Fijian islands, speaking Fijian, Hindustani and Gilbertese. While studying physics at Brigham Young University, he met Amy Christensen who he later married on June 7, 2008 in the Sacramento Temple. He completed his Bachelor of Science degree in physics at Brigham Young University in Provo Utah in April 2009. While attending graduate school at Louisiana University, his two daughters were born—Emily Clarees Kemp and Katelyn "Katie" Talei Kemp. He received his Master of Science degree in medical physics and health physics from Louisiana State University in the summer of 2012. He currently plans to begin a career as a clinical medical physicist in Baton Rouge, Louisiana at Mary Bird Perkins Cancer Center beginning in July 2012 as a resident medical physicist.